

**INTER-ANNUAL VARIABILITY OF THERMAL AND  
CHLOROPHYLL FRONTS IN SELECTED PARTS OF EASTERN  
ARABIAN SEA AND THEIR RELATION TO MARINE FISHERY**

*by*

**ANANTH C BABU**

**(2012 - 20 - 103)**

**THESIS**

**Submitted in partial fulfilment of the  
requirements for the degree of**

**B.Sc. – M.Sc. (Integrated) Climate Change Adaptation**

**Faculty of Agriculture**

**Kerala Agricultural University**



**ACADEMY OF CLIMATE CHANGE EDUCATION AND RESEARCH**

**VELLANIKKARA, THRISSUR – 680 656**

**KERALA, INDIA**


**2017**

## DECLARATION

I, Ananth C Babu (2012 – 20 – 103) hereby declare that this thesis entitled **“Inter-annual variability of thermal and chlorophyll fronts in selected parts of eastern Arabian Sea and their relation to marine fishery”** is a bonafide record of research work done by me during the course of research and the thesis has not previously formed the basis for the award to me of any degree, diploma, associateship, fellowship or other similar title, of any other University or Society.

Vellanikkara

Date: 18/01/18



Ananth C Babu

(2012 – 20 – 103)

## CERTIFICATE

Certified that this thesis entitled “**Inter-annual variability of thermal and chlorophyll fronts in selected parts of eastern Arabian Sea and their relation to marine fishery**” is a record of research work done independently by Mr. Ananth C Babu, under my guidance and supervision and that it has not previously formed the basis for the award of any degree, diploma, fellowship or associateship to him.

Kochi

Date: 18/01/2018

  
Dr. Grinson George

Senior Scientist


Fishery Resources Assessment Division

Central Marine Fisheries Research Institute

Ernakulam North P.O., Kochi- 682 018.

## CERTIFICATE

We, the undersigned members of the advisory committee of Mr. Ananth C Babu, a candidate for the degree of BSc-MSc (Integrated) Climate Change Adaptation agree that the thesis entitled “**Inter-annual variability of thermal and chlorophyll fronts in selected parts of eastern Arabian Sea and their relation to marine fishery**” may be submitted by Mr. Ananth C Babu, (2012-20-103), in partial fulfilment of the requirement for the degree.



18/01/2018

**Dr. Grinson George**

(Major Advisor, Advisory Committee)  
Senior Scientist  
Fishery Resources Assessment Division  
Central Marine Fisheries Research Institute  
Ernakulam North P.O., Kochi



**Dr. Kunhamu T. K**

(Member, Advisory Committee)  
Special Officer  
ACCER, KAU  
Vellanikkara, Thrissur



**Mr. Vivekanand Bharti**

(Member, Advisory Committee)  
Senior Scientist  
Fishery Resources Assessment Division  
Central Marine Fisheries Research Institute  
Ernakulam North P.O., Kochi



**Dr. Sunil K. M**

(Member, Advisory Committee)  
Assistant Professor  
Krishi Vigyan Kendra, Pattambi  
Palakkad



**EXTERNAL EXAMINER**

(K. Agath Joseph)

## ACKNOWLEDGEMENT

I give my glory, honor and praises to my **LIVING GOD** who is my supreme guide and beloved, friend for his favor, guidance, strength and health he provided for me to successfully complete this research work.

I would first like to express my extreme Gratitude and obligation to my major advisor **Dr. Grinson George** of the Central Marine Fisheries Research Institute (CMFRI), Kochi for the useful comments, remarks and encouragement throughout the learning process of this master thesis. It was a great honor and privilege working under his guidance. Furthermore I would like to thank **Mr. Arjun S Putezhath**, Fleming College, Lindsay, Ontario, **Dr. Shalin Saleem**, Research Associate, CMFRI, Kochi, **Dr. Phiros Shah**, Research Associate, CMFRI, Kochi and **Mr. Muhammad Shafeeque** Research Scholar, CMFRI, Kochi for introducing me to the topic as well for the support on the way.

I express my thanks to **Dr. Kunhamu T. K**, Special officer, Academy of Climate Change Education and Research, KAU, Vellanikkara and member of my advisory committee for her scrupulous guidance, advices, valuable and timely suggestions given during my work.

I respectfully thank **Dr. K. M. Sunil**, Assistant Professor, Agrl. Meteorology, KVK Palakkad, Pattambi and member of my advisory committee for his valuable recommendation and help during my work and writing of thesis.

I respectfully thank **Mr. Vivekanand Bharti**, Scientist, CMFRI, Kochi and member of my advisory committee for his suggestions and corrections in my thesis.

I would also like to acknowledge **Dr. Shelton Padua** Scientist, CMFRI, Kochi for his treasured knowledge regarding GIS and remote sensing.

I would also like to extend huge, warm thanks to **Mr. Jason J. Roberts**, Marine Geospatial Ecology Lab, Duke University, USA for his in-depth knowledge regarding Marine Geospatial Ecology Tools and frontal identification techniques.

I thank **Mr. Tarun Joseph**, Cochin University of Science and Technology, for his motivation and encouragement provided over the research period.

I would also like to thank **Ms. Neethu Anto**, Data entry supervisor, CMFRI, Kochi and **Ms. Ammu J. V**, Data analyst CMFRI, Kochi for helping me with handling the data and for their whole hearted support while doing my thesis.

I respectfully thank **Kerala Agricultural University, Academy of Climate Change Education and Research** and all scientists and staff members of **Central Marine Fisheries Research Institute** for providing all the support needed to complete this work.

My heartfelt thanks to all my classmates of **Redhawks-2012** and my seniors of **Spartans-2011** for their support given to me during the whole college days.

I express my sincere gratitude to **my parents** and **my elder brother** who were always there to encourage me in all of my endeavors. Their prayers and blessings were a constant source of inspiration and guidance to me. Without them I would have never been able to complete my work on time.



**Ananth C Babu**

## TABLE OF CONTENTS

---

CHAPTER NO.	TITLE	PAGE NO.
	LIST OF TABLES	i
	LIST OF FIGURES	ii-iii
	SYMBOLS AND ABBREVIATIONS	iv-vii
1	INTRODUCTION	1-6
2	REVIEW OF LITERATURE	7-25
3	MATERIALS AND METHODS	26-37
4	RESULTS AND DISCUSSION	38-82
5	SUMMARY AND CONCLUSION	83-86
	REFERENCES	87-109
	ABSTRACT	

---

## LIST OF TABLES

Table No.	Title	Page No.
1	Regions of Arabian Sea with respective coordinates	34
2	List of the annually averaged combined global land and ocean temperatures and their anomaly for the 9 warmest years on record	77



## LIST OF FIGURES

Figure No.	Title	Page No.
1	Study Area - Arabian Sea	5
2	SST for the period Jan 1-8 2010	26
3	Chl-a for the period Jan 1-8 2010	27
4	Front detection using ArcGIS	32
5	Area calculation using ArcGIS	33
6	Shapefile creation using QGIS	35
7	Extracting features within EEZ using ArcGIS	36
8	Climatology of SST of Arabian Sea from January to June for the period 2002-2016	38
9	Climatology of SST of Arabian Sea from July to December for the period 2002-2016	39
10	Climatology of Chl-a concentration of Arabian Sea from January to June for the period 2000-2016	43
11	Climatology of Chl-a concentration of Arabian Sea from July to December for the period 2000-2016	44
12	Climatology of SSHA of Arabian Sea from January to June for the period 2000-2013	48
13	Climatology of SSHA of Arabian Sea from July to December for the period 2000-2013	49
14	Climatology of winds over Arabian Sea from January to June for the period 2000-2016	53

<b>15</b>	Climatology of winds over Arabian Sea from July to December for the period 2000-2016	54
<b>16</b>	Climatology of surface current velocity of Arabian Sea from January to June for the period 2000-2016	58
<b>17</b>	Climatology of surface current velocity of Arabian Sea from July to December for the period 2000-2016	59
<b>18</b>	Climatology of thermal frontal area (2003-2016) and chlorophyll frontal area (2000-2016) over Arabian Sea	63
<b>19</b>	Climatology of variability in frontal area in the north west, north east, south west and south eastern Arabian Sea	65
<b>20</b>	Percentage spatial distribution of thermal frontal area over Arabian Sea	72
<b>21</b>	Percentage spatial distribution of chlorophyll frontal area over Arabian Sea	72
<b>22</b>	Time series plot of thermal and chlorophyll frontal area in Arabian Sea	75
<b>23</b>	Time series plot of thermal and chlorophyll frontal area in the north western, north eastern, south western and south eastern Arabian Sea	79
<b>24</b>	Time-series plot of chlorophyll frontal area and CPUE in hours	81
<b>25</b>	Time-series plot of thermal frontal area and CPUE in hours	82

## SYMBOLS AND ABBREVIATIONS

---

ANI	Andaman and Nicobar Islands
APDRC	Asia-Pacific Data-Research Centre
AVISO	Archiving, Validation and interpretation of Satellite
CFS	Climate Forecast System
Chl-a	Chlorophyll-a
CMFRI	Central Marine Fisheries Research Institute
CPUE	Catch Per Unit Effort
ECMWF	European Centre for Medium Range Weather Forecasts
EEZ	Exclusive Economic Zone
ERA	European Reanalysis
ERS	European Remote Sensing
ESA	European Space Agency
ESRI	Environmental Systems Research Institute
GFO	GEOSAT Follow-On
GODAS	Global Ocean Data Assimilation Centre
INCOIS	Indian National Centre for Ocean Information Services
IPCC AR5	Inter-Governmental Panel for Climate Change 5 <sup>th</sup> Assessment Report
IPFZ	Integrated Potential Fishing Zones

MBN	mechanised bag net
MDN	mechanised dol net
MDTN	multi day trawl net
MERIS	Medium Resolution Imaging Spectrometer
MGET	Marine Geospatial Ecology Tools
MGN	mechanised gill net
MHL	mechanised hooks and lines
MIED	Multi Image Ede Detection
MODIS	Moderate Resolution Imaging Spectroradiometer
MOTHS	mechanised other gears
MPS	mechanised purse seine
MRS	mechanised ring seine
MTN	mechanised trawl net
NASA	National Aeronautics and Space Administration
NC	NetCDF
NCEP	National Environmental Prediction Centre
NM	non-motorized
NOAA	National Oceanic and Atmospheric Administration
NPP	Net Primary Productivity
NWP	Numerical Weather Prediction
OBBN	outboard bag net

OBBS	outboard boat seine
OBDOLE	outboard dol net
OBGN	outboard gill net
OBHL	outboard hooks and lines
OBOTHS	outboard other gears
OBPG	Ocean Biology Processing Group
OBPS	outboard purse seine
OBRS	outboard ring seine
OBSS	outboard shore seine
OBTN	outboard trawl net
OC-CCI	Ocean Color Climate Change Initiative
	Oceanographic data
PFZ	Potential Fishery Forecast
PML	Plymouth Marine Laboratory
ppt	Parts Per Thousand
PSU	Practical Salinity Units
SCS	South China Sea
SeaWiFS	Sea-viewing Wide Field-of-view Sensor
SIED	Single Image Edge Detection
sp.	Species
SRS	Satellite Remote Sensing

SSHA	Sea Surface Height Anomaly
SSS	Sea Surface Salinity
SST	Sea Surface Temperature
TZCF	Transition Zone Chlorophyll Front
VIIRS	Visible Infrared Imaging Radiometer Suite

**Dedicated to my beloved  
parents and my elder  
brother...**

# INTRODUCTION



## CHAPTER 1

### INTRODUCTION

Climate change is currently the most widely discussed and alarming topic of the 21<sup>st</sup> century. Its impacts are well known and possess great challenge to the society, environment and ecosystem. Climate change has its profound impact due to increase in temperature, and this can be attributed directly to the increasing levels of greenhouse gases in the atmosphere. Also, there are changes in precipitation pattern and sea level rise across the globe. As per the Inter-Governmental Panel for Climate Change 5<sup>th</sup> Assessment Report (IPCC AR5), the phase 1983-2012 was reported as likely the warmest 30year period in the Northern Hemisphere, during the past 800 years. The worldwide averaged, combined land and sea surface temperature showed a warming of 0.85°C during the period 1880-2012, which ranged from 0.65°C to 1.06°C. It is also reported that the upper 75 m of the world oceans showed a warming of 0.11°C [0.09°C to 0.13°C] per decade over the years from 1971 to 2010, and this warming is largest near the surface. It is predicted that there could be a further increase in combined land-sea surface temperature of the magnitude of at least 1.8°C in the 21<sup>st</sup> century, regardless of mitigation measures. The anthropogenic activities that involves combustion of fossil fuels, which results in large scale emissions of greenhouse gases to the atmosphere, is the predominant factor for climate change (Hansen *et al.*, 2013; Vitousek *et al.*, 1997). The emission of GHG due to human activities have reached a level of 49±0.5 Gt CO<sub>2</sub> – eq/yr (Allen *et al.*, 2014). The climate change escalates other problems such as ecosystem degradation, loss of biodiversity, sea level rise, desertification and also strengthened biogeochemical cycles. Many of the present research deals with the impacts of climate change on the ecosystem and necessary adaptive and mitigation measures (Vivekanandan, 2013; Laukkonen *et al.*, 2009; Hallegatte, 2009).

Marine capture fisheries contributes significantly to the food supply and food security in India. It also contributes significantly to the national GDP and foreign

exchange. In India, the potential harvestable marine fishery resources has been estimated as 4.41 million tonnes from the Exclusive Economic Zone. As reported by Central Marine Fisheries Research Institute in the Marine Fisheries Census 2010, about 3.9 million fisher folk works in the fisheries sector and produce about 3.63 million tonnes of marine fish per year. By exporting fish and fishery products to the foreign countries, fisheries sector generated huge investment of 30,213.26 crore INR during 2013-14 (Preethika *et al.*, 2016). Globally, fish provides nourishment for 3 billion people. It is estimated that, in the least developed countries, fish ensure at least half of animal protein and mineral requirement to 400 million people (Yazdi and Shakouri, 2010). As the oceans are not confined, and the resources are not infinite, there is an extreme competition within stakeholders having different interests to access these limited resources in the coastal waters, which has finally resulted in over exploitation and stock depletion of few fish species. Climate change is expected to impact fisheries by altering the abundance and distribution of species and its breeding and migration patterns (Vivekanandan, 2010).

El Niño southern oscillation, commonly called as ENSO is often cited as an example of climate change affecting oceanographic events and is the predominant reason for the inter-annual climatic inconsistency all over the world. ENSO events are considered as variations in atmospheric circulation pattern impacting ocean due to changes in sea surface temperature (SST), variation in vertical thermal structure of oceans and altered coastal and upwelling currents, which occurs irregularly at a time interval of 2-10 years (Enfield, 1988; Wang *et al.*, 2006). ENSO events are linked with varied physical and biological properties of the ocean that alters fish abundance and its distribution. Variations in SST, increased stratification of water column, varied intensity and frequency of upwelling events results in varied primary and secondary production in the coastal waters. In the tropics, the economy of many countries depends crucially on the strength and occurrence of the El Niño (Kumar *et al.*, 2014).

El Niño causes changes in circulation patterns in the atmosphere and ocean (Lix *et al.*, 2016), which results in varied property of water in certain areas of the open ocean. This negatively impacts the fish species of that region by interfering with the species-specific biological thresholds and tolerance levels of the fishes. Fish migrates to those regions where the environment is favorable for its growth and reproduction. Thus, migration of species can be looked upon as a bio-marker of climate change. One of the prime after effects of El-Nino is the loss of an economically significant species which was earlier present in an area (NOAA, 2017a). Loss of even a single species in such a big ecosystem can lead to catastrophe, since each species are closely linked to other in marine food chain. Fish migrate towards favourable environment for their growth and reproduction, thus the aggregation of fish in large quantities can be seen in areas that are favourable for them (Humston *et al.*, 2000, Bertignac *et al.*, 1998). Generally these areas are characterised by a gradient temperature or chlorophyll-a (Chl-a) content, known as thermal fronts and chlorophyll fronts respectively.

A front is a narrow zone of gradient water properties such as temperature, nutrients, density etc. between two relatively uniform water masses (Olson *et al.* 1994; Bakun 2006; Belkin *et al.* 2009). Different physical processes results in the formation of distinctive fronts. Most fronts are associated with a surface convergence towards the front, which causes surface water to sink, resulting in the upwelling of cooler nutrient rich subsurface waters to the surface (Owen, 1981; Cromwell and Reid, 1956). This upwelling of nutrient rich subsurface water contributes to elevated primary productivity along the fronts, making them 'hotspots' of marine biodiversity ranging from phytoplankton to apex predators. These areas are well known as egg laying, feeding and nurturing areas for marine fishes and mammals. Therefore, the thermal and chlorophyll fronts enable an extremely favourable environmental condition for all marine living organisms. Fronts occur either as long stripes or as comma shaped curves. Length wise fronts can range from few metres to many kilometres, while vertically fronts extend from few metres to more than a kilometre. Though most fronts are seasonal in nature and appear for a few days, some fronts can be persistent throughout the

year (Belkin, 2002; Mann & Lazier 2013). Generally surface temperature and salinity across fronts shows a discrepancy in the range of 2-5°C and 0.3-1.0 PSU respectively, but this fluctuation can even be up to 10-15°C and 2-3 PSU respectively (Belkin *et al.*, 2009). These physico-chemical properties of water favour the aggregation of fishes and larvae toward the frontal area.

The area of high biomass of fishes is known as Potential Fishery Zones (PFZ). The period 1989-90 has been marked as the starting phase of PFZ forecasting by making use of the available SST and Chl-a satellite images. Earlier studies have reported that the Catch Per Unit Effort (CPUE) is high in the PFZ as compared to its neighbouring areas and it mostly coincides with thermal and chlorophyll fronts (Choudhury *et al.*, 2007, George *et al.*, 2013, Pillai and Nair, 2010, Bhaware *et al.*, 2013). Thus thermal and chlorophyll fronts are linked with high fish biomass. Zainuddin *et al.* (2006) made use of satellite derived SST and ocean color data to analyse the fishing grounds and reported that the high potential fishing grounds corresponds to the frontal zones and anti-cyclonic eddies.

The Arabian Sea is unique when compared to other low latitude seas since it is landlocked at the north by the Asian landmass. This peculiarity of Arabian Sea draws immense continental effect resulting in improved land-sea thermal gradient causing monsoon. Monsoon winds have marked influence on the variability of upwelling patterns in the Arabian Sea. South west monsoon triggers upwelling of nutrients along the west coast of India which then gradually propagate towards north (Muraleedharan & Prasanna Kumar 1996; Madhuprathap *et al.*, 1996). During north east monsoon, the north east trade winds brings cool and dry continental air to the northern Arabian sea, resulting in higher productivity in the region (Madhuprathap *et al.*, 2001). Hence Arabian Sea is considered as one among the most productive marine ecosystems in the world. Arabian Sea enclosed within the extent of 0-30°N latitude and 50-80°E longitude (fig. 1) is selected for the study.

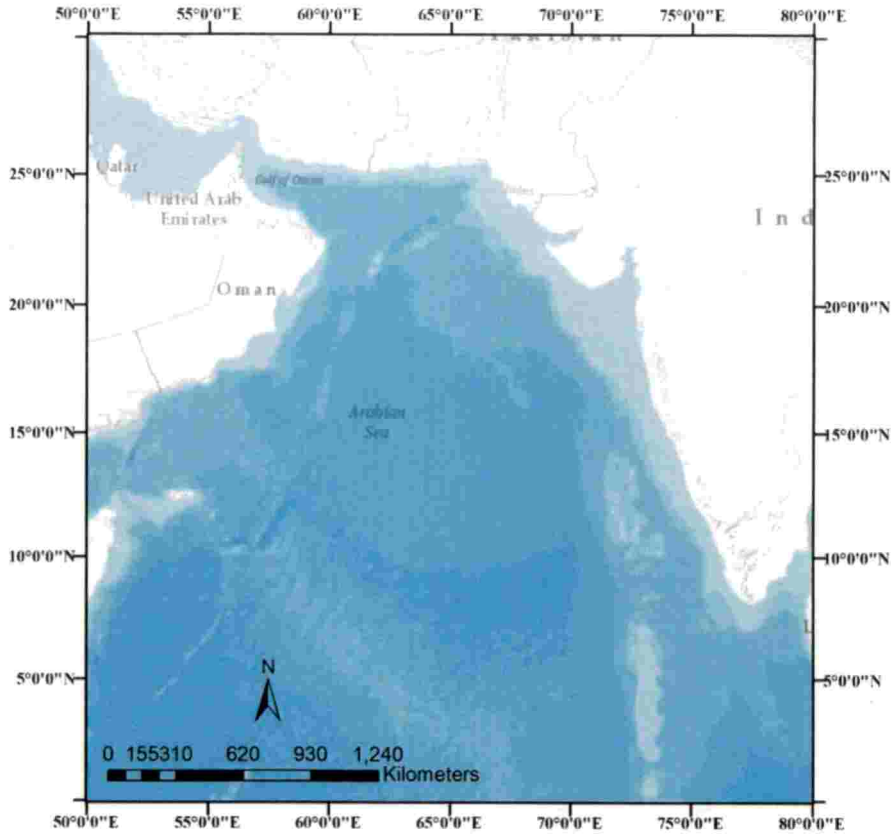


**Figure 1: Study Area - Arabian Sea**

Puthezhath (2014) identified thermal fronts in the Arabian Sea using Cayula-Cornillon Single Image Edge Detection Technique in ArcMap and MODIS Aqua SST data. He found that thermal fronts increase gradually through August-September and an acceleration in the rate of thermal front formation occurs during October-November. A steady decrease in number of thermal fronts during December-January was also reported. However, work was done utilizing monthly data while fronts generally have less life span than a month.

Primary objective in this thesis is to reveal the key factors influencing the inter-annual variability of thermal and chlorophyll fronts and their relation to ocean primary productivity. In the current study, thermal as well as chlorophyll frontal identification is done using SIED technique in ArcGIS, making use of MODIS Aqua SST data and OC-CCI Chl-a data. Temporal resolution of the data

is fixed as 8 day, taking in to consideration the shorter life span of frontal structures (Vipin *et al.*, 2015). This study can also be used to analyse the linkage between frontal and fishery distribution in the area of study.

# REVIEW OF LITERATURE

## CHAPTER 2

### REVIEW OF LITERATURE

#### 2.1 CHARACTERISTICS OF ARABIAN SEA

##### 2.1.1 Upwelling in the Arabian Sea

Arabian Sea has a very productive upwelling system (Banse and English, 2000; Piontkovski *et al.*, 2012). Upwelling refers to the process by which water from deep ocean layers gets advected to the upper ocean layers, very near to the surface of the oceans. This results in shifting of colder nutrient rich subsurface water to the upper oceanic layers (Owen, 1981; Cromwell and Reid, 1956), triggering primary productivity in the ocean. Depending on the location of occurrence, upwelling can be classified into two; open ocean upwelling and coastal upwelling. Open ocean upwelling is induced by currents or winds, which creates divergence zones at the ocean surface due to replacement of surface water mass by water mass from beneath. On the other hand, coastal upwelling is stimulated by along shore winds (Pedlosky, 1978; Rutllant *et al.*, 2004), which results in uplifting of subsurface water. This rise of subsurface water occurs by pushing the surface waters away from the shore as a result of Ekman transport.

Arabian Sea upwelling is of great importance, since it results in advection of huge amounts of cold nutrient rich subsurface water to the surface (Fischer *et al.*, 2002; Wiggert *et al.*, 2002; Montégut *et al.*, 2007). This triggers an enhancement in primary productivity of the ocean, ultimately resulting in enriched ocean biomass and help sustain fishery population. The close relationship of Arabian Sea upwelling with Indian Summer Monsoon makes it a topic of high scientific importance for understanding the effects of climatic variation on upwelling phenomenon of the region (Schott, 1983; Keen *et al.*, 1997; Murtugudde *et al.*, 2007).



During summer monsoon period, since the south westerly winds blow almost parallel to the western Arabian Sea (Findlater, 1969; Brock *et al.*, 1992; Weller *et al.*, 1998), it induces upwelling in the region as a result of offshore Ekman transport. Thus the Arabian Sea upwelling exhibits a strong seasonality in its occurrence. It generally starts by May and winds up by September (Brock *et al.*, 1991). During this period, upwelling lifts water from as deep as 200m at a speed of  $2 \times 10^{-5}$  m/s (Rixen *et al.*, 2000) and can result in cooling of surface waters by 5.5 °C (Weller *et al.*, 2002). A study by Yi (2016) stated that the annual cycle of upwelling velocity exhibited significant positive values starting from May and ending in September with its peak in July.

### **2.1.2 SST – temporal and spatial variability**

Muhammad *et al.* (2016) observed that the maximum SST in the northern Arabian Sea occurs during May and minimum in February. They also reported that 2010 and 2008 had the highest and lowest value of SST respectively in the Arabian Sea. They could not find any long term trend in SST, but were able to draw out some robust seasonal patterns that repeats annually. Their temporal assessment disclosed a four stage warming-cooling variation in SST pattern, during March to May, June to August, September to October and November to February. They suggested the high intensity of solar radiation in May as the reason for the first stage. While transforming to the second stage, an increase in cloud cover and heavy winds during June to August cools down the SST. During September, the low wind speed allows the SST to increase causing warming. The decrease in SST during final stage is caused due to decrease in solar radiation from November to February. While studying the spatial pattern in SST variation, they deduced a four stage variation in SST. They reported that the first stage starts from January where the SST increases and proceeds to the south-east till March. Then the SST increases to south from April till May. The third stage starts from June and the SST increases to north-east till August. In the fourth and final step, SST increases towards south-east till December.

In a study conducted by Vialard *et al.* (2012) they stated that while studying the interaction between SST and active/break monsoon periods, variation in wind patterns within a season is more relevant in case of Arabian Sea when compared to Bay of Bengal.

### **2.1.3 Seasonality in Chl-a concentration**

Bensam (1964) stated that phytoplankton blooms can be identified easily by ocean color in sea water of west coast of India. He observed two seasonal blooms in the west coast of India. First bloom occurs during May-June and it overlaps temporally with the aggregation of pre-spawning adult fishes. The second bloom occurs during September-October, which overlaps temporally with the biomass of juvenile fishes.

A study by Raghavan *et al.* (2006) revealed that the Chl-a concentration in the south western coast of India can reach values up to 5 to 10 mg/m<sup>3</sup> during summer season, whereas the concentration of Chl-a in other seasons ranges from 0.1 to 5 mg/m<sup>3</sup>. Joseph *et al.* (2007) conducted a study in the eastern Arabian Sea, they suggested coastal upwelling as the reason for the increasing Chl-a concentration in the south east Arabian Sea during south-west monsoon. They also reported that the Arabian Sea is acted upon by the effect of improved vertical mixing due to winter cooling in the post monsoon season, resulting in deeper mixed layer depth and a decreased SST. While studying the correlation between Chl-a and SST in the Arabian Sea, they reported that there existed a reverse correlation between SST and Chl-a in the open oceans. Meanwhile it may not be always true for the coastal waters, since availability of nutrients is the major factor that regulates Chl-a concentrations in those areas.

## **2.2 ENHANCED PRIMARY PRODUCTIVITY AT FRONTAL ZONES**

### **2.2.1 Significance of phytoplankton in the oceans**

Photosynthetic phytoplankton forms the base of the ocean food chain accounts for 50 percent of the primary productivity across the globe (Longhurst *et al.*, 1995). It

also adds to the ocean carbon uptake, which is predominantly high at higher latitudes (Longhurst and Harrison, 2001). The distribution of ocean primary productivity is highly heterogeneous. Sometimes it is found as patchy blooms. This results in huge ambiguity in worldwide assessments of ocean primary productivity and uptake of atmospheric carbon by the oceans. Scientists have conducted many studies in this sector (Levy *et al.*, 2001; Mahadevan and Archer, 2000; Mahadevan and Tandon, 2006) and they have reported that occasional blooms are possible in oligotrophic waters, by upwelling of more nutrients into the euphotic zone by the oceanic fronts (Thurman and Trujillo, 1999).

### **2.2.2 Seasonality in phytoplankton production**

A study conducted by Madhupratap *et al.* (2001) reported that the maximum biomass of phytoplankton occurs along the west coast of India during summer monsoon (June–September), due to the influence of Westerlies and Ekman transport, which brings subsurface water to the top resulting in phytoplankton blooms. They also reported that the fraction of total marine fish catch from the western coast of India reaches its maximum during October–December (42%) and January–March (24%), which can be attributed to the effect of winter cooling that results in upwelling and elevated primary productivity, attracting more fishes to the area. They claimed that the intense increase in SST during April–June leads to decreased phytoplankton production. As a result the fishes migrate to other areas in search of food, causing a huge drop in fish catch.

As per the study conducted by Sarma *et al.* (2015) to assess changes in inorganic carbon components in the north western Arabian Sea, they suggested winter convective mixing (Banse and McClain, 1986; Kumar and Prasad, 1996; Madhupratap *et al.*, 1996) as the reason behind increased nutrient availability off Gujarat coast, making it highly productive (Solanki *et al.*, 2003; 2005) during north east monsoon period. During the course of study, they noticed that SST was cooler in the frontal

zones to a magnitude of 0.56-1.02°C. They also observed a similar trend in salinity, where it decreased to an extent of 0.03-0.13 PSU within fronts. Despite of this decreasing trend, they were able to identify a noteworthy increasing trend of Chl-a within fronts by 0.05-0.6 mg/m<sup>3</sup>. Sharma *et al.* (2015) suggested that the elevated plankton biomass was the result of enhanced nutrient supply that followed an increased vertical mixing in that area. Nair (1959) and Bakun *et al.* (2015) reported that fishes migrate towards the coastal areas for feeding and egg laying during the monsoon period and to the deeper waters during the post monsoon period, and the stimulus to such activity is the lowered temperature or salinity which can be attributed to possible upwelling during these periods. This migration is for the sole purpose of consuming the robust growth of phytoplankton that occurs during the starting of monsoon (Chidambaram, 1950; Hornell, 1910; Hornell and Nayudu, 1924; Nair, 1953).

### **2.2.3 High latitude phytoplankton blooms**

Recent studies have shown that despite of unfavorable conditions such as destabilizing winds and intense surface cooling, phytoplankton blooms can occur in high latitudes during winter season by re-grading of the surface waters through frontal variabilities. The problem with high latitudes are the deep surface boundary layer which takes the phytoplankton below the euphotic zone and reduced sunlight availability which inhibits primary productivity. But, as the depth of the surface boundary layer is reduced due to the frontal restratification, sunlight becomes available to the phytoplankton, which ultimately results in phytoplankton blooms in the higher latitudes (Taylor and Ferrari, 2011).

## **2.3 ENHANCED FISH CATCH NEAR FRONTS**

Chavez and Messie (2009) quoted that in the open oceans, there are regions with key changes in water mass, depth, ocean currents and upwelling areas which also have enriched productivity and are regions of higher biodiversity. Olson *et al.* (1994) reported that formation of mesoscale structures in the ocean can cause enriched

productivity and forage as a result of complex physical processes. A study conducted by Houk *et al.* (2007) reported that in the coastal waters near NW Hawaiian islands, 71 percent and 65 percent variance of Chl-a concentration in the Transition Zone Chlorophyll Front (TZCF) could be explained by average monthly SST and meridional Ekman transport measurements respectively. An increase in the Ekman transport and a decrease in the monthly average SST values would lead to elevated phytoplankton densities.

### **2.3.1 Frontal zones and fish abundance**

Royer *et al.* (2004) stated that chlorophyll front formation generally takes place as a result of surface convergence, resulting in the accretion of phytoplankton and other macro organisms which are the preferred food for tunas. They also observed that the accumulation of tuna is more frequently found near chlorophyll fronts and less frequently near thermal fronts. Klemas (2013), reported that blue fin tunas were found to be closely associated with the frontal regions that separated productive greenish waters from less productive blueish waters, which also had a temperature gradient between them.

Platt *et al.* (2009) devised energy conservation strategies in the marine ecosystem using the satellite derived time series data on phytoplankton which plays an important role to build numerous bio-indicators for the pelagic system.

### **2.3.2 Environmental proxies and fish abundance**

Zainuddin and Saitoh (2004) conducted a study in the north-western of north pacific, where the cold Oyashio current and warm Kuroshio Current meets, leading to the formation of a transition zone which is highly productive. They used 20°C SST and 0.3 mg/m<sup>3</sup> Chl-a as proxies to identify potential fishing grounds of albacore tuna and reported that the most potential fishing grounds occurred during winter season, especially during November since the frontal structure were well developed during the period. They observed that as the distance between the 20°C isotherm and 0.3 mg/m<sup>3</sup>

isopleth decreases, the CPUE increases due to well-developed SST and Chl-a fronts. When the distance between them increases, frontal formation spreads over greater spatial extent. This leads to poor development of fronts and thus shift in mean point of abundance of albacore. They suggests that productive tuna fishing ground evolves where there is a close proximity of chlorophyll front near a warm habitat and points out that by tracking the shift in the corresponding proxies, good fishing grounds of albacore can be identified.

In another study by Zainuddin (2011) conducted at Bone Bay, he stated that as per the satellite imageries CPUE was highest where the 30.5°C SST isotherm and 0.3mg/m<sup>3</sup> Chl-a meet. They used these two values as proxies for identifying tuna aggregations and they reported that skipjack tuna aggregates in area where there is suitable environmental conditions. Catch of skipjack tuna was high during January–June, and the favorable SST and Chl-a *in situ* values in the study area were same as the outputs of the study conducted by Zainuddin and Jamal (2009). The study suggests that the union of these two proxies creates fronts that are favorable for skipjack tuna aggregation. The study also indicates that the catch data from these frontal areas are relatively higher as compared to other areas. The outputs from the study indicates that the potential fishing grounds of skipjack is in parallel with the observed thermal and chlorophyll frontal areas from satellite images.

Rana *et al.* (2014) concluded that the open ocean upwelling during tropical cyclones can result in presence of cold surface waters as compared to the higher SST near the coastal waters. Fiedler and Bernard (1986) while conducting a study to analyze the feeding pattern of tuna stated that, skipjack tuna aggregation was found near cool and productive frontal zones, where the prey was abundant. During summer upwelling, an abundance of prey of albacore tuna is found in the southern California current. Fiedler and Bernard (1987) reported that albacore tuna migrates seasonally through the pacific to make the most of this prey abundance. They also reported migrations of

skipjack tuna, as a response to El Niño that causes unusual warmer surface temperatures in the southern California Bight ecosystem.

### 2.3.3 Frontal zones and animals

Many studies in the related sectors have shown that not only fishes but also sea birds have close correlation with frontal occurrence caused due to climate forcing. A robust relationship exists between sea birds and infant sea turtles with the frontal structures and eddies in the Gulf Stream and Kuroshio Current (Haney 1986; Witherington 2002; Thorne and Read, 2013; Polovina *et al.*, 2006). It was reported that surface and near surface foraging seabirds are closely associated with convergent fronts (Durazo *et al.*, 1998; Hunt *et al.*, 1999), while sub surface foragers showed an intimate relation to vertically formed frontal structures (Decker and Hunt, 1996; Begg and Reid, 1997)

Downwelling shelf slopes near Mid-Atlantic Bight (Ryan *et al.*, 1999) and near the edges of Bering Sea (Springer *et al.*, 1996) are reported as significant foraging spots of sea birds. It was reported that large number of fronts are formed as a result of interaction of North Atlantic Current with Mid-Atlantic Ridge (Miller *et al.*, 2013) and it draws surface and near surface foraging sea birds (Egevang *et al.*, 2010; Frederiksen *et al.*, 2012; Edwards *et al.*, 2013).

Nur *et al.* (2011) and Sabarros *et al.*, (2013) stated that high concentration of primary production along fronts formed due to upwelling in the oceans, attracts fish species from distinct foraging groups. In the California Current, there is a strong connection among marine carnivores mammals (Tynan *et al.*, 2005), sea birds (Ainley *et al.*, 2009) and the upwelling induced fronts. A study by Scott *et al.*, (2010) revealed that tidal fronts have potential for producing high chl-a concentration below the surface, attracting many diving predators. Along shelf-edge fronts, accretion of surface feeding and diving sea birds were also observed by Skov and Durinck (1998).

## 2.4 FRONTAL REGIONS AND POTENTIAL FISHERY ZONES

### 2.4.1 Increased fish catch in the PFZ

In a study conducted by George *et al.* (2013) for validating Potential Fishing Zone (PFZ) Forecasts in the Andaman and Nicobar Islands (ANI), they stated even if ANI have an annual fishery potential of 1.48 lakh tonnes (Roy and George, 2010), only 22 percent of its potential is currently being harvested. They registered a substantial increase in the total fish catch and individual catch of most species (example: *Sphyraena sp.*, *Katsuwonus pelamis*, *Euthynnus affinis* and *Scomberomorous sp.*) within the PFZ. They suggested that since the phytoplankton productivity is directly associated with pelagic fishes in the open oceans (Ware and Thomson, 2005), the formation of mesoscale structures such as fronts, eddies and upwelling is the reason behind the accumulation fishes (Nayak *et al.*, 2003; Solanki *et al.*, 2001; 2003 and 2005) within the PFZ. Even though the properties of trawlers like the engine capacity and speed were not suitable for catching tuna species, the trawlers registered a high catch of tuna from the PFZ which revealed that the PFZ that are associated with high Chl-a concentration attracts not only pelagic fishes but also the predatory carnivores. They also examined the gut of several fishes caught from the PFZ and observed that in case of sardines, 92% percent of the fishes had full stomach contents consisting of completely digested greenish mass as the chief food item which is an indicator of enhanced primary production in the PFZ, while from the non PFZ areas, only 46 percent displayed similar gut conditions.

### 2.4.2 Integrated Potential Fishing Zones (IPFZ) forecast

In a similar study conducted by George *et al.* (2011) in the Andaman and Nicobar Islands the Integrated Potential Fishing Zones Forecast helped the fishermen to utilize their under-utilized fishery resources. There was an urgent need to change the focus of fishing to the unexploited resource rich waters since most of the current fishing activity is relatively low productive (as compared to PFZ) waters (Nayak *et al.*, 2003).



In Andaman and Nicobar Islands, the IPFZ Forecast was found to reduce the fishing effort, fuel and operational costs, but still giving higher yields. This supports the existing evidence that satellite advisory based fishing provides better yields.

### **2.4.3 Chlorophyll variation in PFZ and its effect on fisheries**

George *et al.* (2012) conducted a study in the west coast of India to analyze the variations in sardine catch with respect to the presence of Chl-a on a synoptic scale. For this study they used monthly average of surface Chl-a as recorded by the SeaWiFS (Sea-viewing Wide Field-of-view Sensor) ocean color data. They stated that the major cause for the migration of sardines is the intensity and frequency of upwelling events and its effects on the coastal waters. They could also observe a lag phase between initiation of upwelling and high productivity (Kumar *et al.*, 2008; Jayaram *et al.*, 2010). Hence they concluded that Chl-a concentration is the predominant factor that attracts fishes. In this study, they observed that the peak periods of Chl-a concentration (May-October) overlapped with the active reproductive stage of sardines. This substantiates the existing finding that the fish times itself to make the most out of the high phytoplankton production during the south west monsoon (Madhupratap *et al.*, 1994). Earlier studies in the related sector clearly depicts the migrations of spawning and juvenile fishes towards coast and to deeper waters in response to availability of food (Raja, 1972; Longhurst and Wooster, 1990). George *et al.* (2012) concluded that the average Chl-a concentrations during 1998-2006 during the bloom initiation months overlapped with the sardine catches. The study indicated that Chl-a defined 39 percent of the inter-annual variability of sardine landings, implying that the Chl-a concentration can be used as a proxy to predict fish landings from the specified area.

### **2.4.4 Modelling of PFZ**

Tijani *et al.* (2015) conducted a study to create a model that would detect PFZ resulting in increased catch per unit effort (CPUE). Their study was based on mapping of SST and Chl-a concentration as given by the satellite imagery, and also on secondary

data and *in situ* measurements for authentication of the model. They used a normalized scalar product of Chl-a and SST for identifying anti-parallel alignment of high valued gradients of SST and Chl-a. By assessing the output, they reported that vessels operated near the frontal zones caught more fish than other regions. This output also had good correlation with the *in situ* data.

## 2.5 FRONTAL ZONES AS POTENTIAL CONSERVATION SITES

### 2.5.1 Threats due to overfishing

In a study conducted by Scales *et al.* (2014), they stated that most of the marine mammals are known to be well correlated with the frontal zones, which makes the frontal zones most worthy candidate sites for protection. They described frontal zones as hotspots of intersection between favorable habitat for marine species and areas of undoubted intervention of humans through activities such as fisheries (Halpern *et al.*, 2008). Even if ample data is not available, it is clear that tenacious fronts are the major aim of commercial fisheries, especially pelagic long-line fisheries (Podesta *et al.*, 1993; Hartog *et al.*, 2011). This offers huge pressure and competition for the apex predators, which can result in an ecological imbalance leading to major ecological problems. Halpern *et al.* (2008) and Lewison *et al.* (2014) stated that this overlapping of favorable habitat and areas of increased human intervention is particularly high near the coastal areas. So, these areas are to be given prime importance while considering conservation of marine habitats.

### 2.5.2 Threats due to accumulation of contaminants

Apart from the risks associated with increased fishing activity in the frontal zones, convergent zones amplifies the threat by causing the accumulation of contaminants such as oil and plastic near the frontal area (Bourne and Clark, 1984; Carman *et al.*, 2014). Miller and Christodoulo (2014) stated that the Marine Renewable Energy Machineries are concentrated near tidal mixing fronts and have possible

adverse effects on marine vertebrates (Inger *et al.*, 2009; Grecian *et al.*, 2010; Scott *et al.*, 2014).

With the evolution of computers and satellites, tracking of frontal zones have been automated and can be done with ease. Howell *et al.* (2008) have reported an effective decline in loggerhead turtle bycatch along the Tropical Zone Convergence Front north of Hawaii, by utilizing coupled real time SST-satellite SST and fisheries data. Thus, the improved coupling between satellite remote sensing, fisheries management and oceanographic features have endless possibilities to be used as measures in marine biodiversity conservation practices.

## 2.6 EXTREME EVENTS: IMPACTS ON FISHERIES AND MARINE ENVIRONMENT

### 2.6.1 El Niño and fisheries

Niquen and Bouchon (2004) stated that El Niño events can cause very strong SST anomalies, even up to 8°C above mean temperatures. They also observed significant changes in distribution, size, reproductive process and landings of fishes in response to the temperature anomaly. They observed that the distribution of anchovy which is an inhabitant of Peruvian coast, changed their distribution to patchy and irregular rather than being uniformly spread over the entire Peruvian coast. Similarly, the shoal of sardines shifted from Paita (normal condition) toward Pimentel and Chicama. They also stated that, during less intense El Niño years (2000) anchovy were distributed over the entire Peruvian coast compared to high intense El Niño period (1997-1998), where anchovy concentrated mostly to south of 13°S. This confirmed that fish migrations are linked to the intensity of extreme events such as El Niño. Niquen and Bouchon (2004) also observed that El Niño had effects on size of fishes. During 1972-73, 1982-83, 1997-98 El Niño adult anchovy were more in numbers and juveniles were more or less absent. They also stated that El Niño had effects on reproductive processes of fishes. During 1997-98 El Niño, reproductive cycle of anchovy was

disturbed and caused huge loss in fish stocks (Perea *et al.*, 1998). But in case of sardines and pacific mackerels, the same El Niño resulted in an increase in intensity of spawning and increase in stocks of the species. These observations suggests that El Niño have specific impacts on each species of marine ecosystem. They could also observe the impact of El Niño on the relative dominance of biomass in an area. During 1971-73, the beginning of El Niño marked the predominance of anchovy. But at end of the El Niño event, the species that dominated the most were sardines, jack mackerel and mackerel. El Niño had an effect of converting single-species landings to multi-species landings in the Peruvian coast, where there is a reduced fraction of anchovy and an increased fraction of other pelagic fishes.

### **2.6.2 El Niño and productivity change**

Behrenfeld *et al.* (2001) used SeaWiFS data to compare concurrent ocean and land Net Primary Production (NPP) in response to a major El Niño La Niña transition which occurred between September 1997 and August 2000. During this period, biospheric NPP fluctuated by 6 pentagrams of carbon per year. Impacts of ENSO on upwelling and availability of nutrients were more in the tropical regions and hence oceanic NPP is also more prominent here.

### **2.6.3 ENSO and fisheries**

Western equatorial warm pool has the warmest surface waters of the world's oceans and hence corresponds to very low productivity rates. But recent studies shows that the tuna catches in this region are close to one million tonnes and are sustainable. Lehodey *et al.* (1997) reported that this spatial shift in tuna population is related to the large zonal displacement of warm pool, which is fundamental to ENSO

A study conducted by Zainuddin *et al.* (2004) stated that the proxies for identifying skipjack tuna ( $29^{\circ}\text{C}$  SST and  $0.3 \text{ mg/m}^3$  Chl-a) in the western pacific is strongly correlated to ENSO events. During 1999 La Niña, there was a very high catch of skipjack tuna near  $30^{\circ}\text{N}$  and  $35^{\circ}\text{N}$  and from  $60^{\circ}\text{E}$ - $75^{\circ}\text{E}$ . In this region, the proxy

indicators were also very close to each other. During La Niña period, the proxy indicators were far away from each other and hence the potential fishing grounds were very poorly developed. They claimed that the remarkable weakening of southward intrusion of the Oyashio current during El Niño event, resulted exceptionally low Chl-a content (Sugimoto *et al.*, 2001). Kumar *et al.* (2014) stated that the maximum tuna landings were recorded during 2004 and 2006, which were weak El Niño periods. Kumar *et al.* (2014) also stated that the three vital environmental variables that affect the tuna abundance and distribution in the Indian Ocean are sea surface temperature, sea level pressure and wind actions. They concluded that SST can be judged as the best habitat predictor in the Indian Ocean, since it described highest deviation in generalized additive models.

#### **2.6.4 Tropical cyclone and fisheries**

In a study conducted by Subrahmanyam *et al.* (2002) to explore the impacts of tropical cyclone on Chl-a concentration in the Arabian Sea, they reported that the passage of tropical cyclone had a severe impact on the Chl-a concentration. Before occurrence of the cyclone, the Chl-a values ranged from 0.1-0.4 mg/m<sup>3</sup>, which is in harmony with the low levels of Chl-a during May owing to the nutrient depletion due to intense heating (Bhattathiri *et al.*, 1996; Prasannakumar *et al.*, 2000). After the cyclone passage, the Chl-a concentration in the area got enhanced to >5-8 mg/m<sup>3</sup> and it appeared as blooms. They suggested forced increase in mixed layer depth as a result of severe winds, and an increase in upwelling frequency due to cyclone driven divergent currents as the reasons for the enhanced Chl-a concentration. This period also marked a steep decrease in the SST values ranging from 22.5°C to 27.5°C which is much low compared to normal SST during the period (29.3-30.2°C) in the eastern Arabian Sea (Levitus and Boyer, 1994) as recorded by AVHRR.

According to Lin *et al.* (2003), tropical cyclones have substantial impacts on the SST and Chl-a content of the South China Sea (SCS). They reported that the tropical

cyclone Kai-Tak, triggered a 30 fold increase in Chl-a content and reduction in SST by almost 9°C in the SCS which resulted in an Integrated Primary Production of 2800 mg/cm<sup>2</sup>/d compared to 300 mg/cm<sup>2</sup>/d before the typhoon occurrence.

## 2.7 SATELLITE REMOTE SENSING (SRS) AND OCEANOGRAPHY

SRS has turned out to be a strategic tool in marine ecology studies, providing wider opportunities for monitoring the environment and aiding in assessing the impacts on environment, proving itself as a handy tool when it comes to conservation issues. (Turner *et al.*, 2003; Mumby *et al.*, 2004).

### 2.7.1 Basic Concepts

In SRS studies, a sensor is defined as an electronic device which senses emitted/reflected electromagnetic (EM) radiation, converts to a value, which is then stored and dealt with. Based on the energy source, sensors can be classified as active and passive sensors. Active sensors sends out a signal, and detects after reflecting from the object. This kind of sensor needs an external source for generating signals. Passive sensors do not need an external source, but it simply receives signals that are irradiated by other objects (Butler *et al.*, 1988). Based on spectral regions of solar radiation, sensors can be classified as visible/reflective infrared, thermal infrared and microwave (Martin, 2004)

Another fundamental classification of SRS sensors are based on temporal, spatial and spectral resolutions. Spatial resolution of a sensor is defined as the measure of the smallest area on the Earth, of which independent measurement can be made by the sensor. Temporal resolution refers to the time required for the satellite to revisit a point on the Earth's surface and gather data. The ability of the sensor to sort out the detected energy and characterize it into different constituents on Earth is termed as spectral resolution (Gibson, 2000).

### **2.7.2 Data Processing Levels**

As the processing of data proceeds, level of data also varies starting from level 0, containing only raw data as collected by satellite which includes orbital information, different calibration coefficients and so on. Level 1 data is almost the same as the earlier except that they are rearranged by channels from raw data to geophysical units. Level 2 data is prepared by including satellite corrections and geo-referencing the data. This is the first level of exploitable data for the scientific community. Level 3 data is the most extensively used and enclosing most number of parameters plotted with appropriate projection system, and averaged temporally and spatially (Chassot *et al.*, 2011).

### **2.7.3 Remote Sensing of Oceanic Data and Mesoscale Structures**

The main atmospheric window which is used to measure SST by satellite sensors are 3.7 micrometer in the mid-infrared and 11-12 micrometer in the far-infrared regions of solar spectrum. Chassot *et al.* (2011) stated that while measuring SST, high frequency of geostationary satellites (METEOSAT) results in better cloud free images, while Tropical Rainfall Measuring Mission Microwave Imager (TMI) is completely unaffected by cloud cover and hence provides completely cloud free data, but at the cost of thin swath, lack of data near coastal waters and coarser resolution (25 km). They also concluded that merging SST data products from various satellites will result in good cloud free images, but the merging procedure will make the data unfit for identifying mesoscale oceanic features such as fronts and eddies.

Over the years, scientists and researchers are more centered on studies relating to thermal fronts than chlorophyll fronts (Miller, 2004; Royer *et al.*, 2004). Belkin and O'Reilly (2009) stated that chlorophyll fronts results from complex interactions between physical, chemical and biological factors and turns out with complex spatial patterns and features making it more difficult to identify than thermal fronts. Though

the above constraints exist, the same edge detection technique used for identifying SST fronts can be applied in case of chlorophyll also.

Tew Kai and Marsac (2010) stated that remotely sensed sea surface height data can provide valuable information regarding sea surface height anomaly and geostrophic currents, aiding in the identification of cyclonic and anticyclonic eddies. Miller (2004) reported that biophysical processes in an ecosystem can be clearly understood by overlaying thermal and chlorophyll fronts in a single map.

#### **2.7.4 SRS and Modelling studies**

In the context of ecosystem modelling combining data from SRS and *in situ* observations has proved to be an effective source of input for the scientific community (Chassot *et al.*, 2011). Fine resolution daily and global datasets of variables obtained by SRS proves to be highly reliable and beneficial when it comes to integrating habitat factor to changing fish population studies. (Polovina and Howell, 2005; Dulvy *et al.*, 2009).

Kurien *et al.* (2010) stated that the possible mechanisms behind the mesoscale structure formation and the higher productivity that accompanies the phenomena can be better understood by incorporating the remotely sensed mesoscale formations to the three dimensional ocean circulation models.

### **2.8 IDENTIFYING FRONTS USING GIS**

Satellite data is a boon for oceanographers as they supply voluminous time series data regarding the physical and biological processes taking place in the open oceans. One of the most time consuming and cumbersome processes in manual satellite data processing is the identification of edges of mesoscale oceanic features such as frontal zones, which have been completely computerized with the evolution of high end computers (Prat *et al.*, 1991; Podesta *et al.*, 1993).



### 2.8.1 Different algorithms for edge detection

Hoyer and Peckinpaugh (1989) developed an algorithm for automated edge detection of oceanic features from satellite images, based on gray level co-occurrence matrix (GLC) used in image texture studies. This cluster shade texture measure, obtained from the previously mentioned GLC matrix proved to be highly effective in identifying mesoscale oceanic features, since it retained the sharpness of edges of the oceanic features.

Another edge – detection algorithm was developed by Cayula and Cornillon (1991), which is completely automated, widely used, and most accurate among other edge detection algorithms for SST. It is based on relative strength of the features in satellite data rather than on its absolute strength, making the algorithm independent of the scale of the feature. It also help to rule out the problems associated with cloudiness in satellite images, which other algorithms would detect as frontal zones. Cayula and Cornillon (1991) further developed Single-Image Edge Detection (SIED) as well as a Multi-Image Edge Detection (MIED) techniques. SIED identifies frontal regions, when there is a temperature gradient of at least  $0.4^{\circ}\text{C}$  between adjoining water masses. They also reported that the reliability of the identified frontal zones using both SIED and MIED techniques are as close to that analyzed by a human expert, by comparing the obtained results with data from 98 different satellites and *in situ* data. The SIED technique has some handful of success stories when it was practically put to use in many different regions (Kahru *et al.*, 1995; Ullman and Cornillon, 2001; Hickox *et al.*, 2000; Podesta *et al.*, 1993). MIED technique is simply the SIED applied to a series of satellite images. As the next step, the coordinates of those frontal zones which are continuing in the first image analyzed using SIED and in the subsequent image, are delivered to SIED algorithm so that the continuing fronts in the succeeding images can be recognized (Cayula and Cornillon, 1994)

### **2.8.2 Marine Geospatial Ecology Tools: Framework for ecological geoprocessing in ArcGIS**

Marine Geospatial Ecology Tools (MGET) are an assembly of prefabricated software tools that is of immense use to the analysts having expertise in GIS. By incorporating it with Arc GIS, scientists and analysts are able to carry out scientific analysis without the need of writing cumbersome codes. MGET comprised of more than 180 tools under seven categories. Among this, Oceanographic Analysis tools can be used for locating frontal zones by allowing the user to apply logical algorithms on oceanographic data sets. It also provides assistance in numerous modelling and research oriented works. MGET's Cayula-Cornillon fronts tool make use of the Cayula-Cornillon SIED algorithm for identifying frontal zones in the open oceans. Connectivity with in ocean ecosystems can be analyzed using MGET's Connectivity tools. One such work (Trembl *et al.*, 2008) is the study of distribution of coral larvae away from reefs due to ocean currents, with the help of Eulerian advection-diffusion algorithm (Roberts *et al.*, 2010).

# MATERIALS AND METHODS

## CHAPTER 3

### MATERIALS AND METHODS

#### 3.1 DATA USED

##### 3.1.1 Sea surface temperature (SST)

Sea Surface Temperature of the global ocean were downloaded from the NASA Ocean Color (<https://oceancolor.gsfc.nasa.gov/>). The website is maintained by Ocean Biology Processing Group (OBPG) of NASA's Goddard Space Flight Center, USA. They deal with data collection, handling, correction, validation and dissemination of numerous ocean related products like SST, Sea Surface Salinity (SSS) and so on since 1996. The data for the study is monthly climatology as well as 8 day composites of SST ( $^{\circ}\text{C}$ ) (fig. 2), downloaded from Aqua-MODIS (Moderate Resolution Imaging Spectroradiometer) satellite sensor of 4 km \* 4 km spatial resolution for the time period 2002-2016 as NetCDF (NC) files. These 8 day composite data were used to identify frontal zones using ArcGIS software.

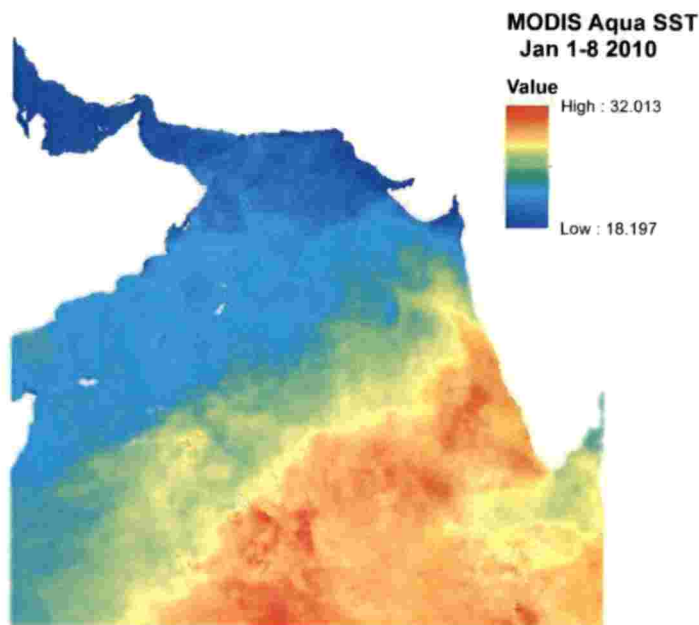


**Figure 2: SST for the period Jan 1-8 2010**

### 3.1.2 Chlorophyll - a concentration (Chl-a)

The data regarding concentration of Chl-a in the surface waters was downloaded from Ocean Color Climate Change Initiative (OC-CCI) website ([www.oceancolour.org](http://www.oceancolour.org)). The downloaded data was in the form of NC files containing monthly climatology as well as 8 day composites of Chl-a ( $\text{mg}/\text{m}^3$ ) (fig. 3) with a spatial resolution of  $4 \text{ km} * 4 \text{ km}$  for the period 2000-2013. OC-CCI is a multi-sensor satellite data platform that develops and validates algorithms, and produces possibly the most comprehensive, stable and reliable time series global satellite data products from multi-sensor data records since 1998. The various satellites that are used for generating OC-CCI datasets include MERIS (Medium Resolution Imaging Spectrometer), Aqua-MODIS, VIIRS (Visible Infrared Imaging Radiometer Suite), and SeaWiFS. The downloaded global Chl-a data was used to identify frontal zones with the aid of ArcGIS.

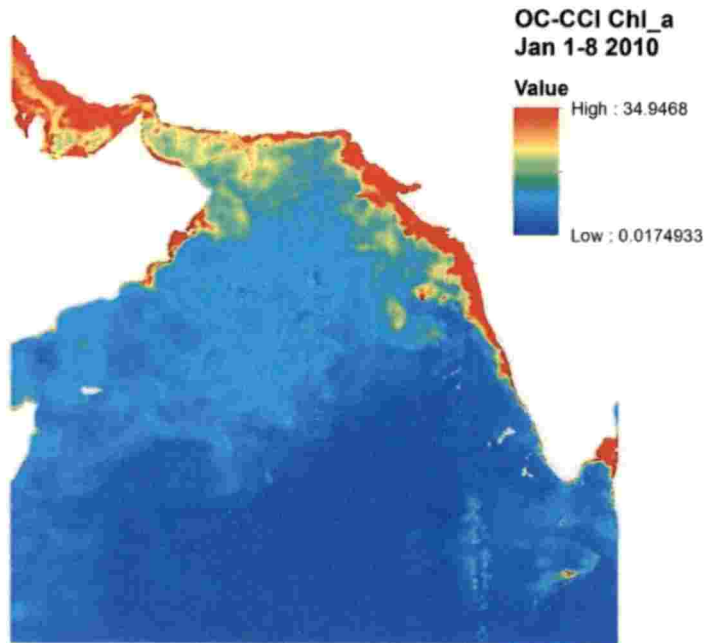


Figure 3: Chl-a for the period Jan 1-8 2010

### 3.1.3 Fishery data

Fishery data includes the quantity of fish that has been landed in various landing centers in the vicinity of the study area from various fishing gears as well as the effort data of the crafts. The various fishing gears are mechanized bag net (MBN), mechanized dol net (MDN), multi day trawl net (MDTN), mechanized gillnet (MGN), mechanized hooks and lines (MHL), mechanized other gears (MOTHS), mechanized purse seine (MPS), mechanized ring seine (MRS), mechanized trawl net (MTN), non-motorized (NM), outboard bag net (OBBN), outboard boat seine (OBBS), outboard dol net (OBDOL), outboard gillnet (OBGN), outboard hooks and lines (OBHL), outboard other gears (OBOTHS), outboard purse seine (OBPS), outboard ring seine (OBRS), outboard shore seine (OBSS) and outboard trawl net (OBTN). Effort data for each fishing craft is available in actual fishing hours as well as in unit operation. Such precious information on fish catch and effort was provided by Central Marine Fisheries Research Institute (CMFRI), Kochi. CMFRI estimates marine fish landings and provide reliable data regarding annual national and state level fish landings since 1950 and 1961 respectively. The landing centers considered for the study belongs to the maritime states and union territories of the west coast of India namely, Kerala, Karnataka, Goa, Maharashtra, Gujarat and Daman and Diu. Monthly marine fish catch for the period 2007 – 2016 was used for the study.

### 3.1.4 Wind data

The daily wind data used for the study is the ERA Interim data, available from ECMWF (European Centre for Medium Range Weather Forecasts) website (<http://apps.ecmwf.int>). ERA stands for European Reanalysis and it represents a series of ongoing research projects at ECMWF that generates various datasets. ERA interim make use of a numerical weather prediction (NWP) system and provides the global reanalysis of data from 1979 to present. The data with a spatial resolution of 0.125 degree\*0.125 degree for the period 2000 to 2016 was downloaded to

understand wind distribution over the study area. ERA consists of various parameters average over various time intervals and can be downloaded in a variety of data types.

### **3.1.5 Current data**

Ocean current information from Global Ocean Data Assimilation System (GODAS) was extracted from the Asia-Pacific Data-Research Center website (<http://apdrc.soest.hawaii.edu/>). GODAS was developed by National Environmental Prediction Center (NCEP) for the purpose of providing the global Climate Forecast System (CFS) with initial oceanographic conditions. GODAS has been providing the scientific community with reliable reanalysis of data from 1979 to present. In this work, five day composite information on ocean current with spatial resolution of 1 degree \*1 degree extending from 2000 to 2016 was utilized.

### **3.1.6 Sea surface height anomaly (SSHA)**

SSHA data of 7-day temporal resolution and 0.25 degree \* 0.25 degrees spatial resolution for the period 2000-2013 was extracted from AVISO (Archiving, Validation and Interpretation of Satellite Oceanographic data). AVISO program has been providing the scientific community with reliable and continuous satellite altimetry data since 1992. AVISO combines datasets from multiple present and past altimetry missions. Currently it makes use of the satellite data from Jason-1, TOPEX/Poseidon, The European Remote Sensing (ERS) Satellites 1 and 2, and GEOSAT Follow-On (GFO) to provide reliable SSHA data.

## **3.2 SOFTWARE USED**

### **3.2.1 ArcGIS**

ArcGIS is one among the major components in the ESRI's ArcGIS software platform for processing of the geographic data. It represents geographic data as an assemblage of various layers and corresponding map components. ArcGIS supports an infrastructure that enables users for recording and analyzing geospatial data,

creating and exploring custom made maps, symbolize features, maintaining database of geographic information and so on. ArcGIS can handle shapefiles, NetCDF files and many other file formats which allows for easy storage and analysis of voluminous data from various sources for scientific studies. Tools such as Multi-Dimensional Tools, Marine Geospatial Ecology Tools, Conversion Tools, Data Management Tools are used in this work.

### **3.2.2 Marine geospatial ecology tools (MGET)**

MGET is a python based open source toolbox for ArcGIS that assists in geoprocessing tasks, developed and updated by Marine Geospatial Ecology Lab, Duke University, USA. It consists of more than 300 prefabricated tools assigned for a wide range of purposes. It helps marine researchers and GIS specialists to do a wide range geoprocessing tasks ranging from gaining access to various oceanographic datasets, identification of mesoscale oceanographic features to building species distribution models, modelling habitat connectivity in an aquatic ecosystem and so on.

### **3.2.3 QGIS**

QGIS or Quantum GIS is an open source geographic information system software which allows users to view, analyze and make necessary changes in geographic as well as spatial data. QGIS is widely used for simpler tasks such as georeferencing an image, creating and editing custom maps, marking features on a map, etc. Scientists and researchers also use QGIS for complex tasks such as planning habitat management strategies, modelling ecological corridors for animals, mapping biodiversity hotspots, water resource management, urban planning and so on. QGIS supports vector layers, raster layers, shapefiles, personal geodatabases, dxf, MapInfo, PostGIS and other formats



### **3.2.4 Ferret**

Ferret is a Linux based interactive computer software that aids users in visualizing and analyzing various gridded datasets, which could be of single dimension or multi-dimensional. Ferret is of immense use for researchers in the field of meteorology and oceanography since it could produce high quality output images for publication purposes using simple logical commands. Ferret is capable of generating line plots, scatter plots, line contours, filled contours, raster output, vector output, polygons and 3D wire frames. Calculations embedded in this software were utilized to average data from daily time scale to 8-day composites.

### 3.3 METHODOLOGY

#### 3.3.1 Methodology for detecting fronts in ArcGIS

Initially the SST/Chl-a image was opened in ArcGIS using ‘Multidimension Tools’. Further processing of the data was done using MGET, which consists of the SIED technique for identifying frontal features. The SIED technique utilized Cayula-Cornillon algebra for carrying out this task. Cayula-Cornillon algebra performs a set of statistical tests on the data within a 30\*30 pixel window with a stride of 16 pixels. It runs a histogram algorithm and identifies those windows which has a bimodal distribution of values representing two different populations and identifies the value of the variable (SST/Chl-a) that separates the two populations. Further this value is used to classify the pixels into two different populations and applies a spatial cohesion algorithm to confirm that these different populations are spatially distinct. If any window contains such distinct populations, then it marks any pixels in any of the population that is adjacent to pixels in the other population. These pixels separate the two populations and are in the direction of the front. After identifying all the along-front pixels, a contour-following algorithm is executed. This algorithm joins all these pixels based on the SST/Chl-a gradient in the direction of the front. This results in the identification of the SST/Chl-a fronts.

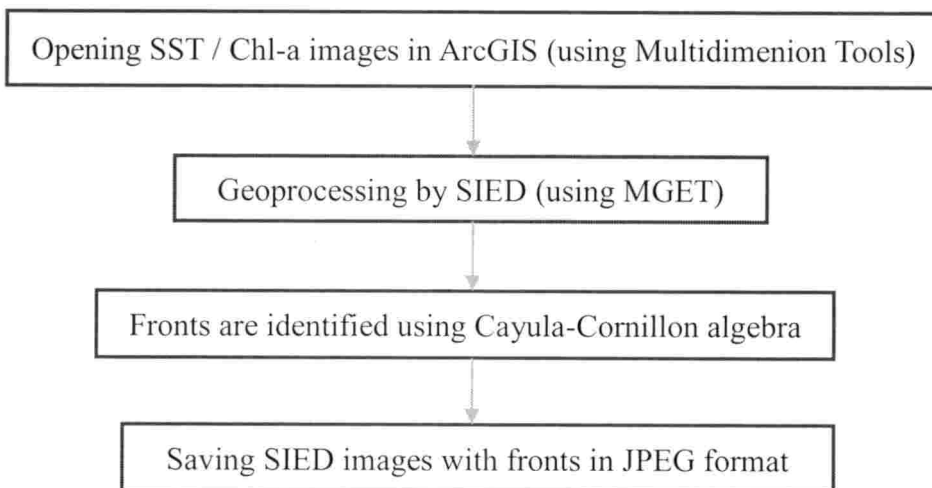


**Figure 4: Front detection using ArcGIS**

### 3.3.2 Methodology for computing area of frontal zones in ArcGIS

The output from the Cayula-Cornillon algebra is a raster layer containing the frontal zones, which is in the WGS-1984 Geographic Coordinate System. But for calculating area, this layer needs to be re-projected to a new Projected Coordinate System. For this purpose, each raster layer was converted to vector using 'Conversion Tool' in ArcGIS. Then appropriate projection was selected from the 'Projections and Transformation' option under 'Data Management Tools'. I have used 'Asia South Albers Equal Area Conic' projection as it is the appropriate one for the study area. This applies a new projection to the vector layer. To the newly projected layer frontal area was calculated using 'Calculate Geometry' option.

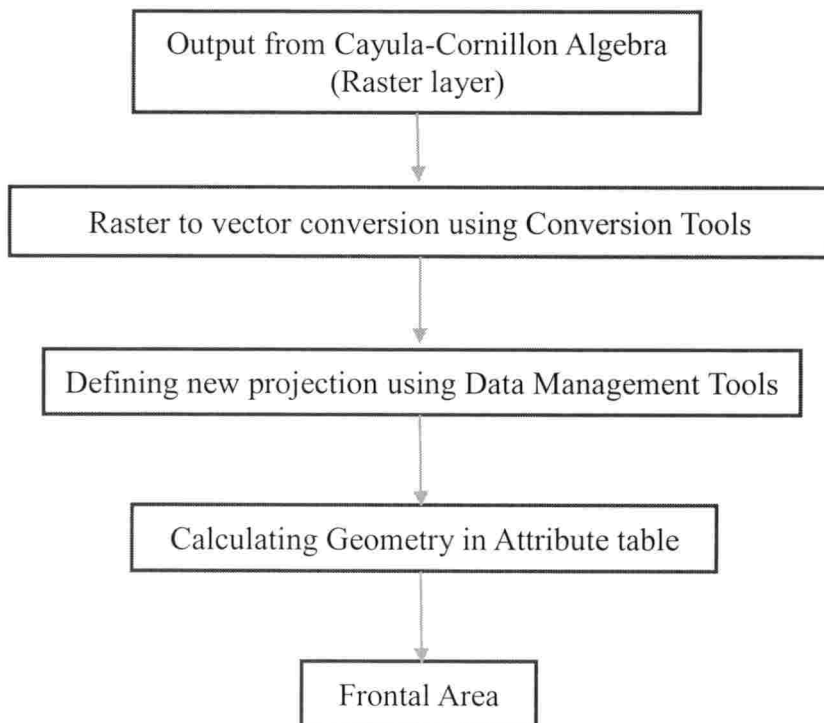


**Figure 5: Area calculation using ArcGIS**

### 3.3.3 Creating boxes for the north east, north west, south east and south west Arabian Sea in QGIS

For the purpose of investigating patterns in the spatial variability of thermal and chlorophyll frontal area in the Arabian Sea, the study domain was divided into four regions. The four regions and their coordinates are given in the table below.

**Table 1: Regions of Arabian Sea with respective coordinates**

REGIONS	COORDINATES
North eastern Arabian Sea	12°-26°N, 65°-78°E
North western Arabian Sea	12°-26°N, 50°-65°E
South eastern Arabian Sea	0°-12°N, 65°-78°E
South western Arabian Sea	0°-12°N, 50°-65°E

For creating shapefiles for different regions of the Arabian Sea, an NC file for SST or Chl-a was opened using 'Open Raster' option. This was done so as to get an idea regarding the coordinates of the study area. Then 'Create Layer' option under 'Layer' toolbar was selected. Then using 'Add Feature' option, a polygon was drawn over the desired coordinate points to create a shape file for the area of interest.

### 3.3.4 Creating shapefile for Exclusive Economic Zone (EEZ) in QGIS

EEZ map available from INCOIS website was utilized here ([www.incois.gov.in](http://www.incois.gov.in)). This map was opened as a raster layer in QGIS and was georeferenced to appropriate latitude and longitude co-ordinates using the 'georeferencer' tool. Using 'create layer' tool, a new polygon layer was created. Individual points were added in the polygon layer over the EEZ line using 'add feature' tool in such a way that the added point and the EEZ line overlaps perfectly.

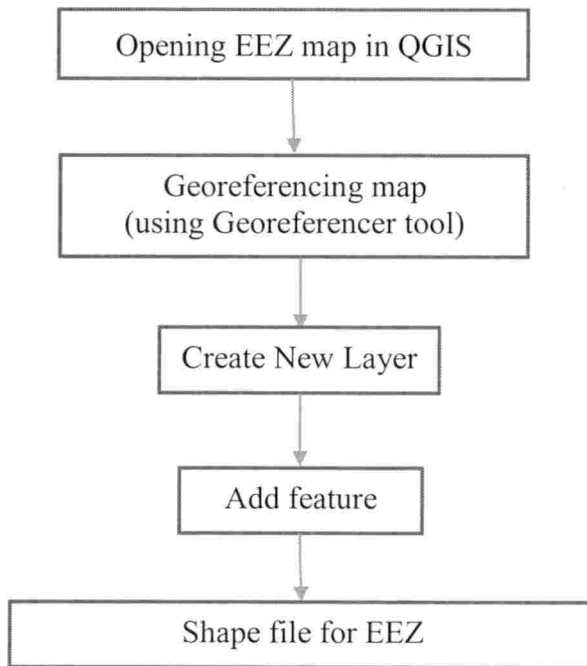


**Figure 6: Shapefile creation using QGIS**

### 3.3.5 Extracting frontal features within EEZ

Majority of the fishing activity of India is carried out within the EEZ. So, for getting a more reliable relationship between frontal zones and fish catch, the frontal area that occurs within the EEZ is selected rather than which occurs in the open oceans. The frontal map for the entire area for the required time was opened in ArcGIS. EEZ shapefile generated as mentioned in section 3.3.4 was superimposed on to the frontal map. Using 'Extract by mask' option under 'spatial analyst' tool, EEZ was masked (here masked means it selects EEZ). This resulted in the formation of a new layer, with frontal layer within EEZ. Further, attribute table was used to obtain total frontal area within the defined zone using method as mentioned in section 3.3.2.

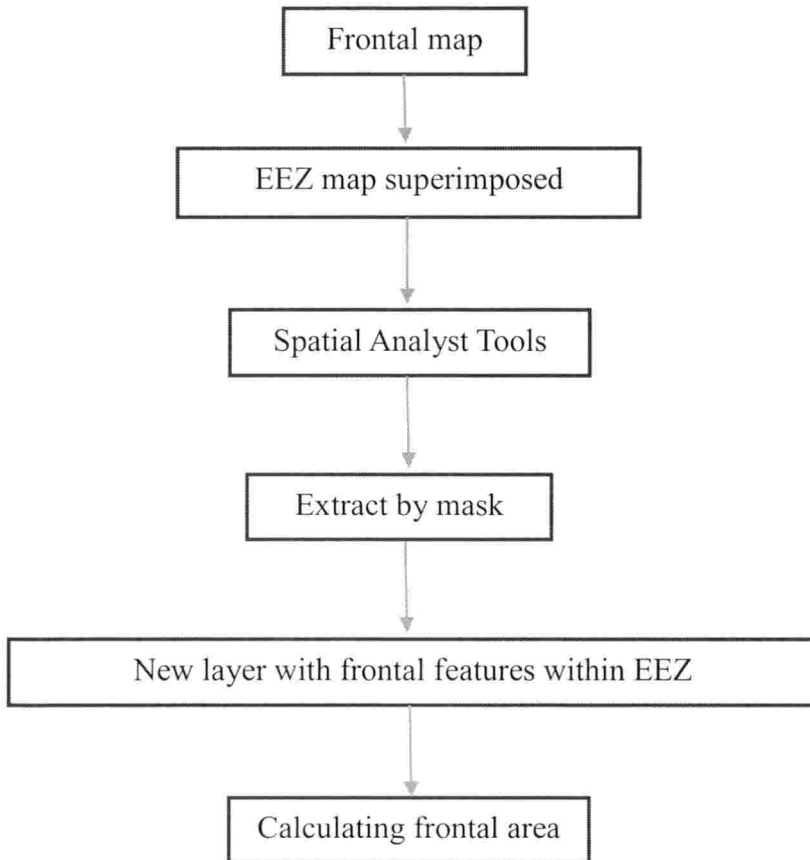


**Figure7: Extracting features within EEZ using ArcGIS**

### **3.3.6 Finding out CPUE from catch and effort data**

Marine fish catch is generally assessed based on landing data from different fishing gears at various landing centers across the country. All fishing gears do not have uniform efforts and hence taking only the total amount of fish caught by the gears in a particular month may not represent the fish abundance during that time in the EEZ. So there is a need to standardize the fish caught by each gear, giving adequate weightage based on the effort of the respective gear. The gear-wise fish landing data (in kilograms) was provided on a monthly basis by CMFRI, along with the individual efforts (in hours of operation) for each gear. This data was used to generate Catch Per Unit Effort (CPUE) by dividing the total quantity of fish caught by a gear by the respective hours of operation (effort) of the gear, so as to give a more ideal representation of the total fish landings along the west coast of India.

## RESULTS AND DISCUSSION



## CHAPTER 4

### RESULTS AND DISCUSSION

#### 4.1 CLIMATOLOGY OF UPPER OCEANOGRAPHIC PARAMETERS IN THE ARABIAN SEA

##### 4.1.1 SST - climatology

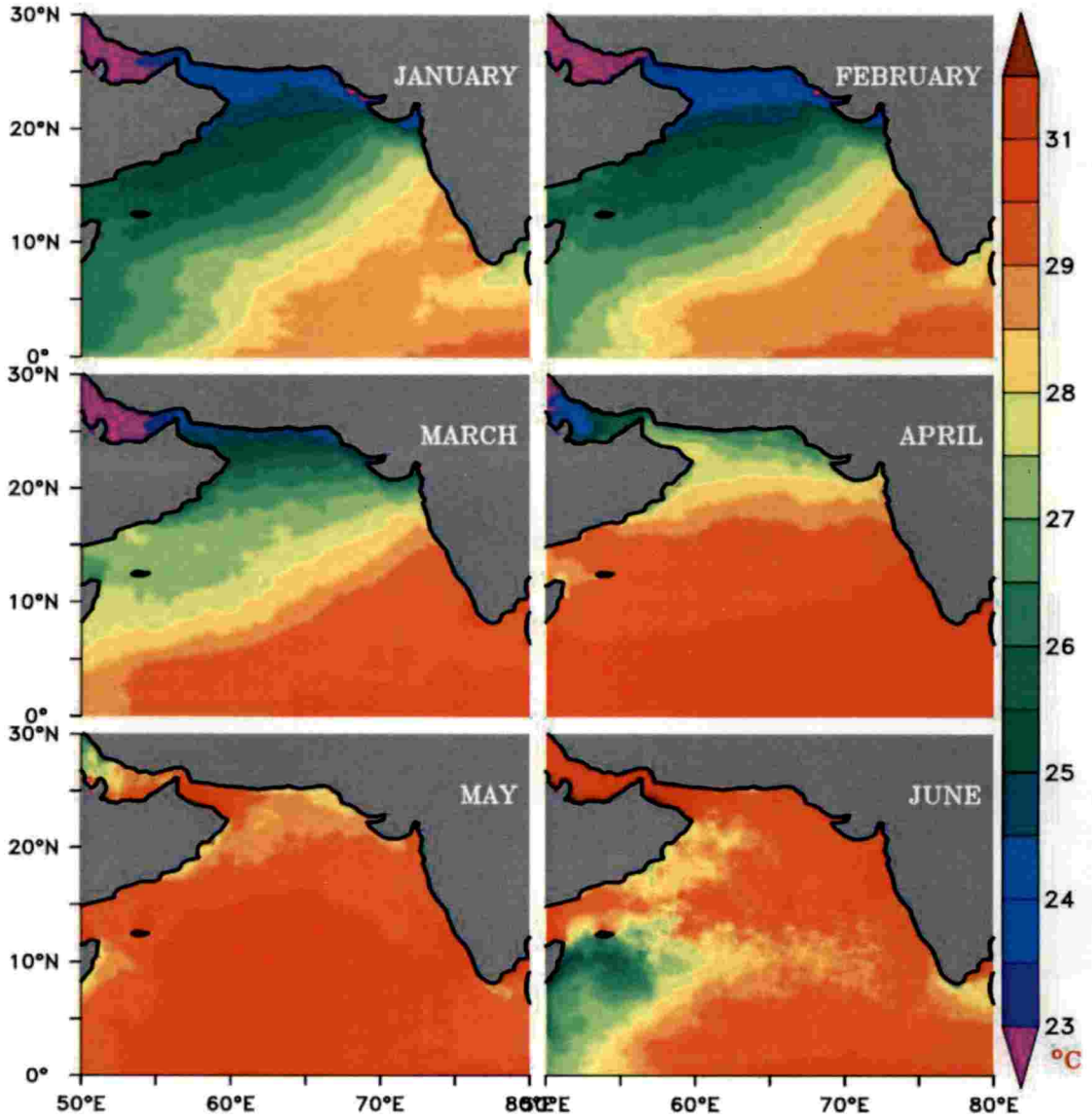
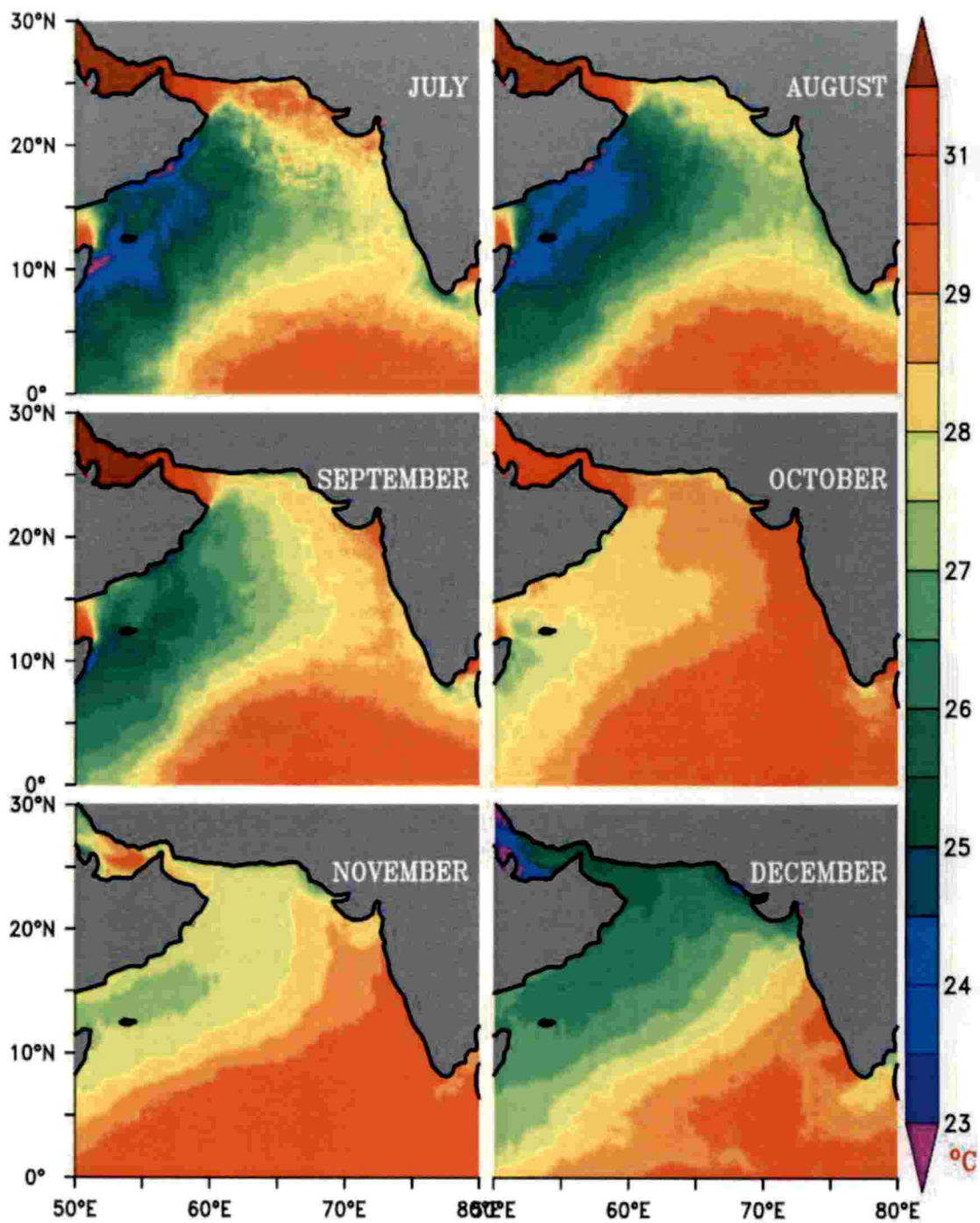


Figure 8: Climatology of SST of Arabian Sea from January to June for the period 2002-2016



**Figure 9: Climatology of SST of Arabian Sea from July to December for the period 2002-2016**

57A

Monthly climatology of SST in the Arabian Sea (fig. 8 and 9) brought out seasonal fluctuations, the intensity and spatial extent of cooling/warming is subject to the seasonal fluctuations. The temperature increased in the study area during April-June and SST attained values up to 26-31°C in the central Arabian Sea during the period. North east Arabian Sea is usually cooler (23-27°C) except during the south west monsoon months (29-31°C) (Pillai *et al.*, 2000). Persian Gulf experienced high seasonal fluctuations, where a very low SST (18-25°C) during the period November-March and high SST (25-34°C) in the period May-October can be seen. The monthly variability in cooling/warming of sea surface has been examined in detail as follows:

### **January**

During January, the central and western Arabian Sea recorded temperatures of 26-28°C, while that of south east Arabian Sea recorded slightly higher temperatures (29-30°C). Persian Gulf showed a significantly low temperature of magnitude 17-23°C.

### **February**

Conditions of the central and western Arabian Sea remained the same as January. Temperature at the Kerala coast increased to about 29-30°C and showed an increase in its spatial extent (74-77°E and 8-12°N). This period also marked the shifting of warm sea surface towards western part of southern Arabian Sea.

### **March**

The expansion of high temperature (29-31°C) along the western part of southern Arabian Sea continued. Thus the entire region to the south of 20°N was warmed and the temperature became 25-29°C by March (Pillai *et al.*, 2000)

## **April**

The warming further continued even during April, such that region with higher temperature covered the central Arabian Sea (0-16°N), with temperature of 29-31°C and southern part of Arabian Sea showed a temperature of 30-31°C.

## **May**

During May, the entire Arabian Sea experienced an increase in temperature in the range of 28-31.5°C, with its peak value in the northern region encompassing an area of 22-26°N and 54-60°E (30.5-31.5°C) and in the central Arabian Sea (31°C).

## **June**

The temperature in the south west Arabian Sea started to decrease (25-27°C) during June (Shetye, 1986). Persian Gulf experienced a significant warming trend, resulting in a SST hike up to 30.5-32.5°C.

## **July**

The temperature drop intensified (22-26.5°C) during July along the south western region and covered the entire western and some parts of central Arabian Sea. The maritime states of India also experienced a drop in temperature (25.5-28°C), while Persian Gulf recorded exceptionally high values of temperature (31.5-33.5°C).

## **August**

The cooling trend continued in the western, central and northern Arabian Sea, while Persian Gulf continued the warming trend (32-34.5°C)

## **September**

Over the course of time, the cooling trend observed in the western Arabian Sea slowly transformed into a warming trend (Shetye, 1986) with temperatures ranging from 24.5-27°C, while Persian Gulf region got slightly cooled (32-34°C). The

southernmost part of Arabian Sea maintained the same temperature range as in previous months.

### **October**

During October, temperature of the western Arabian Sea increased (26.5-28°C), marking a clear end to the cooling trend of the region. Eastern and southern Arabian Sea displayed a significant warming trend with temperatures varying from 29-30.5°. As a result, the coastal waters of the west coast of India covering the coastal waters of Kerala, Karnataka, Goa, Maharashtra and some parts of Gujarat showed a hike in SST. October also marked the start of cooling period for Persian Gulf where the temperature reduced to 30-32°C compared to previous months (32-34°C)

### **November**

Temperature dropped (26-28°C) during November and slightly cooler surface water was noticed along the northern, north western and western Arabian Sea. Persian Gulf also expressed significant cooling trend with temperature ranging from 25.5-30°C. Highest temperature (30-30.5°C) was recorded near the south east Arabian Sea.

### **December**

During December, the temperature throughout Arabian Sea decreased. The significant cooling trend of the Persian Gulf sustained with temperature ranging from 21-25°C. Northern and north western Arabian Sea showed low temperatures (25.5-27°C) while the south east Arabian Sea recorded temperature of 28-30°C.

#### 4.1.2 Chl-a - climatology

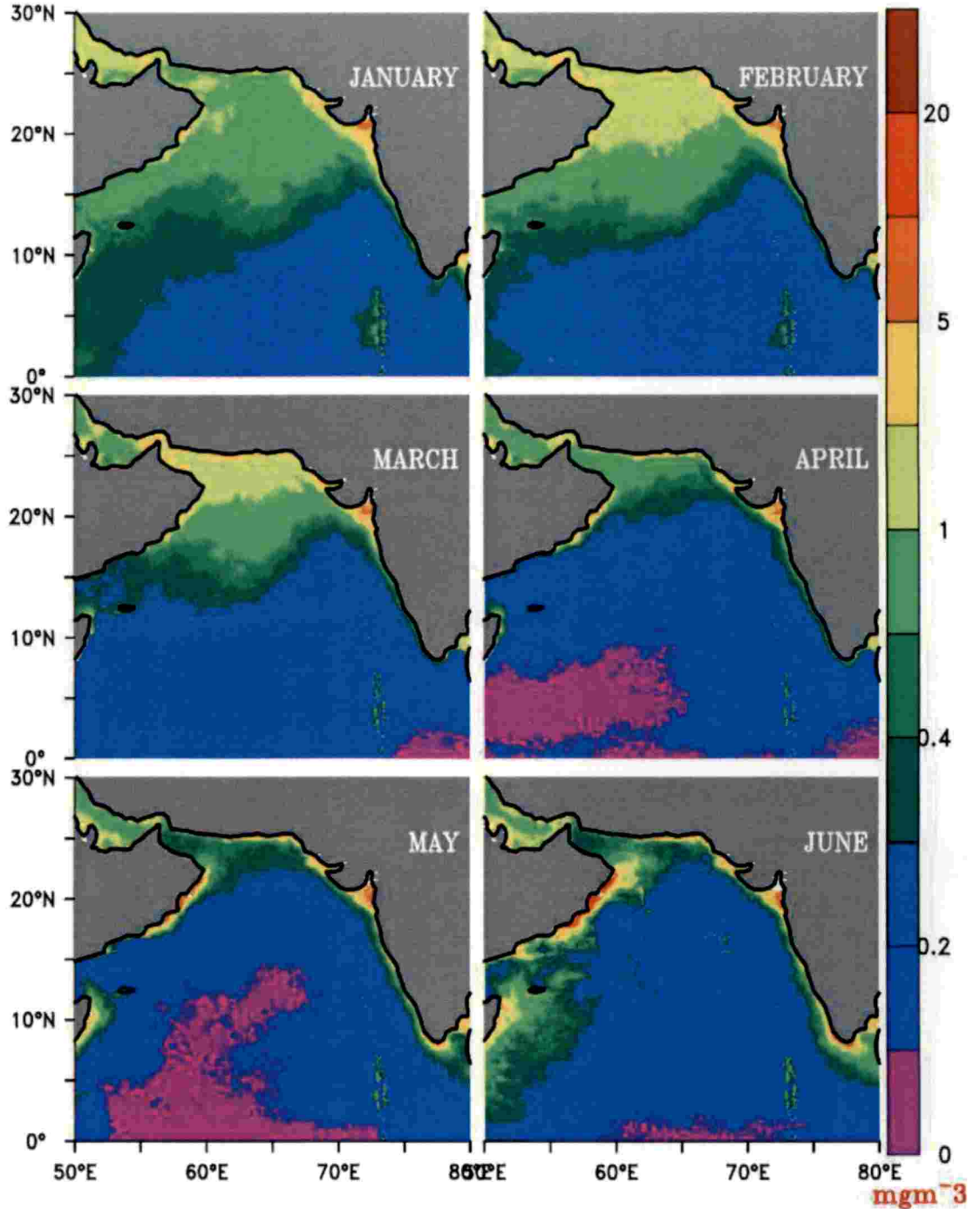


Figure 10: Climatology of Chl-a concentration of Arabian Sea from January to June for the period 2000-2016

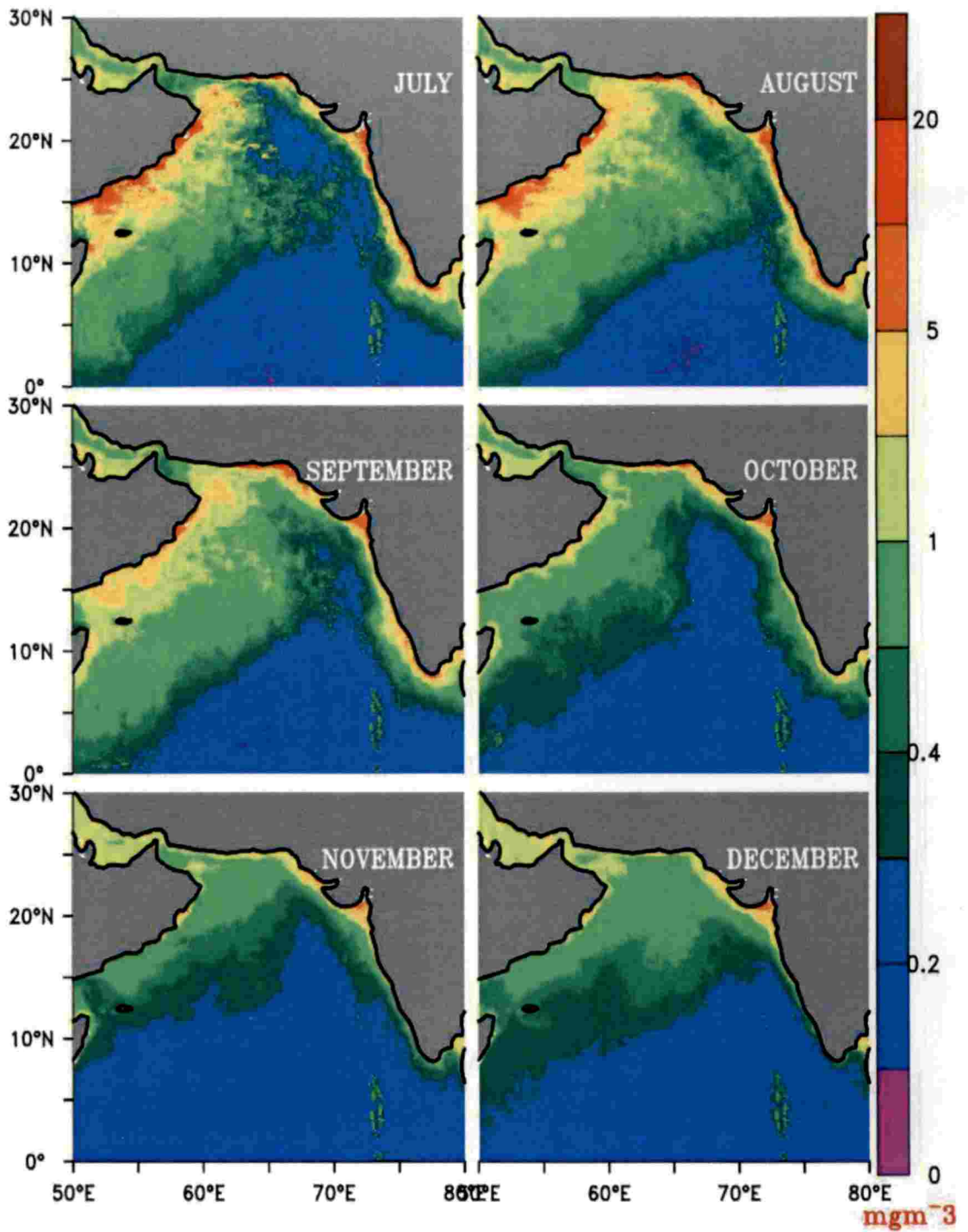


Figure 11: Climatology of Chl-a concentration of Arabian Sea from July to December for the period 2000-2016

In general, near coastal areas experienced high values of Chl-a, while very low levels of chlorophyll existed in the open waters of southern and south eastern Arabian Sea. During southwest monsoon, phytoplankton bloom occurred in the western and south east Arabian Sea (Subrahmanyam, 1959; Banse 1959, 1968). The aerial extent of west is large compared to the south eastern part. For the north east monsoon, only the northern as well as north western regions have high Chl-a concentration in the sea water (Radhakrishna *et al.*, 1978; Qasim, 1982). The details based on monthly data (fig. 10 and 11) is explained below:

### **January**

In January, low Chl-a concentration ( $0.1-0.3 \text{ mg/m}^3$ ) was found in the south and south east Arabian Sea, while Persian Gulf and coastal areas of Gujarat showed higher Chl-a values of the range  $0.5-5 \text{ mg/m}^3$ . Northern as well as central Arabian Sea experienced moderate Chl-a concentrations ( $0.3-1 \text{ mg/m}^3$ ).

### **February**

Low Chl-a concentrations ( $0.1-0.3 \text{ mg/m}^3$ ) in the south and south east Arabian Sea continued, while northern and central Arabian Sea experienced higher Chl-a concentrations ( $0.3-2 \text{ mg/m}^3$ )

### **March**

In March, the area with lower Chl-a concentration ( $0-0.3 \text{ mg/m}^3$ ) drastically increased its aerial spread and covered almost the entire southern and central Arabian Sea. A region of very low Chl-a concentration was found at the southern tip of Arabian Sea ( $0-0.1 \text{ mg/m}^3$ ), while the northern Arabian Sea had higher Chl-a values ( $0.3-5 \text{ mg/m}^3$ ).



## **April**

The high Chl-a concentration along the northern Arabian Sea has decreased by April. The lowest value of Chl-a was recorded in the south east and south west Arabian Sea. (0-0.1 mg/m<sup>3</sup>). Except for the northern Arabian Sea (0.2-1 mg/m<sup>3</sup>), all other areas showed lower Chl-a values of 0.1-0.2 mg/m<sup>3</sup>.

## **May**

The lowest value of Chl-a (0-0.1 mg/m<sup>3</sup>) was recorded near central and south west Arabian Sea in May. Except for the northern tip of Arabian Sea (0.3-1 mg/m<sup>3</sup>), the entire area showed lower Chl-a values of 0-0.2 mg/m<sup>3</sup>.

## **June**

June marked the beginning of increase in Chl-a in the western Arabian Sea, with the Chl-a values increasing eastwards with a range of 0.3-2 mg/m<sup>3</sup>. Except western Arabian Sea, all other regions experienced Chl-a values ranging from 0-0.3 mg/m<sup>3</sup>. A marginal increase in Chl-a was also seen in the south east Arabian Sea during this month.

## **July**

The phytoplankton bloom (0.4-20 mg/m<sup>3</sup>) had an eastward propagation during July in the western Arabian Sea. At the same time an increase in Chl-a concentration occurred along the west coast of India.

## **August**

During August, the Chl-a concentration of the entire western (Brock *et al.*, 1991) and central Arabian Sea increased to 0.5-20 mg/m<sup>3</sup>, while southern Arabian Sea recorded low Chl-a values (0.1-0.3 mg/m<sup>3</sup>)

## **September**

Low chlorophyll region ( $0.1-0.3 \text{ mg/m}^3$ ) of the southern Arabian Sea showed an expansion in its area, spreading to the eastern Arabian Sea, while Chl-a values in the western and central Arabian Sea was around  $0.3-5.0 \text{ mg/m}^3$ .

## **October**

In October the low chlorophyll region further extended its aerial spread towards north east Arabian Sea with a Chl-a concentration of  $0.1-0.3 \text{ mg/m}^3$ . At the same time Chl-a values in western Arabian Sea ranged between  $0.3$  to  $5.0 \text{ mg/m}^3$ .

## **November**

In November, Chl-a values in the southern Arabian Sea ranged from  $0-0.1 \text{ mg/m}^3$  and from  $0.2-0.4 \text{ mg/m}^3$  in the central Arabian Sea. Northern Arabian Sea exhibited an increase in Chl-a concentration ( $0.5-5 \text{ mg/m}^3$ ) compared to previous months.

## **December**

In December, the entire Arabian exhibited similar Chl-a concentration in sea water as of the previous month.

### 4.1.3 SSHA - climatology

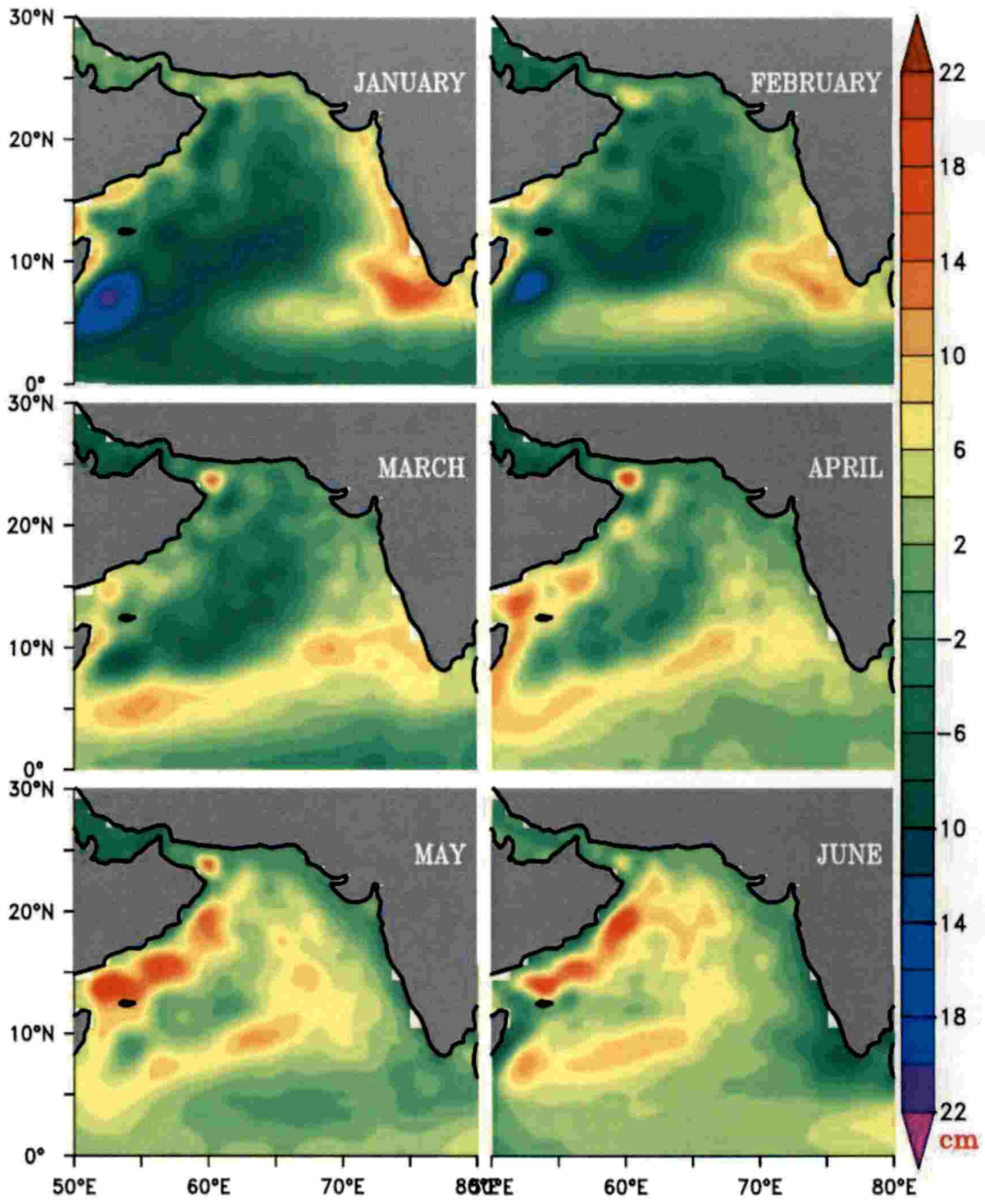


Figure 12: Climatology of SSHA of Arabian Sea from January to June for the period 2000-2013

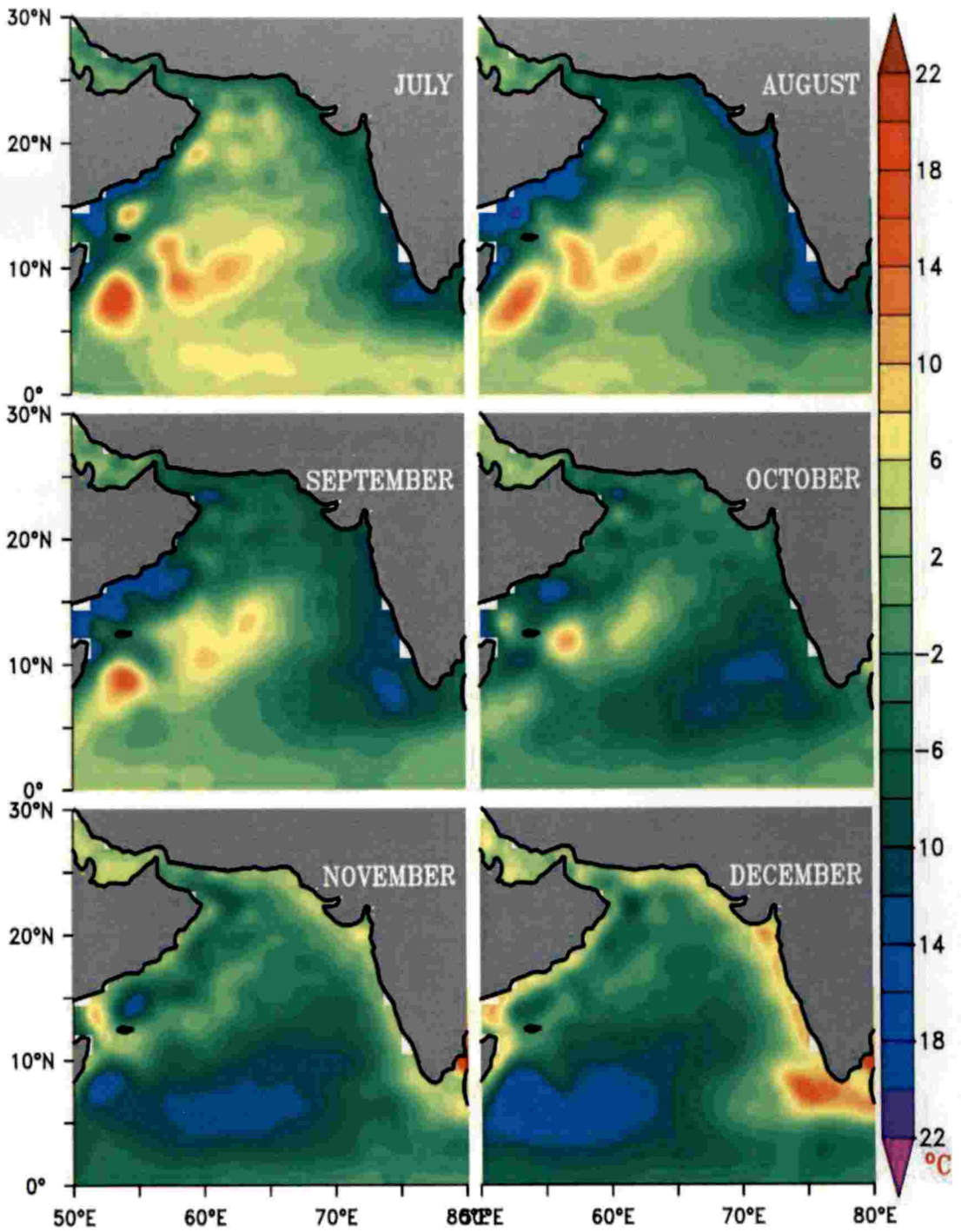


Figure 13: Climatology of SSHA of Arabian Sea from July to December for the period 2000-2013

During December-February, higher SSHA values (10 to 14.5 cm) occurred in the southern tip of Indian peninsula. The higher SSHA region in the south east Arabian Sea propagated to the west during January-February and reached the western Arabian Sea by March. It further shifted to the northern Arabian Sea through the Saudi Arabia coast by April-June period, recording very high values of SSHA (11 to 20 cm) near the Saudi Arabia coast which can be attributed to downwelling due to anticyclonic eddy formation in the region (Nerem *et al.*, 1994; Kumar and Narvekar, 2005). From July to September, the eastern and western Arabian Sea experienced negative SSHA values (-14 to -22 cm) which can be attributed to upwelling in that region (Shankar and Shetye, 1997). This negative SSHA region started shifting through southern Arabian Sea during September, reaching the south western Arabian Sea by December. This resulted in much negative SSHA values by January which can be attributed to possible upwelling in the region. Month wise distribution of SSHA along the Arabian Sea (fig. 12 and 13) has been given below.

### **January**

In January, the west coast of India experienced SSHA values from -4 cm to 14 cm with higher positive values (11 to 15 cm) near the coastal waters of Kerala and Karnataka. SSHA values ranged from 2 cm to -14 cm along the central Arabian Sea, while the south western Arabian Sea had much negative SSHA values (-14 to -22 cm). This negative SSHA value can be attributed to the upwelling due to cyclonic eddy formation as reported by Al Saafani *et al.* (2007)

### **February**

February experienced almost the same conditions as of the previous month, with the propagation of the higher positive SSHA from south eastern Arabian Sea to the western Arabian Sea.

## **March**

The westward propagation of SSHA values persisted and it reached the western Arabian Sea where SSHA values ranged from 6 to 12 cm. All other regions experienced relatively lower SSHA values (2 to -7 cm).

## **April**

The positive SSHA region in the western Arabian Sea started shifting towards north along the Saudi Arabia coast during April with values ranging from 7 to 14 cm.

## **May**

During May, the positive SSHA region covered the north western Arabian sea with values of 3 to 21 cm. Anticyclonic eddies started forming along the Saudi Arabia coast with values ranging from 10 to 21 cm, while the eastern Arabian sea experienced moderately lower SSHA values (-2 to 6 cm).

## **June**

Anticyclonic eddy formation continued in the north western Arabian Sea while eastern Arabian Sea continued recording lower values (4 to -9 cm).

## **July**

SSHA started to decrease along the western and eastern Arabian Sea with values of -4 to -14 cm, while positive SSHA (12 to 15 cm) existed in the south west Arabian Sea.

## **August**

In august, the SSHA further decreased in the western and eastern Arabian Sea (-14 to -22), which can be attributed to upwelling in this region due to cyclonic eddy during this month.

## **September**

The negative SSHA values of the eastern Arabian Sea started shifting towards western Arabian Sea during September.

## **October**

Westward shift of low SSHA values persisted throughout October. Lower SSHA values (-2 to 6 cm) existed in the central Arabian Sea, while western Arabian sea recorded higher SSHA values compared to previous months.

## **November**

In November, the southern part of Arabian Sea (2-12°N and 50-74°E) experienced greater negative SSHA values (-11 to -19 cm), while the west coast of India and the Saudi Arabia coast experienced SSHA values ranging from -2 to 10 cm during this month.

## **December**

In December, large negative SSHA values (-14 to -20 cm) was observed in the south west Arabian Sea, while the west coast of India experienced higher positive SSHA values (0 to 14.5 cm), implying upwelling in south west Arabian Sea and downwelling in west coast of India.

#### 4.1.4 Winds - climatology

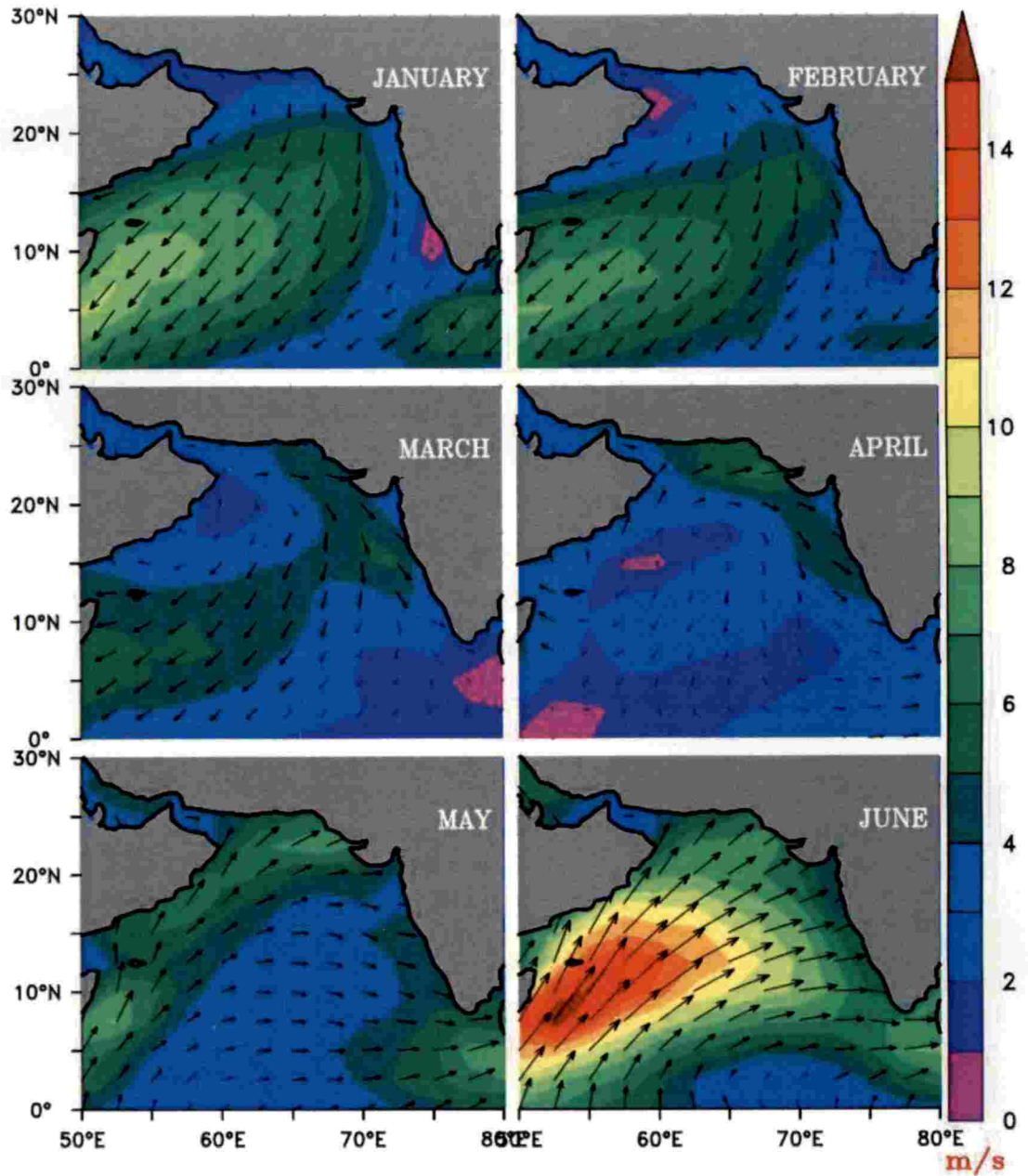
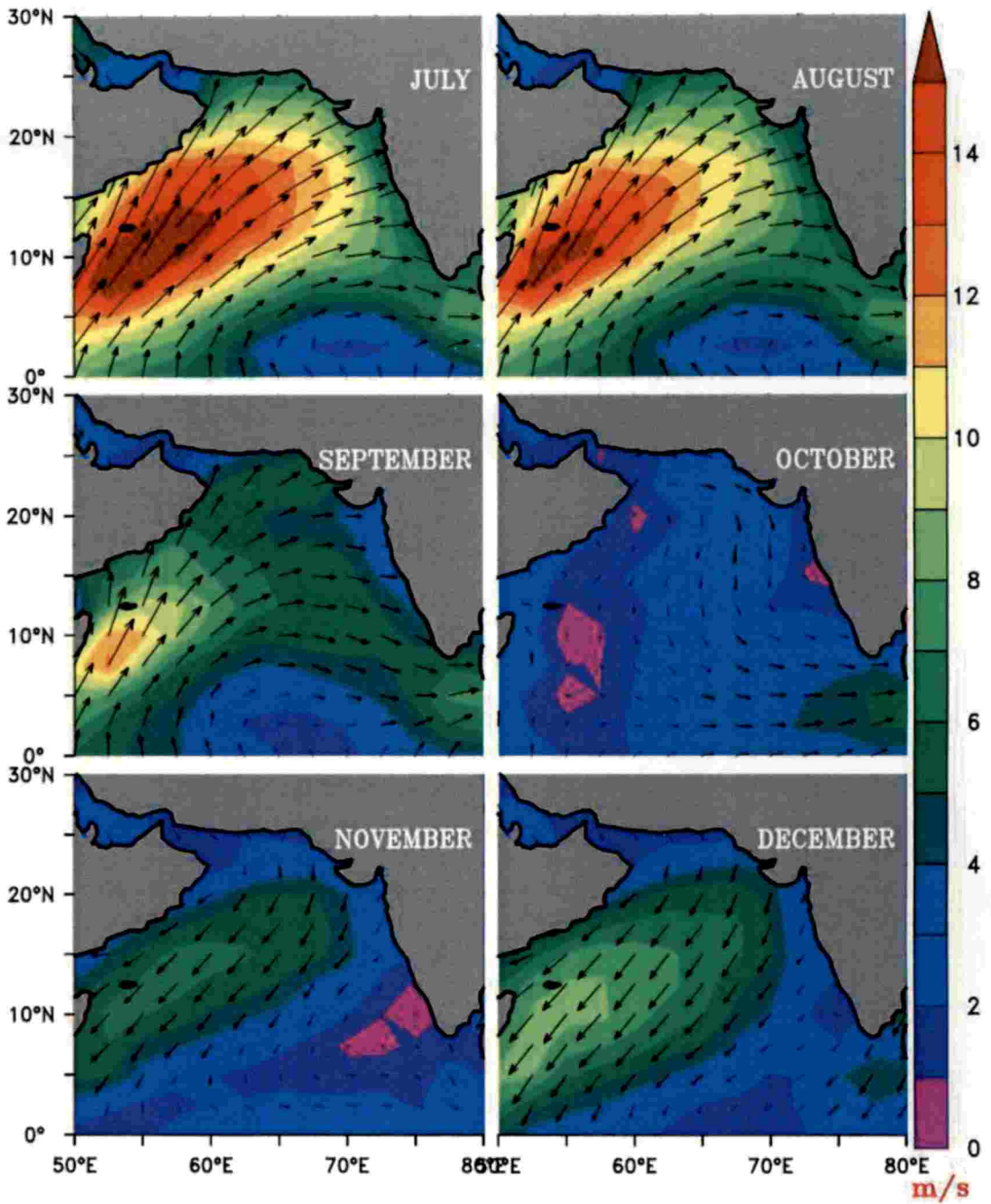


Figure 14: Climatology of winds over Arabian Sea from January to June for the period 2000-2016





**Figure 15: Climatology of winds over Arabian Sea from July to December for the period 2000-2016**

South westerlies prevailed during April, where high wind speeds (6-9 m/s) existed near the western and south east Arabian Sea. During May to July, the wind speeds drastically increased (12-15 m/s) in the central and western Arabian Sea (Findlater, 1969) while south east Arabian Sea experienced lower wind speed (0-5 m/s). West coast of India recorded moderate wind speeds of 5-8 m/s during this period (Pillai *et al.*, 2000). The wind speed started decreasing by August. During October winds gradually changed its direction to north easterlies (Goes *et al.*, 2005). During this period very low wind speeds (0-4 m/s) existed in the in the eastern, northern and southern Arabian Sea. Central and south west Arabian Sea recorded moderate wind speeds of 5-10 m/s during this period. During February to March, Arabian Sea experienced a weakening of the north easterly winds resulting in very low wind speeds (0-4 m/s) over the entire Arabian Sea. A detailed observation of monthly wind movement (fig. 14 and 15) has been provided below.

### **January**

North easterly winds prevailed in the northern Arabian Sea and the region experienced very low wind speeds (1-5 m/s) during January. The same conditions prevailed in the west coast of India, with lowest wind speed (0-2 m/s) near Kerala coast. Central and south western Arabian Sea experienced higher wind speeds of magnitude 5-10 m/s. The coasts of Kerala and Karnataka recorded very low wind speeds (1-2 m/s) during January.

### **February**

In February, the low wind speed region in the northwest and southeast Arabian Sea started expanding towards the central Arabian Sea and recorded values around 0-4 m/s. Only a small region in the north east and south west Arabian Sea recorded slightly higher wind speeds of magnitude 4-7 m/s.

## **March**

In March, almost the entire Arabian Sea recorded very low wind speeds (0-4 m/s) except for a small region in the north east Arabian Sea, where wind speeds ranged from 4-8 m/s

## **April**

The wind reversed its direction and became south westerlies for the month of April. Wind speeds started increasing gradually along the northern, north western and south eastern Arabian Sea with values ranging from 4-9 m/s. Central and southern Arabian Sea still had very low wind speeds of magnitude 1-3 m/s during the period, while south east Arabian Sea experienced wind speeds of magnitude 4-6 m/s. The wind also reversed its direction and became south westerlies for the month of April

## **May**

In May, except for a small region in the southern Arabian Sea, all other regions exhibited higher wind speeds ranging from 6-16 m/s with highest values near the western Arabian Sea (12-15 m/s). The south westerly winds strengthened during this period when compared to previous months.

## **June**

In June, the high wind speed region in the western Arabian Sea expanded its spatial extent and the entire Arabian Sea had wind speeds of 7-15 m/s except for the south east region (0-6 m/s). High south westerly winds prevailed during this period.

## **July**

In July, the low wind speed region started shifting from south east towards western Arabian Sea. Conditions in the south east region continued while all other areas exhibited higher wind speeds with greatest wind speed (11-15 m/s) near western Arabian Sea.

## **August**

August marked the start of retreating phase of high wind speed region in the western Arabian Sea. The spatial shift of low wind speed region towards west continued even during August, resulting in lower wind speeds (0-6 m/s) over the entire Arabian Sea except for western region (7-13 m/s)

## **September**

In September, wind speeds were drastically reduced and the wind speeds in the entire Arabian Sea ranged from 0-5 m/s, except for south eastern tip where slightly higher wind speed (4-7 m/s) was recorded. The south westerly winds gradually weakened and changed its direction during this period.

## **October**

North easterly wind prevailed over the entire Arabian Sea during this month. Wind speeds of central and south western Arabian Sea were slightly higher (3-9 m/s) in October, compared with the low wind speed at other regions (0-3 m/s). Wind speeds along the south east Arabian Sea were exceptionally low (0-2 m/s) during this period. North easterly wind prevailed during this month.

## **November**

November marked the beginning of expansion of high wind speed region in the central and western Arabian Sea, where wind speeds ranged from 6-10 m/s, while the west coast of India still recorded very low wind speeds (0-3 m/s) during this period. Strong north easterly winds prevailed in the northern and central Arabian Sea

## **December**

Strong north easterly winds prevailed almost in the entire Arabian Sea. South western and central Arabian Sea showed higher wind speeds (6-11 m/s), while northern and eastern Arabian Sea recorded lower values (0-4 m/s).

### 4.1.5 Surface current velocity - climatology

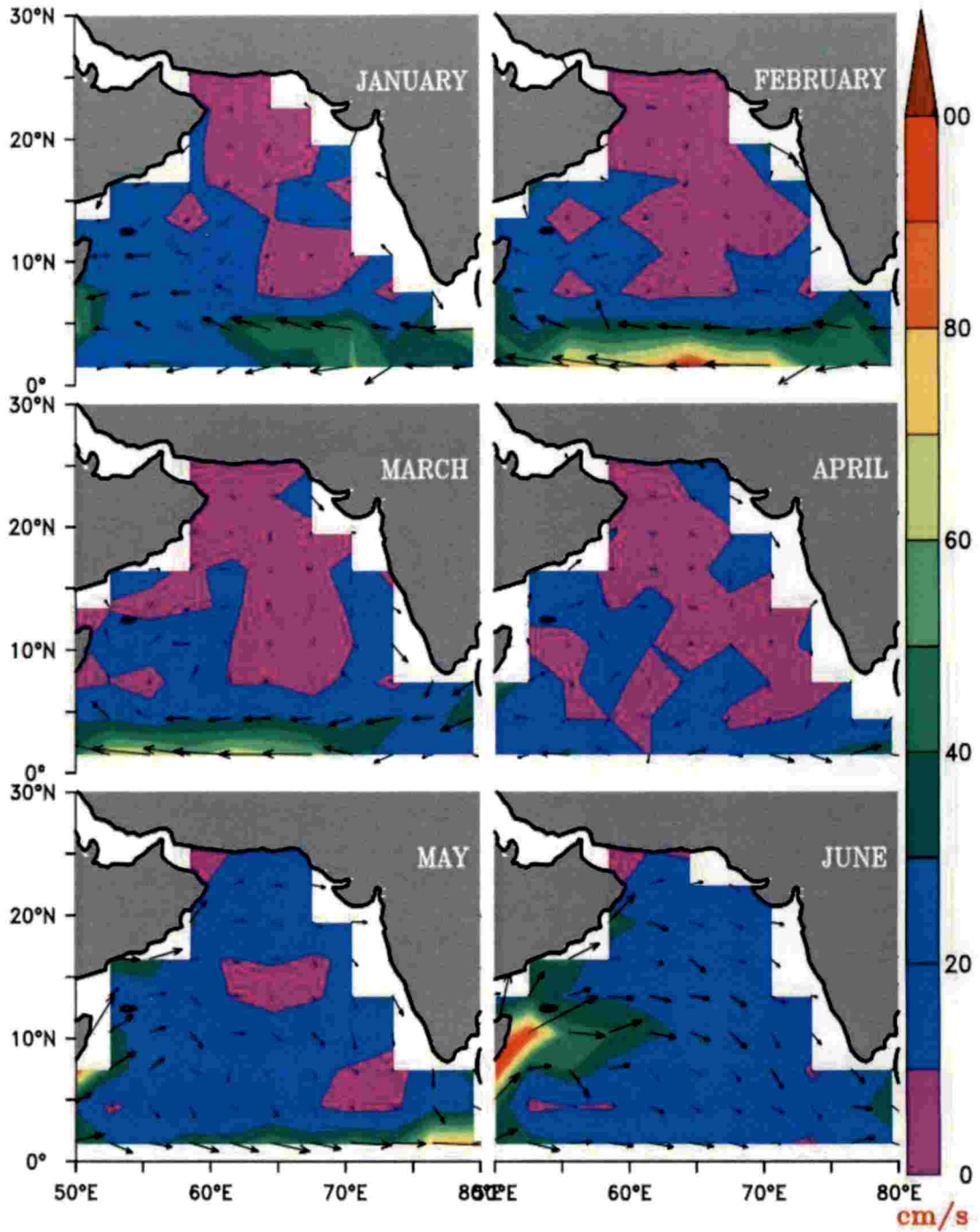


Figure 16: Climatology of surface current velocity of Arabian Sea from January to June for the period 2000-2016

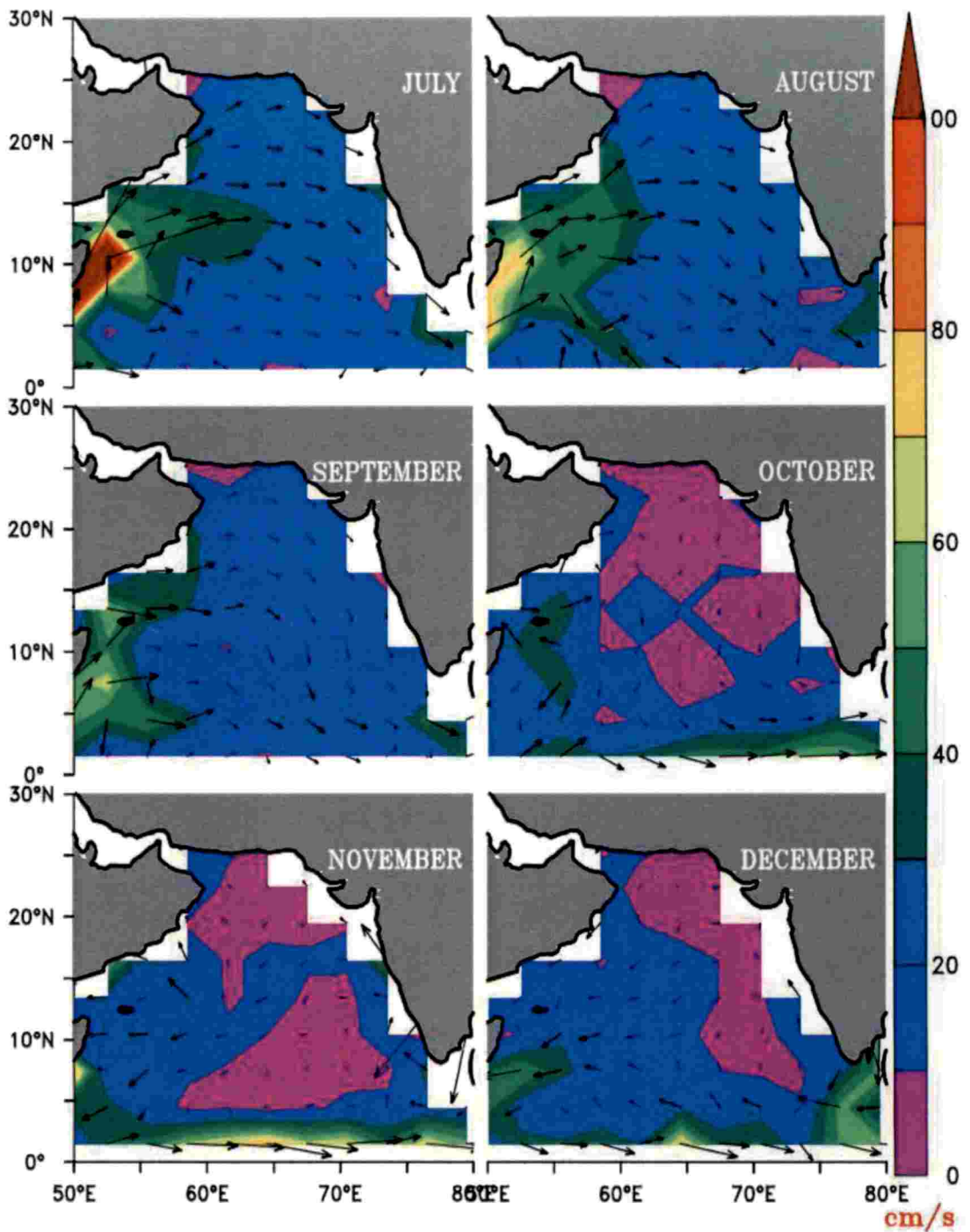


Figure 17: Climatology of surface current velocity of Arabian Sea from July to December for the period 2000-2016

In general, the surface current velocity of waters near the central and eastern Arabian Sea showed lower values ranging from 10-40 cm/s throughout the year. Western Arabian Sea recorded higher values of surface current velocity (60-120 cm/s) during the period from May to November. Surface current velocity values reached its peak (100-160 cm/s) at the south western Arabian Sea during July. Surface current velocity values were generally lower during the period January to April (Shankar *et al.*, 2002). Month wise analysis of the current pattern (fig. 16 and 17) is given below.

### **January**

In January, the central and eastern Arabian Sea experienced very low surface current velocity (10-30 cm/s). While the southern Arabian Sea had a moderate surface current velocity (50-70 cm/s) were recorded.

### **February**

In February, very low values of surface current velocity (10-30 cm/s) existed in the central Arabian Sea. At the same time, southern Arabian Sea experienced a high surface current velocity of the range 70-110 cm/s.

### **March**

Same current pattern existed during March, but the current velocity was reduced to 60-80 cm/s at the southern Arabian Sea during the period.

### **April**

In April, the south east Arabian Sea exhibited very low surface current velocity values of the range 0-30 cm/s with the lowest current velocity near southern tip of Kerala coast.

## **May**

An eastward intrusion of the high surface velocity currents was visible from May onwards. This resulted in moderate values of surface current velocity (60-90 cm/s) near the south western tip of Arabian Sea, while west coast of India still had lower values (0-30 cm/s)

## **June**

The eastward shifting of higher surface velocity currents was easily visible by June. This created currents with higher velocities of 60-110 cm/s near the south western Arabian Sea, while the eastern Arabian Sea showed comparatively lower values (10-40 cm/s).

## **July**

Currents with higher surface velocity became more pronounced in the western Arabian Sea with surface velocity values of 110-170 cm/s. West coast of India still had lower surface current velocity.

## **August**

During august, the surface velocity of currents near the south east Arabian Sea decreased (60-120 cm/s) when compared to previous month. Surface current pattern near west coast of India remained unchanged.

## **September**

September marked the shift of lower surface current velocity value from west coast of India towards central Arabian Sea, resulting in low velocity of currents (10-40 cm/s) near the central and eastern Arabian Sea. The current velocity was reduced to 60-140 cm/s in the western Arabian Sea during September.



## **October**

In October, the low surface current velocity region spread further towards central Arabian Sea, causing reduction in current velocity in the area. A high surface current velocity (60-130 cm/s) was recorded in the western Arabian Sea.

## **November**

In November, western Arabian Sea recorded relatively lower values of surface current velocity (50-90 cm/s) when compared to previous months. Low surface current velocity region shifted further towards central Arabian Sea.

## **December**

In December, surface velocity of currents in the western Arabian Sea recorded lower values (50-60 cm/s) compared to previous month. But the south eastern tip of Arabian Sea recorded higher values (70-90 cm/s) during the period.

#### 4.2 CLIMATOLOGY OF THERMAL AND CHLOROPHYLL FRONTAL AREA IN THE ARABIAN SEA

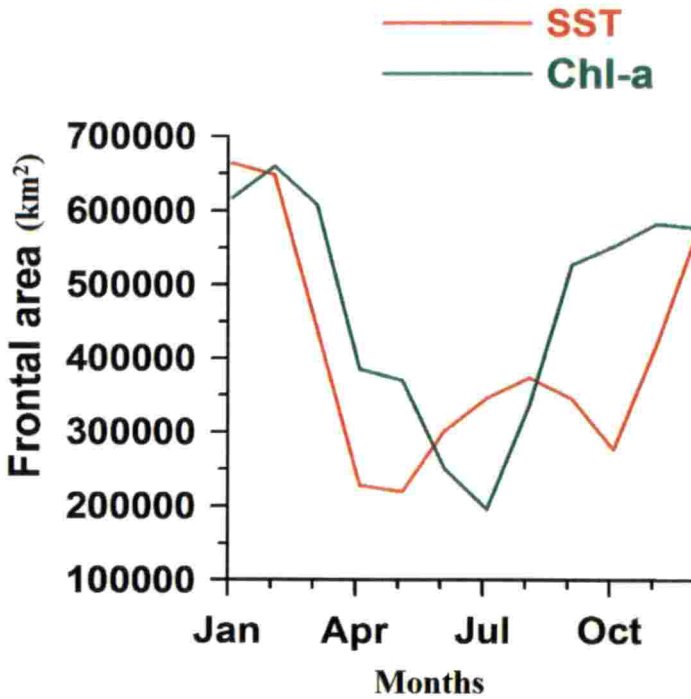


**Figure 18: Climatology of thermal frontal area (2003-2016) and Chl-a frontal area (2000-2016) in the Arabian Sea**

The thermal frontal area was given as an output by the SIED technique in ArcMAP and a study was conducted to analyze the climatology of the thermal frontal area for the period 2003-2016 (fig. 18). The results showed that October marked the beginning of an increasing trend in thermal frontal area which sustained till February, with its peak value in the month of January. This indicated that the maximum thermal frontal area occurred during the winter monsoon period. The study also pointed out that the period from March to May experienced a steady decrease in thermal frontal area with its lowest value occurring during the month of May. The study also revealed lower values during August to October, indicating that lower values of thermal frontal area

during pre and post monsoon periods. An increase in thermal frontal area occurred during May to September, attaining secondary peak in August.

Climatological analysis of chlorophyll frontal area from 2000-2016 (fig. 18) showed an increase in frontal coverage from November to February with its peak value in February. This indicated that the maximum chlorophyll frontal area occurred during winter monsoon period. From February onwards the chlorophyll frontal area started decreasing steadily till July indicating low chlorophyll frontal area coverage during pre-monsoon period. Chlorophyll frontal area again started to increase steadily from July to September with its second peak in November.

The monthly climatology study of thermal and chlorophyll frontal area revealed the intensity of frontal occurrences in the entire Arabian Sea during each month. A spatial analysis of frontal coverage was conducted to further gain insight into the patterns of frontal coverage in the north eastern, north western, south eastern and in the south western Arabian Sea.

### 4.3 CLIMATOLOGY OF SPATIAL VARIABILITY IN FRONTAL AREA IN THE ARABIAN SEA

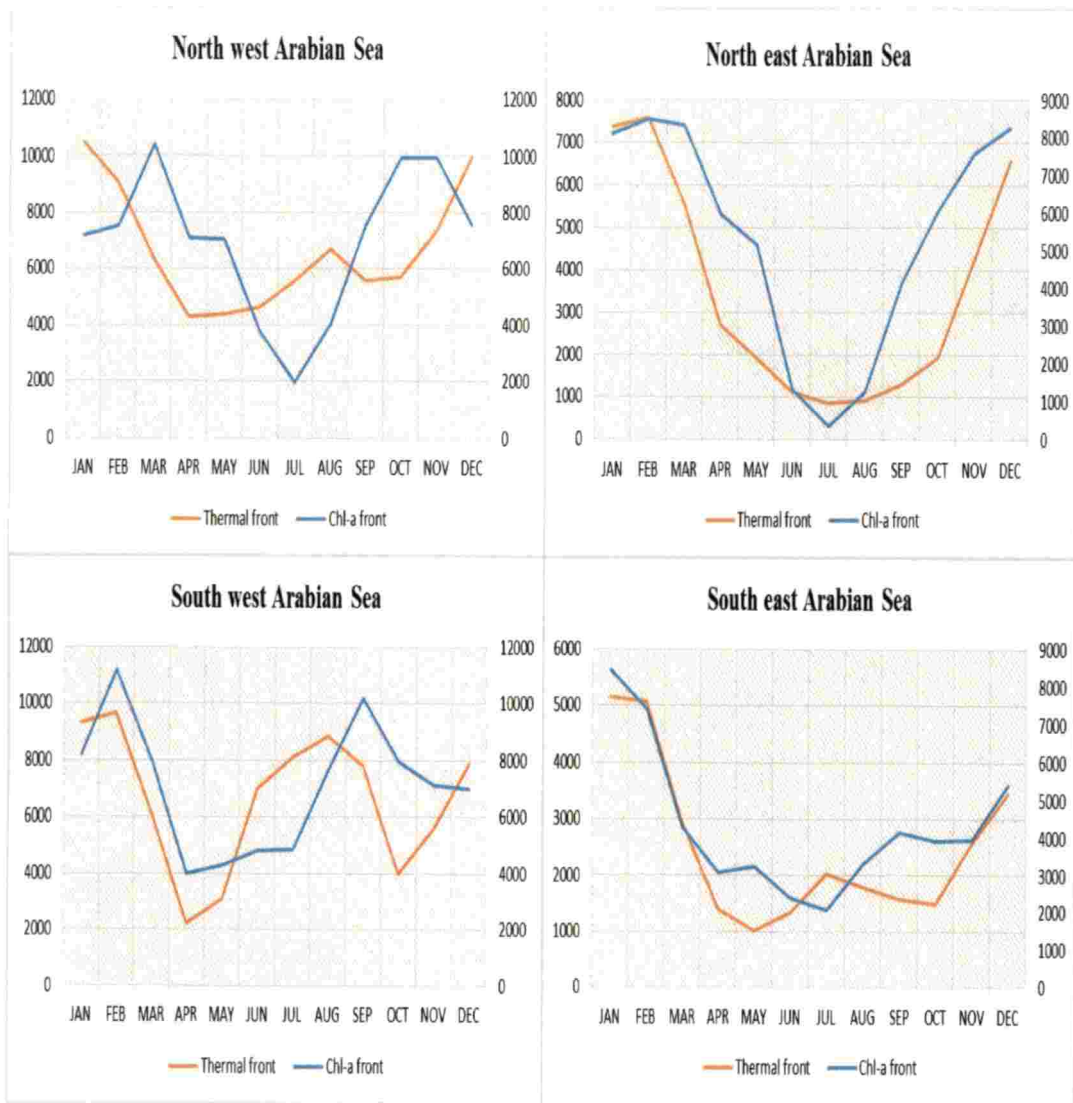


**Figure 19: Climatology of variability in frontal area in the north west, north east, south west and south eastern Arabian Sea**

Despite of the area, the maximum thermal as well as chlorophyll frontal occurrences were observed during the north east monsoon. Minimal thermal frontal coverage was observed during the pre-monsoon period for the north western, south

western and south eastern Arabian Sea and during summer monsoon period in the north eastern Arabian Sea. In the case of minimal chlorophyll frontal occurrence, it was observed during July for the north eastern, northwestern and south eastern Arabian Sea and during April in the south western Arabian Sea. This study revealed high correlation among thermal and Chl-a frontal area in the north east (86%) and south east (91%) Arabian Sea. Correlation values were low among thermal and Chl-a frontal area in the north west (20%) and south west (59%) Arabian Sea compared to eastern Arabian Sea. This indicated that the pattern of spatial variability in frontal zones in the eastern Arabian Sea is different compared to the western Arabian Sea. A detailed study on the spatial variation in thermal and chlorophyll frontal occurrences in the Arabian Sea based on monthly climatology data (fig. 19) is presented below.

### **North western Arabian Sea**

In the north western Arabian Sea, the thermal frontal area increased during the winter monsoon period and attained its maximum value in January. Another episode of increase in thermal frontal area in the NW Arabian Sea occurred during the summer monsoon period and it attained a secondary and less prominent peak by the month of August. However, the pre and post monsoon periods experienced a decline in thermal frontal area with a steady decrease during pre-monsoon period, recording the lowest thermal frontal coverage during April.

Chlorophyll frontal area in the NW Arabian Sea recorded a slightly different pattern. The chlorophyll frontal area started its increasing phase from January, attaining its peak value by March. Then a steady decline in the chlorophyll frontal area was observed from March to July, and recorded the lowest frontal area. A secondary increase in chlorophyll frontal area started from July, reaching its second highest value during October-November period.

### **South western Arabian Sea**

In the south west Arabian sea, thermal frontal area increased from October and attained its highest value by the month of February. Then from February onwards the thermal frontal area started to decline steadily and attained its lowest value during April. Then a secondary increase in thermal frontal area started during April and the thermal frontal area peaked by the month of August. Then again thermal frontal area decreased from August to September.

Chlorophyll frontal area recorded a slightly different pattern in the south western Arabian Sea. The chlorophyll frontal area increased from December and reached its highest value by February. Then starting from February the chlorophyll frontal area decreased and attained its lowest value by April. Then a secondary increase in chlorophyll frontal area started from April and it attained its second highest value by the month of September.

### **North eastern Arabian Sea**

In the north eastern Arabian Sea, both the thermal and chlorophyll frontal area started to increase from July and attained its peak value during February. Then, starting from March, both thermal and chlorophyll frontal area marked the beginning of a declining phase which persisted throughout the pre-monsoon and summer monsoon periods, attaining its lowest value by the end of July.

### **South eastern Arabian Sea**

In the south east Arabian Sea, the thermal frontal area increased from October and attained its peak value by January. Then thermal frontal area decreased steadily from March and attained its lowest value by the month of May. The secondary increase in thermal frontal area started from May and attained its secondary peak by July. From July to October, again the thermal frontal area decreased, recording its second lowest value in October.

Chlorophyll frontal area in the south eastern Arabian Sea increased steadily from November and attained its maximum frontal coverage by the month of January. From January to July, the chlorophyll frontal area experienced a steady decrease, with its lowest value by July. The secondary increase in chlorophyll frontal area occurred from July, which persisted throughout the summer monsoon period and attained its secondary peak by September. Chlorophyll frontal area again decreased from September to November.

#### 4.4 SPATIAL DISTRIBUTION OF FRONTAL AREA IN THE ARABIAN SEA – A SEASONAL ANALYSIS

The monthly climatology study of the thermal and chlorophyll frontal area in the north eastern, north western, south eastern and south western Arabian Sea clearly brought out patterns of seasonal variability in the total frontal coverage. So, further analysis was done on a seasonal scale for clearly identifying seasonal trends in spatial distribution of frontal area in the Arabian Sea and understanding the factors governing such trends.

##### **North east monsoon**

Seasonal distribution of the percentage of total frontal area brought out maximum of thermal (fig. 20) as well as chlorophyll (fig. 21) frontal occurrences during the north east monsoon. In case of thermal fronts, maximum occurrence during the north east monsoon was in the north western Arabian Sea (33%). Whereas in case of chlorophyll fronts, maximum frontal occurrences were almost equally distributed in the south west (27%), north east (26.3%) and in the north western Arabian Sea (26%). From the analysis it was evident that higher chlorophyll frontal areas coincided with high Chl-a distribution. Also, higher thermal frontal occurrence was observed in areas with higher SST gradient. This can be sufficiently substantiated using the climatological observations of the upper oceanographic parameters in the Arabian Sea. During north east monsoon, the northern Arabian Sea recorded lower values of SST compared to other areas. High Chl-a content was also observed in the area during the same period. The reason for higher productivity in the northern Arabian Sea during north east monsoon is discussed below.

During north east monsoon, insolation rates are very low resulting in very low sea surface temperature. The winds during north east monsoon are generally gentle and are north easterly in nature. These trade winds brings in cool and dry continental air to the northern Arabian Sea. These cooler winds enhances the evaporation rates and



accelerates the surface cooling of northern Arabian Sea. The reduction in sea surface temperature due to this evaporative cooling is estimated at about 3°C (Kumar and Prasad, 1996). The already lower sea surface temperature along with the enhanced cooling by the trade winds results in an increase in salinity causing the surface waters of the northern Arabian Sea to densify. (Kumar and Prasad, 1996). This densification of the surface waters generates a convective mixing process. Thus the nutrient lacking surface waters goes down, resulting in a vertical movement of less denser, nutrient rich water from the base of mixed layer to the surface of northern Arabian Sea. This causes higher SSHA values in the northern Arabian Sea during this period. This is the reason behind the enhanced productivity along the northern Arabian Sea during north east monsoon. (Madhupratap *et al.*, 1996)

### **South west monsoon**

During south west monsoon, the highest incidence of thermal (48.9%) and chlorophyll (45.6%) fronts were in the south western Arabian Sea. During this period, low temperatures as well as chlorophyll blooms occurred in the Arabian Sea. Analysis of SSHA revealed very low values near the eastern and western Arabian Sea during this period, which can be attributed to possible upwelling in the region. Wind velocities in the Arabian Sea were also higher compared to other seasons, especially in the western Arabian Sea which is known to intensify upwelling in the region. Surface current velocity plots during south west monsoon showed higher values in the western Arabian Sea, which peaked during July coinciding its occurrence with the Findlater jet. These facts also contribute to upwelling and hence an increased productivity in the region.

South west monsoon is generally characterised by very high wind speeds (Findlater jet). This high wind speed induces a cyclonic wind stress curl on the north of the Findlater jet (north western Arabian Sea) (Bauer *et al.*, 1991). This generates a divergent Ekman transport in the north western Arabian Sea through Ekman pumping.

This results in vertical transport of nutrients from sub surface waters to the surface of north western Arabian Sea, resulting in high productivity in the region (Prasannakumar *et al.*, 2000, Madhupratap *et al.*, 2001). In addition to this, during south west monsoon period, anti-cyclonic wind stress curl is induced to the south of the Findlater jet (south western Arabian Sea). This creates a convergent Ekman transport that results in deepening of the mixed layer depth (MLD) finally resulting in lower nutrient availability along the surface waters of the south west Arabian Sea. But this does not answer the higher productivity trend and hence higher frontal area found in the south west Arabian Sea during this period. Lateral convection is the reason for this increased productivity in south western Arabian Sea (Kumar *et al.*, 2001). During south west monsoon, large scale coastal upwelling and eddy advection occurs along the Somalian coast (Brock *et al.*, 1992; Rixen *et al.*, 1996). These eddies transports large amounts of advected, cold, nutrient rich subsurface water from depths of about 100-150m to the surface of Somalia coast with very high speeds ( $>200$  cm/s) (Schott *et al.*, 1990; Baars *et al.*, 1994; Fischer *et al.*, 1996) . But the Somalia current is very fast during this period due to the influence of the Findlater jet which reduces the residence time of upwelled waters near the Somalia coast, ultimately resulting in lower primary productivity in the region (Wiebinga *et al.*, 1997). Thus most of the unexploited nutrients reaches the south west Arabian Sea through lateral advection from the Somalian upwelling zones. This results in higher productivity in the south western Arabian Sea compared to north west (Prasannakumar *et al.*, 2000).

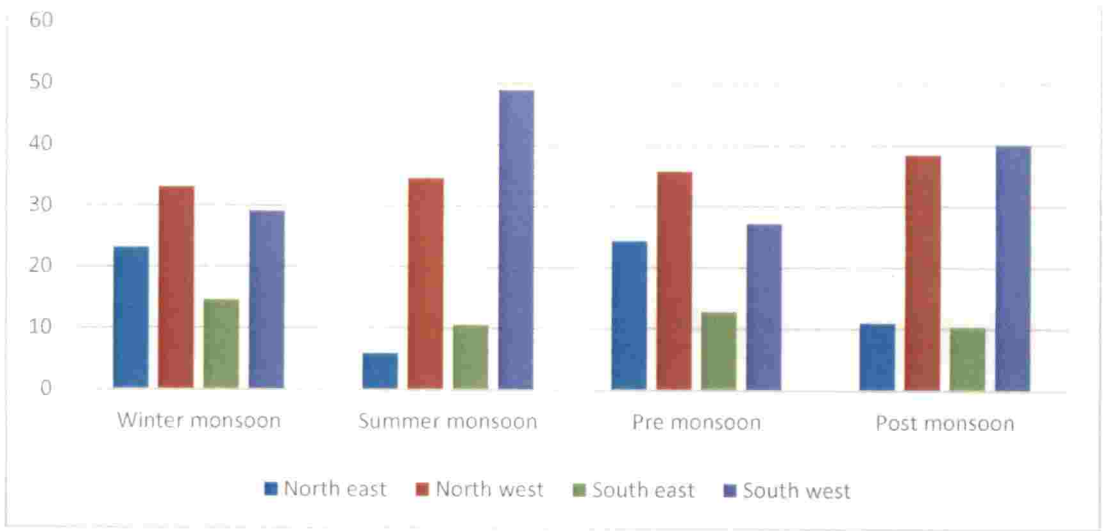


**Figure 20: Percentage spatial distribution of thermal frontal area over Arabian Sea**

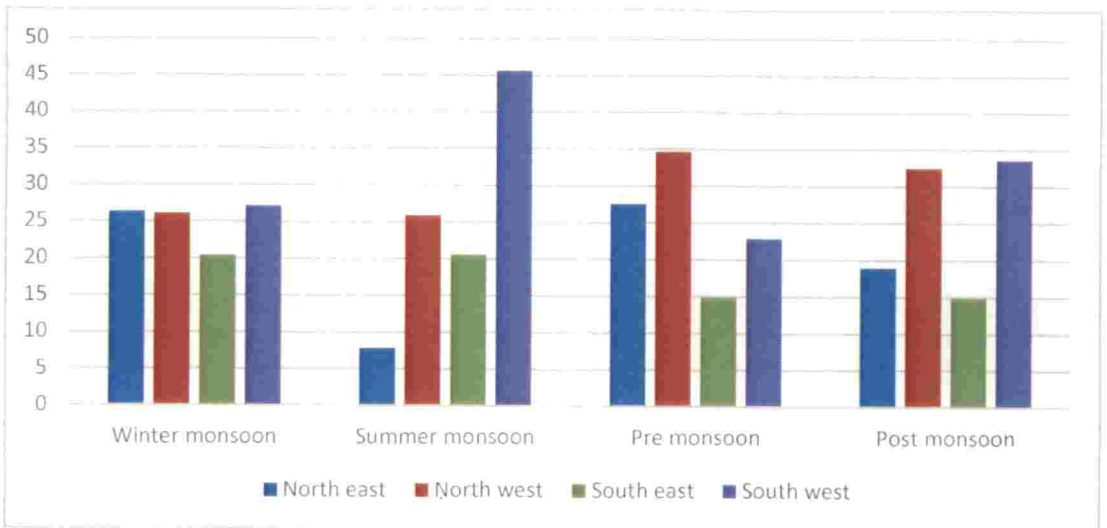


**Figure 21: Percentage spatial distribution of chlorophyll frontal area over Arabian Sea**

## **Pre-monsoon**

During pre-monsoon season, maximum thermal (35.7%) and chlorophyll (34.6%) frontal occurrences takes place in the north western Arabian Sea. During this period the northern Arabian Sea is characterised by cool waters, and high chlorophyll persisted in the northern Arabian Sea when compared to other regions. Analysis of wind pattern also revealed a change in its direction from north easterlies to south westerlies which were strong in the western and northern Arabian Sea during April and they strengthened during May. SSHA was also high in the western Arabian Sea during this period.

During pre monsoon season, intense heating of the Arabian Sea takes place with highest insolation rates of about  $260\text{W/m}^2$ . During this period, since availability of sunlight is not a limiting factor for primary productivity, availability of nutrients is the predominant factor deciding the primary productivity of Arabian Sea. Persistence of higher insolation rates over Arabian Sea results in higher sea surface temperature, causing the surface waters to stratify. This stratified surface water, in the presence of low wind speeds prevents vertical mixing and vertical transport of nutrients to the surface. Since current velocity is very low during this period, any chance for lateral advection is also ruled out, making pre monsoon season one of the least productive seasons for the Arabian Sea.

## **Post-monsoon**

During the post monsoon season, the highest thermal (40%) and chlorophyll (33.6%) frontal incidence was observed in the south west Arabian Sea. This was followed by the north western region with 38.4% of total thermal and 32.48% of total chlorophyll frontal area during the post monsoon period. During post-monsoon season, the entire western Arabian Sea experienced lower temperatures. Chlorophyll values were also higher in the western Arabian Sea during this period. Sea surface height anomaly along western and eastern Arabian Sea exhibited very low negative values

which may be due to upwelling in the region. The current velocity along the south western surface waters recorded high values during the post monsoon periods. All these conditions can induce higher productivity in the south western Arabian Sea during post-monsoon period.

#### 4.5 INTER-ANNUAL VARIABILITY IN THERMAL AND CHLOROPHYLL FRONTAL AREA

This section investigates the pattern of variability in thermal as well as chlorophyll frontal area on an inter-annual time scale. Spatial and temporal variability of frontal occurrences for the north western, north eastern, south western as well as in the south eastern regions of Arabian Sea were also analyzed.

##### 4.5.1 Inter-annual variability of thermal and chlorophyll frontal area in the Arabian Sea

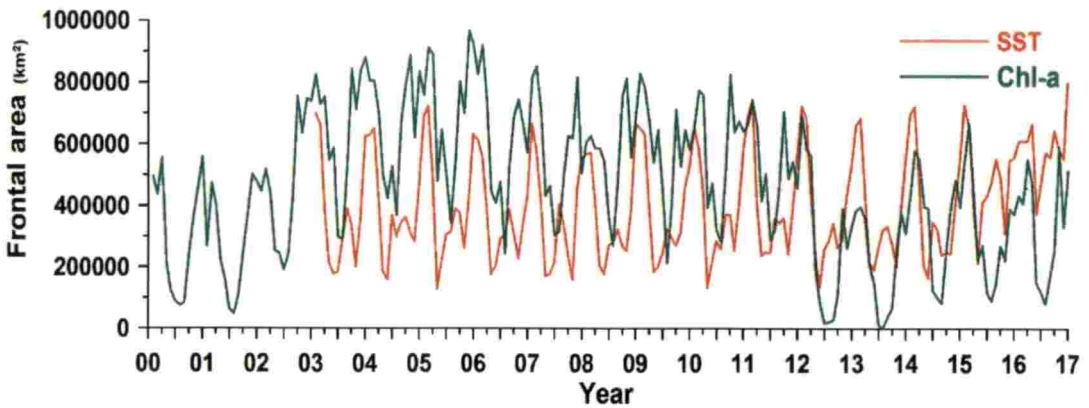


**Figure 22: Time series plot of thermal and chlorophyll frontal area in Arabian Sea**

Analysis of time series data of thermal frontal area revealed a bimodal oscillation pattern for the years from 2002 to 2014 (fig. 22). This pattern is not observed from mid-2015 as an increasing trend replaces this clear bimodal variability. Hence, this variation observed on thermal frontal occurrence is quite unusual.

Analysis of inter annual variability of chlorophyll fronts from 2000-2016 (fig. 22) indicated an overall decreasing trend in chlorophyll frontal area with high variability in patterns over the years. From 2000 to 2002, inter annual variability of

chlorophyll frontal area showed patterns similar to its climatology, with maximum value in February, then a decrease in values till July and then again an increase in chlorophyll frontal area. From 2002 to 2011, the chlorophyll frontal area increased such that the entire chlorophyll frontal distribution shifted to higher values during the period. During the mid-2012 to 2016, the entire chlorophyll frontal area got shifted to a smaller scale, with very low values during the summer monsoon period.

As per the annual Global Climate Report for 2016 generated by National Centers for Environmental Information under National Oceanic and Atmospheric Administration (NOAA), 2016 is reported as the warmest year in NOAA's 137 year series. The average global temperature over land and ocean surface for 2016 was estimated at about  $0.94^{\circ}\text{C}$ , above the entire 20<sup>th</sup> century average value of  $13.9^{\circ}\text{C}$ . The report also highlighted 2015 as the second warmest year on the globe with average global temperature over land and ocean surfaces estimated at  $0.04^{\circ}\text{C}$  above the 20<sup>th</sup> century average. This record warming trend of the globe can be attributed to the immense increase in the global sea surface temperatures. During 2015, the annually averaged sea surface temperature anomaly for the northern hemisphere was estimated as  $+0.86 (\pm 0.16)^{\circ}\text{C}$  above the 20<sup>th</sup> century average, which was the warmest SST among the consecutive 137 years. Higher sea surface temperatures were recorded across the globe, with sea surface temperature of December reported at  $0.61^{\circ}\text{C}$  above 20<sup>th</sup> century average. This strong warming trend can be attributed to the persistence of a near-record strong El Nino conditions during 2015-2016 (NOAA, 2017b). In addition to the strong El Nino event, these abnormalities can also be attributed to a strong negative phase of Indian Ocean Dipole (IOD) that occurred during this period attaining its lowest values in July and in September (WMO, 2016). The unusual increasing trend in thermal frontal area as observed in its time series analysis can be attributed to the occurrence of the above mentioned extreme events. The sudden decrease in overall values of chlorophyll frontal area during 2012 to 2016 can also be attributed to the higher anomalies in globally averaged temperatures during these

years, since the ranks among the top nine years with highest temperature anomalies (table. 2).

**Table 2: List of the annually averaged combined global land and ocean temperatures and their anomaly for the 9 warmest years on record**

RANK 1 = WARMEST PERIOD OF RECORD: 1880–2016	YEAR	ANOMALY °C	ANOMALY °F
1	2016	0.94	1.69
2	2015	0.90	1.62
3	2014	0.74	1.33
4	2010	0.70	1.26
5	2013	0.67	1.21
6	2005	0.66	1.19
7	2009	0.64	1.15
8	1998	0.63	1.13
9	2012	0.62	1.12



#### **4.5.2 Inter-annual variability of thermal and chlorophyll frontal area within the north west, north east, south west and south east Arabian Sea**

In the north western Arabian Sea, values of thermal and chlorophyll frontal areas followed similar pattern in variability with coinciding higher and lower values of thermal and chlorophyll frontal areas (fig. 23). A similar trend with coinciding periods of higher and lower values of chlorophyll and thermal frontal area also occurred in the south west Arabian Sea. But the chlorophyll frontal area experienced a sudden decrease in overall values from July 2012 onwards. The chlorophyll frontal area during this period still preserved the same pattern as of thermal frontal area, but with reduced overall values.

The pattern of occurrence of thermal and chlorophyll frontal area in the north east and south east Arabian Sea were different from that of the western Arabian Sea. Frontal occurrences in the north eastern and south eastern Arabian Sea did not exhibit much correlation among them as in the western Arabian Sea. These results supports our earlier observation that the pattern of variability in frontal area in the western Arabian Sea is different from that of the eastern Arabian Sea.

The time series analysis of spatial variability in thermal and Chl-a frontal area in the Arabian Sea also indicated that higher correlation existed among the thermal and Chl-a frontal occurrence in the north east (66%) and south east (46%) Arabian Sea compared to north west (7%) and south west (30%) Arabian Sea. These results reinforces our earlier finding that the pattern of variability in frontal zones in the east Arabian Sea is different from the west Arabian Sea.

The unusual increasing trend in the total thermal frontal area which was observed in the time series analysis of frontal area in the Arabian Sea during 2015 to 2016, reflected only in the thermal frontal area trend in the north eastern and south eastern Arabian Sea. The overall decrease in the chlorophyll frontal areas from mid-2012 observed in the time series analysis reflected in the north eastern, south western

and in the south western Arabian Sea, which was much more pronounced in the southern Arabian Sea.

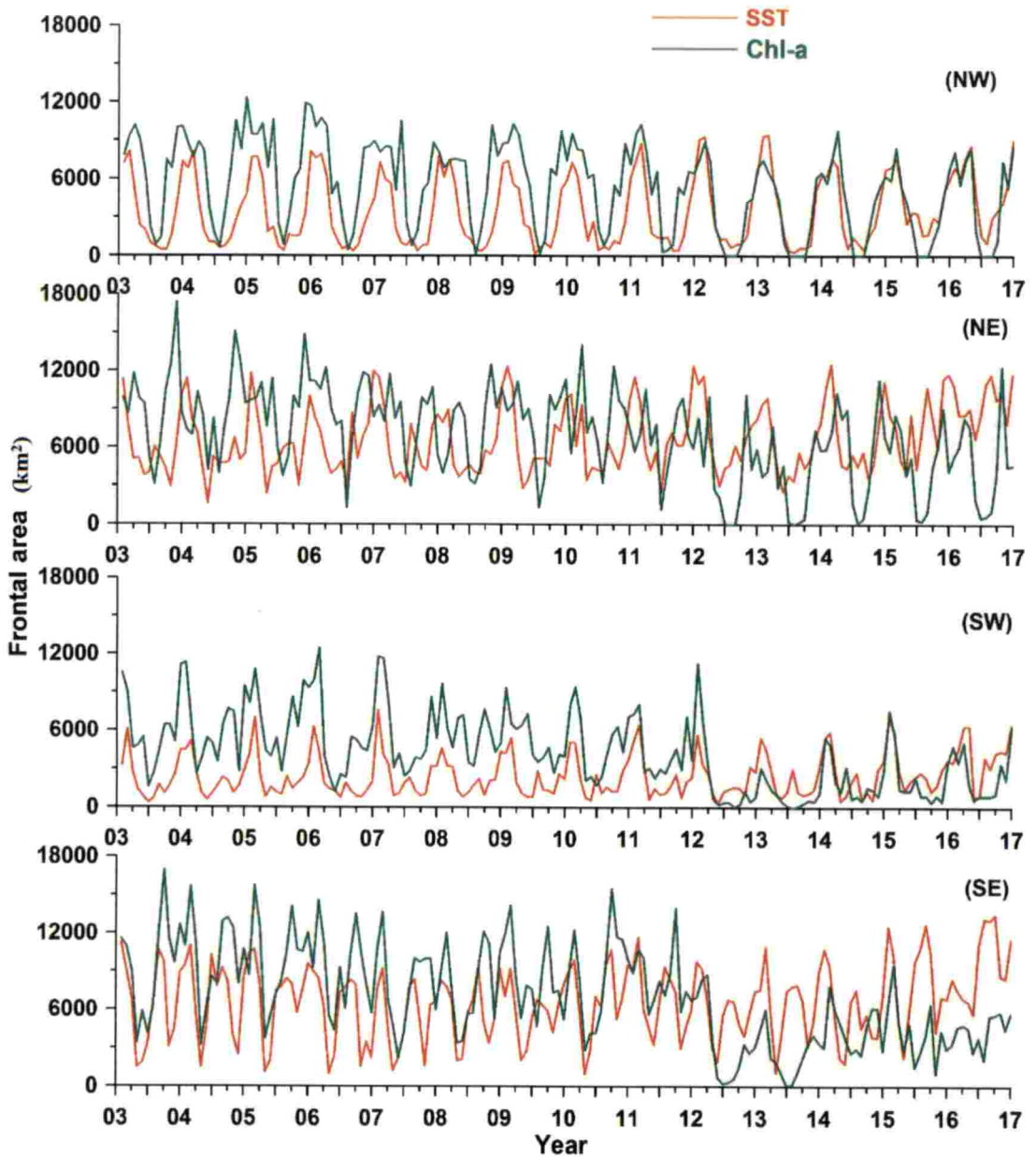


**Figure 23: Time series plot of thermal and chlorophyll frontal area in the north western, north eastern, south western and south eastern Arabian Sea**

#### 4.6 RELATION BETWEEN FRONTAL AREA AND FISHERY DISTRIBUTION ALONG THE WEST COAST OF INDIA

In this section an attempt was made to relate the pattern of variability in total monthly fish landings recorded at various landing centres along the west coast of India, with the occurrence of thermal and chlorophyll fronts within the respective exclusive economic zone.

The landing centres taken into consideration include the maritime states and union territories of Kerala, Karnataka, Goa, Maharashtra, Gujarat and Daman and Diu. The landing data as well as the total effort of each gear was provided by CMFRI from 2007 onwards since monthly fish landings are available only from 2007 onwards.

A shapefile of EEZ was generated as mentioned in section 3.3.4 and the values of both thermal and chlorophyll frontal area within the EEZ was extracted as per procedure mentioned in section 3.3.5. This was done so as to get a more reliable relationship between fish catch and frontal area, since majority of the fishing activity is carried out within the EEZ. The CPUE data as calculated in section 3.3.6 was used in the analysis so as to get a more ideal representation of the total fish landings along the west coast of India. The fishing vessels are broadly classified as mechanised, motorised and traditional or non-mechanised sectors. Among these three sectors, the major contribution towards the fish landings is from the mechanised sector compared to motorised and non-motorised sectors (CMFRI (2013, 2017); Pillai *et al.*, 2009). So this study was conducted utilizing the CPUE (in hours) for mechanised sector only.

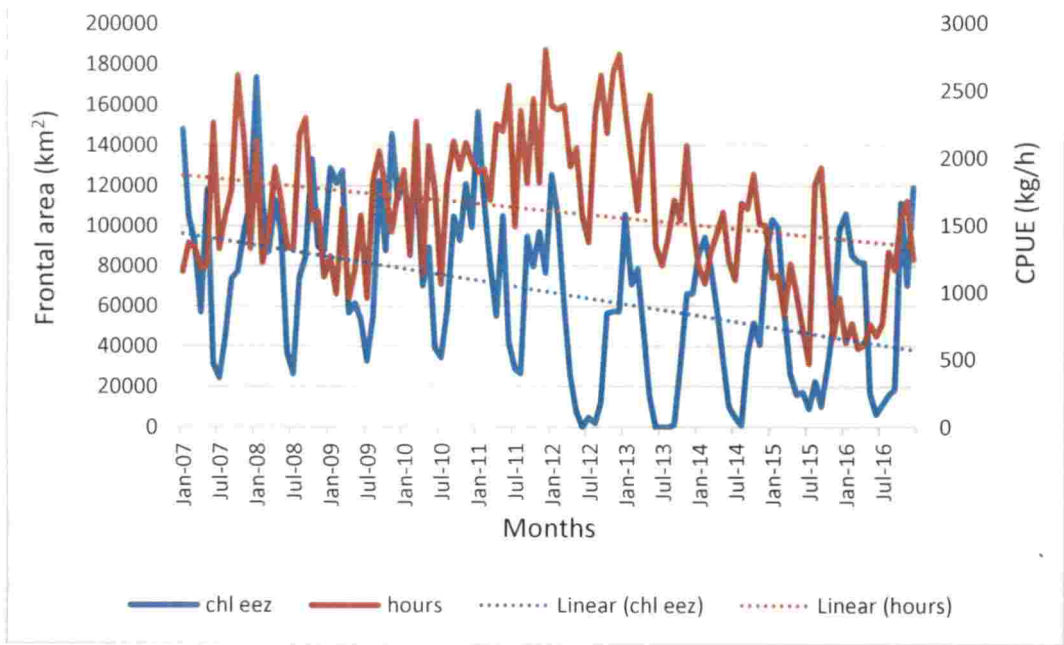


**Figure 24: Time-series plot of chlorophyll frontal area and CPUE in hours**

The time series plot between chlorophyll frontal area (within the EEZ) and CPUE (in hours) along the west coast of India (fig. 24) revealed an overall decreasing trend in both of the variables. Both the chlorophyll frontal area and fish landings exhibited similarity in the pattern of variation over time. Both the chlorophyll frontal area and CPUE showed a sudden decrease in values from early 2008 onwards. This decrease in the variables persisted till mid-2009. Then chlorophyll frontal area increased from July 2009 and it continued till January 2011. But the CPUE continued this increasing trend till the start of 2012. The chlorophyll frontal area then decreased from 2011 onwards, and continued recording lower values till 2017. CPUE also followed the same trend with a decrease in values from 2012 to 2017. This indicates that the variation in the CPUE is similar to that of the chlorophyll frontal occurrence.

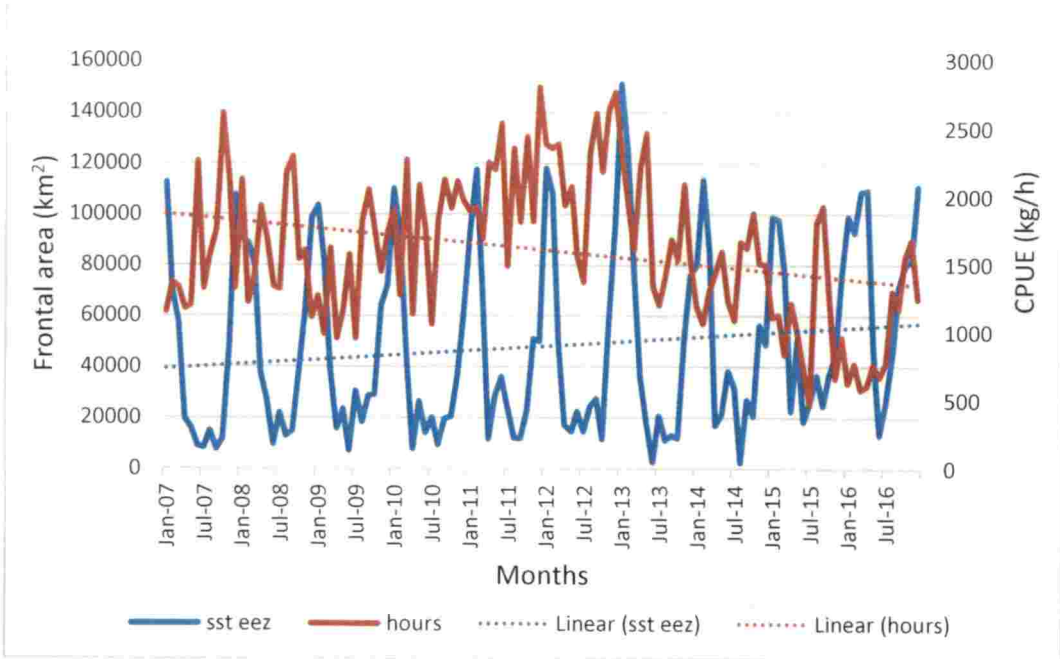


**Figure 25: Time-series plot of thermal frontal area and CPUE in hours**

A time series analysis of thermal frontal area and CPUE was conducted (fig. 25). CPUE along the west coast of India showed an overall decreasing trend, whereas thermal frontal area within the EEZ indicated an overall increasing trend over time. Both the thermal frontal area and CPUE started decreasing by late 2007. From June 2009 onwards, both the thermal frontal area and CPUE increased in value which persisted till early 2013. Again from 2013 onwards, the thermal frontal area and CPUE started decreasing, indicating similarity in their pattern of variability over time.

These results implies that the occurrence of frontal zones in the Arabian Sea has some impact on the fishery distribution along the west coast of India. As a future extension of this study, frontal occurrence could be related to standardized CPUE data for individual species so as to find out species specific response to frontal formation in the Arabian Sea.

# SUMMARY AND CONCLUSION

## CHAPTER 5

### SUMMARY AND CONCLUSION

Arabian Sea is considered as one among the most productive marine ecosystems of the world, with increased productivity due to enhanced upwelling and Ekman pumping during the south west monsoon period and higher productivity due to effect of winter cooling during the north east monsoon period. The present study was conducted in the eastern Arabian Sea for identifying patterns in the inter-annual variability in thermal as well as chlorophyll frontal area. This study also focuses on the spatio-temporal variability in the frontal zones in different regions of the Arabian Sea. The possible impacts of extreme events as well as the relation between frontal occurrence and marine fishery distribution was also investigated.

The climatology study of the thermal frontal zones in the Arabian Sea revealed that the occurrence of the thermal frontal area peaked during the winter monsoon period (0.5 – 0.6 million km<sup>2</sup>) followed by a secondary peak during the summer monsoon season (0.3 – 0.4 million km<sup>2</sup>). Thermal fronts have their least incidence (0.2 – 0.3 million km<sup>2</sup>) during pre and post monsoon period. However chlorophyll frontal area displayed a slightly different pattern with highest incidence during winter monsoon (0.5- 0.6 million km<sup>2</sup>) and least incidence during summer monsoon periods (0.2 – 0.3 million km<sup>2</sup>). Chlorophyll fronts have their moderate incidence during pre and post monsoon periods (0.4 – 0.5 million km<sup>2</sup>). Climatology analysis of spatial variation in frontal area also exhibited maximum frontal occurrence during north east monsoon and it brought out clear seasonal patterns in the frontal occurrence. The study also indicated that the pattern of variability in frontal zones in the eastern Arabian Sea is different from that of the western Arabian Sea.

Since the spatial variability in the of the frontal zones displayed season patterns, a seasonal study on frontal occurrence was conducted which indicated that the maximum frontal incidence during north east monsoon was in the northern Arabian Sea. The main reason for the higher incidence of frontal zones in the area

during winter monsoon period is due to the effect of north easterly trade winds. These winds bring cool and dry continental air to the northern Arabian Sea resulting in lower SST and an enhanced evaporative cooling of the sea surface. This in turn results in densification of surface waters (Kumar and Prasad, 1996), generating a convective mixing process. This causes nutrient lacking surface waters to move deeper, resulting in upward movement of nutrient rich subsurface water to the surface causing higher productivity (Madhupratap *et al.*, 1996) and hence increased frontal occurrence. The study also indicated that the highest incidence of frontal zones during south west monsoon season was in the south west Arabian Sea. Lateral convection from the Somalian upwelling zones during this period is the reason behind this phenomenon (Kumar *et al.*, 2001). Somalia experiences very strong coastal upwelling and eddy convection during summer monsoon period (Brock *et al.*, 1992; Rixen *et al.*, 1996). These eddies transport huge amounts of nutrients from subsurface waters to the surface at very high speeds. But the Findlater jet existing during the period reduces the residence time of nutrients in the surface waters near Somalia coast and causes the major part of unutilized nutrients to reach the south western Arabian Sea due to very swift Somalia current. This causes higher productivity in the south west Arabian Sea (Prasannakumar *et al.*, 2000) and hence higher incidence of frontal zones during the summer monsoon season.

Seasonal variability in frontal area indicated third highest frontal occurrence during the post monsoon season with highest incidence in the western Arabian Sea. This can be attributed to favourable conditions in the western Arabian Sea during this period as observed from the climatology analysis of the upper ocean parameters in the Arabian Sea. During this period, the entire western Arabian Sea recorded lower temperatures with higher Chl-a content. SSHA was also highly negative which can be an indication of upwelling in the area. Swift surface currents during this period also supports higher productivity in the western Arabian Sea during post monsoon and hence higher frontal occurrence. The study showed least frontal occurrence during the pre-monsoon period which can be attributed to the higher insolation rates persisting over the entire Arabian Sea during the period. This causes the surface waters to stratify, inhibiting vertical mixing and movement of nutrients



to the surface. Very low surface currents persisting during the period rules out any chance for lateral advection making Arabian Sea one of the least productive areas and hence least frontal incidence during pre-monsoon season.

Analysis of inter-annual variability of thermal frontal area displayed a bimodal oscillation pattern which existed till 2014. From mid-2015, this bimodal pattern was replaced by an increasing trend in thermal frontal area, which can be attributed to a near record strong El-Nino (NOAA, 2016) and to a very strong negative IOD (FAO, 2016) which persisted during 2015-2016 period. Time series analysis of chlorophyll frontal area indicated an overall decrease in its values from 2012-2016, which can be attributed to the fact that those years ranked among the top 9 warmest years in the 1880-2016 series. Time series analysis was conducted for identifying patterns in spatial variability of thermal and chlorophyll fronts. The findings revealed that in the north eastern and south eastern Arabian Sea, thermal and chlorophyll fronts followed same pattern of variation with higher correlation among themselves, unlike in the north western and south western Arabian Sea where they followed different patterns with lower value of correlation. This supports the earlier finding that the pattern of variability of frontal zones in the western Arabian Sea is different from the eastern Arabian Sea. The analysis revealed that the increasing trend in thermal frontal area in the Arabian Sea from mid-2015 onwards, reflected in the frontal variability of the eastern Arabian Sea (north east and south east Arabian Sea) only. From the study it was also evident that the sudden drop in Chl-a frontal area from mid-2012 onwards was more pronounced in the southern Arabian Sea (south east and south west Arabian Sea) compared to other regions.

Time series plot between CPUE (in hours) along the west coast of India and chlorophyll frontal occurrence within the EEZ revealed similar pattern of variability over time with an overall decreasing trend in both the variables. The chlorophyll frontal area and CPUE showed a sudden decrease in values from 2008 onwards which persisted till July 2009. Then both the variables exhibited an increase in values which continued till January 2011 for chlorophyll frontal area and early 2012

for CPUE. Then both the variables decreased till 2017. Time series plot between CPUE (in hours) and thermal frontal area showed a decrease in values from late 2007 to mid-2009. From mid-2009 onwards both the variables increased in values, which extended till early 2013. Then from 2013 onwards both the variables started decreasing, indicating similarity in pattern of variability over time.

## REFERENCES

## CHAPTER 6

### REFERENCES

- Ainley, D. G., Dugger, K. D., Ford, R. G., Pierce, S. D., Reese, D. C., Brodeur, R. D., Tynan, C.T. and Barth, J. A. 2009. Association of predators and prey at frontal features in the California current: competition, facilitation, and co-occurrence. *Mar. Ecol. Prog. Ser.* 389:271–294.
- Al Saafani, M. A., Shenoi, S. S. C., Shankar, D., Aparna, M., Kurian, J., Durand, F. and Vinayachandran, P.N., 2007. Westward movement of eddies into the Gulf of Aden from the Arabian Sea. *J. Geophys. Res.* 112(C11):1-12
- Allen, M. R., Barros, V. R., Broome, J., Cramer, W., Christ, R., Church, J. A., Clarke, L., Dahe, Q., Dasgupta, P., Dubash, N. K. and Edenhofer, O. 2014. IPCC Fifth Assessment Synthesis Report-Climate Change 2014 Synthesis Report: 40p.
- APDRC [Asia-Pacific Data-Research Center]. 2017. APDRC home page [on line]. Available: <http://apdrc.soest.hawaii.edu/index.php> [5 Jul. 2017].
- Baars, M. A., Bakker, K. M. J., de Bruin, T. F., van Couwelaar, M., Hielde, M. A., Kraaij, G. W., Oosterhuis, S. S., Schalk, P. H., Sprong, I., Veldhuis, M. J. W., Wiebinga, C. J. and Witte, J. I. J. 1994. Seasonal fluctuations in plankton biomass and productivity in the ecosystems of the Somali current, Gulf of Aden and southern Red Sea. In: Baars, M.A. (ed.), *Monsoons and Pelagic Systems, Cruise Reports Netherlands Indian Ocean Programme*, National Museum of Natural History, Leiden, pp. 13–34.
- Bakun, A. 2006. Fronts and eddies as key structures in the habitat of marine fish larvae: opportunity, adaptive response and competitive advantage. *Scientia Marina*. 70(S2):105-122.

- Bakun, A., Black, B. A., Bograd, S. J., Garcia-Reyes, M., Miller, A. J., Rykaczewski, R. R. and Sydeman, W. J. 2015. Anticipated effects of climate change on coastal upwelling ecosystems. *Current Climate Change Reports*. 1(2): 85-93.
- Banase K. and McClain, C. R. 1986. Winter blooms of phytoplankton in the Arabian Sea as observed by the coastal zone color scanner. *Mar. Ecol. Prog. Ser.* 34 (3):201-211.
- Banase, K. 1959. On upwelling and bottom-trawling off the southwest coast of India. *J. Mar. Biol. Ass. India*. 1(1):33-49.
- Banase, K. 1968. Hydrography of the Arabian Sea shelf of India and Pakistan and effects on demersal fishes. *Deep Sea Res. Part I*. 15 (1):45-48.
- Banase, K. and English, D. C. 2000. Geographical differences in seasonality of CZCS-derived phytoplankton pigment in the Arabian Sea for 1978–1986. *Deep Sea Res. Part II: Topical Studies in Oceanography*. 47(7): 1623-1677.
- Bauer, S., Hitchcock, G. L., and Olson, D. B. 1991. Influence of monsoonally forced Ekman dynamics of upper layer depth and phytoplankton biomass distribution in the Arabian Sea. *Deep Sea Res.* 38(5):531-553.
- Begg, G. S. and Reid, J. B. 1997. Spatial variation in seabird density at a shallow sea tidal mixing front in the Irish Sea. *ICES J. Mar. Sci.* 54(4):552–565.
- Behrenfeld, M. J., Randerson, J. T., McClain, C. R., Feldman, G. C., Los, S. O., Tucker, C. J., Falkowski, P. G., Field, C. B., Frouin, R., Esaias, W. E., Kolber, D. D. and Pollack, N. H. 2001. Biospheric primary production during an ENSO transition. *Science*. 291(5513):2594- 2597.
- Belkin, I. 2002. New challenge: ocean fronts. *J. Mar. Syst.* 37(1-3):1-2.

- Belkin, I. M. and O'Reilly, J. E. 2009. An algorithm for oceanic front detection in chlorophyll and SST satellite imagery. *J. Mar. Syst.* 78(3):319-326.
- Belkin, I. M., Cornillon, P.C. and Sherman, K. 2009. Fronts in large marine ecosystems. *Prog. Oceanogr.* 81(1):223- 236.
- Bensam, P. 1964. Growth variation in oil sardine. *Indian J. Fish.* 11 (2): 699–708.
- Bertignac, M., Lehodey, P. and Hampton, J. 1998. A spatial population dynamics simulation model of tropical tunas using a habitat index based on environmental parameters. *Fish. Oceanogr.* 7:326-334.
- Bhattathiri, P. M. A., Pant, A., Sawant, S. S., Gauns, M., Matondkar, S. G. P. and Mahanraju, R. 1996. Phytoplankton production and chlorophyll distribution in the eastern and central Arabian Sea in 1994-1995. *Curr. Sci.* 71(11):857-862
- Bhaware, B. G., Kurhe, A. R. and Mane, U. H., 2013. The Catch per Unit Efforts (CPUE) through Validations of Potential Fishing Zone Advisories along Sindhudurg District Coast of Maharashtra State. *Int. J. Pharm. Biol. Sci.* 3(01):20-29
- Bourne, W. and Clark, G. 1984. The occurrence of birds and garbage at the Humboldt Front off Valparaiso, Chile. *Mar. Pollut. Bull.* 15(9):343–344.
- Brock, J. C., McClain, C. R., Anderson, D. M., Prell, W. L. and Hay, W. W. 1992. Southwest Monsoon circulation and environments of recent planktonic foraminifera in the northwestern Arabian Sea. *Paleoceanography.* 7(6):799-813.
- Brock, J. C., McClain, C. R., Luther, M. E. and Hay, W. W. 1991. The phytoplankton bloom in the northwestern Arabian Sea during the southwest monsoon of 1979. *J. Geophys. Res.* 96(C11): 20623-20642.

- Butler, M. J. A., Mouchot, M. C., Barale, V. and LeBlanc, C. 1988. The application of remote sensing technology to marine fisheries: an introductory manual. FAO, Fisheries Technical Paper no. 295, 165p.
- Carman, V. G., Acha, E. M., Maxwell, S. M., Albareda, D., Campagna, C. and Mianzan, H. 2014. Young green turtles, *Cheloniemydas*, exposed to plastic in a frontal area of the SW Atlantic. *Mar. Pollut. Bull.* 78(1):56-62.
- Cayula, J. F. and Cornillon, P. 1992. Edge detection algorithm for SST images. *J. Atmos. Ocean. Technol.* 9(1):67-80.
- Cayula, J. F. and Cornillon, P. 1995. Multi-image edge detection for SST images. *J. Atmos. Ocean. Technol.* 12(4):821-829.
- Cayula, J. F., Cornillon, P., Holyer, R. and Peckinpaugh, S. 1991. Comparative study of two recent edge-detection algorithms designed to process sea-surface temperature fields. *IEEE Trans. Geosci. Remote Sens.* 29(1):175-177.
- Chassot, E., Bonhommeau, S., Reygondeau, G., Nieto, K., Polovina, J. J., Huret, M., Dulvy, N. K. and Demarcq, H. 2011. Satellite remote sensing for an ecosystem approach to fisheries management. *ICES Journal of Marine Science.* 68(4):651-666.
- Chavez, F. P. and Messié, M. 2009. A comparison of eastern boundary upwelling ecosystems. *Prog. Oceanogr.* 83(1):80-96.
- Chidambaram, K. 1950. Studies on the length frequency of oil sardine, *Sardinella longiceps* Cuv. & Val. and on certain factors influencing their appearance on the Calicut coast of the Madras Presidency. *Proc. of Indian Academy of Sciences.* 31(5):252-286.
- Choudhury, S. B., Jena, B., Rao, M. V., Rao, K. H., Somvanshi, V. S., Gulati, D. K. and Sahu, S. K. 2007. Validation of integrated potential fishing zone

(IPFZ) forecast using satellite based chlorophyll and sea surface temperature along the east coast of India. *Int. J. Remote Sens.* 28(12):2683-2693.

CMFRI [Central Marine Fisheries Research Institute]. 2012. Marine Fisheries Census - 2010. Ministry of Agriculture, Krishi Bhavan, New Delhi and CMFRI, Cochin, 201p.

CMFRI [Central Marine Fisheries Research Institute]. 2013. Annual Report 2012-13. Ministry of Agriculture, Krishi Bhavan, New Delhi and CMFRI, Cochin, 204p.

CMFRI [Central Marine Fisheries Research Institute]. 2017. Marine Fish Landings in India 2016. Technical Report, Kochi, 16p.

Cromwell, T. and Reid Jr, J. L. 1956. A study of oceanic fronts. *Tellus.* 8(1):94-101.

Dam Roy, S. and George, G. 2010. Marine resources of islands: status and approaches for sustainable exploitation/conservation with special emphasis to Andaman and Nicobar. *Indian J. Anim. Sci.* 80(4):57-62

Decker, M. B. and Hunt Jr, G. L. 1996. Foraging by murre (Uria spp.) at tidal fronts surrounding the Pribilof Islands, Alaska, USA. *Mar. Ecol. Prog. Ser.* 139: pp. 1-10.

Dulvy, N. K., Chassot, E., Hyemans, J., Hyde, K. and Pauly, D. 2009. Climate change, ecosystem variability and fisheries productivity. Remote Sensing in Fisheries and Aquaculture: The Societal Benefits, IOCCG report. (8):11-28.

Durazo, R., Harrison, N. and Hill, A. 1998. Seabird observations at a tidal mixing front in the Irish Sea. *Estuar. Coast. Shelf Sci.* 47(2):153-164.

ECMWF [European Centre for Medium Range Weather Forecasts]. 2017. ECMWF home page[on line] Available: <http://apps.ecmwf.int> [5 Jul. 2017].





- Edwards, E. W., Quinn, L. R., Wakefield, E. D., Miller, P. I. and Thompson, P. M. 2013. Tracking a northern fulmar from a Scottish nesting site to the Charlie-Gibbs Fracture Zone: evidence of linkage between coastal breeding seabirds and Mid-Atlantic Ridge feeding sites. *Deep Sea Res. Part II*. 98:438–444.
- Egevang, C., Stenhouse, I. J., Phillips, R. A., Petersen, A., Fox, J. W. and Silk, J. R. D. 2010. Tracking of Arctic terns *Sterna paradisaea* reveals longest animal migration. *Proc. of the National Academy of Sciences*. 107:2078–2081.
- Enfield, D. B. 1988. Is El Niño becoming more common? *Oceanography*. 1(2):23–59.
- Fiedler, P. C. and Bernard, H. J. 1987. Tuna aggregation and feeding near fronts observed in satellite imagery. *Cont. Shelf Res.* 7(8):871–881.
- Findlater, J. 1969. A major low-level air current near the Indian Ocean during the northern summer. *Q. J. Roy. Meteorol. Soc.* 95(404):362–380.
- Fischer, A. S., Weller, R. A., Rudnick, D. L., Eriksen, C. C., Lee, C. M., Brink, K. H., Fox, C. A. and Leben, R. R. 2002. Mesoscale eddies, coastal upwelling, and the upper-ocean heat budget in the Arabian Sea. *Deep Sea Res. Part II: Topical Studies in Oceanography*. 49(12):2231–2264.
- Fischer, J., Schott, F. and Stramma, L. 1996. Currents and transports of the Great Whirl-Socotra Gyre system during the summer monsoon, August 1993. *J. Geophys. Res.* 101(C2):3573–3587
- Frederiksen, M., Moe, B., Daunt, F., Phillips, R. A., Barrett, R. T., Bogdanova, M. I., Boulinier, T., Chardine, J. W., Chastel, O., Chivers, L. S. and Christensen-Dalsgaard, S. 2012. Multicolony tracking reveals the winter distribution of a pelagic seabird on an ocean basin scale. *Divers. Distrib.* 18(6):530–542.

- George, G., Krishnan, P., Roy, S. D., Sarma, K., GouthamBharathi, M.P., Kaliyamoorthy, M., Krishnamurthy, V., and Srinivasa Kumar, T. 2013. Validation of Potential Fishing Zone (PFZ) forecasts from Andaman and Nicobar Islands. *Fish. Tech.* 50:1-5.
- George, G., Krishnan, P., Sarma, K., Kirubasankar, R., Goutham-Bharathi, M. P., Kaliyamoorthy, M., Krishnamurthy, V. and Kumar, T. S. 2011. Integrated Potential fishing Zone (IPFZ) forecasts: a promising information and communication technology tool for promotion of green fishing in the Islands. *Ind. J. Agric. Econ.* 66(3):513-519.
- George, G., Meenakumari, B., Raman, M., Kumar, S., Vethamony, P., Babu, M. T. and Verlecar, X. 2012. Remotely sensed chlorophyll: a putative trophic link for explaining variability in Indian oil sardine stocks. *J. Coast. Res.* 28(1A): 105-113.
- Gibson, P. 2000. Introductory remote sensing principles and concepts. Routledge. 187p.
- Goes, J. I., Thoppil, P. G., do R Gomes, H. and Fasullo, J. T. 2005. Warming of the Eurasian landmass is making the Arabian Sea more productive. *Science.* 308(5721):545-547.
- Grecian, W. J., Inger, R., Attrill, M. J., Bearhop, S., Godley, B. J., Witt, M. J. and Votier, S.C. 2010. Potential impacts of wave-powered marine renewable energy installations on marine birds. *Ibis.* 152(4):683-697.
- Hallegatte, S., 2009. Strategies to adapt to an uncertain climate change. *Glob. Environ. Change.* 19(2):240-247.
- Halpern, B. S., Walbridge, S., Selkoe, K. A., Kappel, C. V., Micheli, F., D'agrosa, C., Bruno, J. F., Casey, K. S., Ebert, C., Fox, H. E. and Fujita, R. 2008. A global map of human impact on marine ecosystems. *Science.* 319(5865):948-952.

- Haney, J. C. 1986. Seabird segregation at Gulf Stream frontal eddies. *Mar. Ecol. Prog. Ser.* 28(3):279–285.
- Hansen, J., Sato, M., Russell, G. and Kharecha, P., 2013. Climate sensitivity, sea level and atmospheric carbon dioxide. *Phil. Trans. R. Soc. A*, 371(2001): 31p.
- Hartog, J. R., Hobday, A. J., Matear, R. and Feng, M. 2011. Habitat over-lap between southern bluefin tuna and yellowfin tuna in the east coast longline fishery—implications for present and future spatial management. *Deep Sea Res. Part II.* 58(5):746-752.
- Holyer, R. J. and Peckinpaugh, S. H. 1989. Edge detection applied to satellite imagery of the oceans. *IEEE Trans. Geosci. Remote Sens.* 27(1):46-56.
- Hornell, J. 1910. Report on the results of the fishery cruise along the Malabar coast and the Laccadive Islands in 1908. *Madras Fish. Bull.* 4(4):71-126.
- Hornell, J. and Nayadu, M. R., 1924. A contribution to the life history of the Indian oil sardine with notes on the plankton of the Malabar Coast. *Madras Fish. Bull.* 17:127-129.
- Houk, P., Bograd, S. and van Woosik, R. 2007. The transition zone chlorophyll front can trigger *Acanthaster planci* outbreaks in the Pacific Ocean: Historical confirmation. *J. Oceanogr.* 63(1):149-154.
- Howell, E. A., Kobayashi, D. R., Parker, D. M., Balazs, G. H. and Polovina, J. J. 2008. Turtle Watch: a tool to aid in the bycatch reduction of loggerhead turtles *Carettacaretta* in the Hawaii-based pelagic longline fishery. *Endanger. Species Res.* 5:267–278.
- Humston, R., Ault, J. S., Lutcavage, M. and Olson, D. B., 2000. Schooling and migration of large pelagic fishes relative to environmental cues. *Fish. Oceanogr.* 9(2):136-146.

- Hunt, G. L., 1999. Physical processes, prey abundance, and the foraging ecology of seabirds. In Proceedings of the 22nd International Ornithological Congress, 16-22 August 1998, Durban. BirdLife South Africa, pp. 2040–2056.
- Hunt, G. L., Mehlum, F., Russell, R., Irons, D., Decker, M., and Becker, P. 1999. Physical processes, prey abundance, and the foraging ecology of seabirds. Proc. of the 22nd International Ornithological Congress, pp. 2040-2056.
- INCOIS [Indian National Center for Ocean Information Services]. 2017. INOIS home page [on line]. Available: <http://www.incois.gov.in>. [9 Apr. 2017].
- Inger, R., Attrill, M. J., Bearhop, S., Broderick, A. C., Grecian, W. J., Hodgson, D. J., Mills, C., Sheehan, E., Votier, S. C., Witt, M. J. and Godley, B. J. 2009. Marine renewable energy: potential benefits to biodiversity? An urgent call for research. *J. Appl. Ecol.* 46(6):1145-1153.
- Jayaram, C., Chacko, N., Joseph, K. A. and Balchand, A. N. 2010. Interannual variability of upwelling indices in the Southeastern Arabian Sea: A satellite based study. *Ocean Science Journal*, 45(1):27-40.
- Joseph, K. A., Thejna, T. and Balchand, A. N. 2007. Studies on the seasonal variability of Chlorophyll-a concentration and SST in the Eastern Arabian Sea using satellite imageries. *J. Mar. Atmos. Res.* 3(2):41-50.
- Kahru, M., Håkansson, B. and Rud, O. 1995. Distributions of the sea-surface temperature fronts in the Baltic Sea as derived from satellite imagery. *Cont. Shelf Res.* 15(6): 663-679
- Kai, E. T. and Marsac, F. 2010. Influence of mesoscale eddies on spatial structuring of top predators' communities in the Mozambique Channel. *Prog. Oceanogr.* 86(1):214-223.

- Keen, T. R., Kindle, J. C. and Young, D. K. 1997. The interaction of southwest monsoon upwelling, advection and primary production in the northwest Arabian Sea. *J. Mar. Sys.* 13(1-4): 61-82.
- Klemas, V. 2013. Fisheries applications of remote sensing: an overview. *Fish. Res.* 148:124-136.
- Kumar, K. V., Kumar, P. D., Smitha, B. R., Rahman, H. H., Josia, J., Muraleedharan, K. R., Sanjeevan, V. N. and Achuthankutty, C. T. 2008. Hydrographic characterization of southeast Arabian Sea during the wane of southwest monsoon and spring intermonsoon. *Environ. Monit. Assess.* 140(1-3):231-247.
- Kumar, P. S., Pillai, G. N. and Manjusha, U. 2014. El Nino southern oscillation (ENSO) impact on tuna fisheries in Indian Ocean. *Springer Plus.* 3(1):591.
- Kumar, S. P. and Narvekar, J. 2005. Seasonal variability of the mixed layer in the central Arabian Sea and its implication on nutrients and primary productivity. *Deep Sea Res. Part II.* 52(14):1848-1861.
- Kumar, S. P. and Prasad, T.G. 1996. Winter cooling in the northern Arabian Sea; *Curr. Sci.* 71(11):834-841.
- Kumar, S. P., Madhupratap, M., Kumar, M. D., Muraleedharan, P. M., De Souza, S. N., Gauns, M. and Sarma, V. V. S. S. 2001. High biological productivity in the central Arabian Sea during the summer monsoon driven by Ekman pumping and lateral advection. *Curr. Sci.* 81(12):1633-1638.
- Kurien, P., Ikeda, M. and Valsala, V. K. 2010. Mesoscale variability along the east coast of India in spring as revealed from satellite data and OGCM simulations. *J. Oceanogr.* 66(2):273-289.

- Laukkonen, J., Blanco, P. K., Lenhart, J., Keiner, M., Cavric, B. and Kinuthia-Njenga, C. 2009. Combining climate change adaptation and mitigation measures at the local level. *Habitat Int.* 33(3):287-292.
- Lehodey, P., Bertignac, M., Hampton, J., Lewis, A. and Picaut, J. 1997. El Niño Southern Oscillation and tuna in the western Pacific. *Nature.* 389(6652):715-718.
- Levitus, S. and Boyer, T. P. 1994. Temperature. NOAA Atlas NESDIS 4. World Ocean Atlas 4. 117 p
- Lévy, M., Klein, P. and Treguier, A. 2001. Impact of sub-mesoscale physics on production and subduction of phytoplankton in an oligotrophic regime. *J. Mar. Res.* 59(4):535–565.
- Lewison, R. L., Crowder, L. B., Wallace, B. P., Moore, J. E., Cox, T., Zydalis, R., McDonald, S., DiMatteo, A., Dunn, D. C., Kot, C. Y. and Bjorkland, R. 2014. Global patterns of marine mammal, seabird, and sea turtle bycatch reveal taxa-specific and cumulative megafauna hotspots. *Proc. of the National Academy of Sciences.* 111(14):5271-5276.
- Lin, I., Liu, W. T., Wu, C. C., Wong, G. T., Hu, C., Chen, Z., Liang, W. D., Yang, Y. and Liu, K. K. 2003. New evidence for enhanced ocean primary production triggered by tropical cyclone. *Geophys. Res. Lett.* 30(13):1-4
- Lix, J. K., Venkatesan, R., Grinson, G., Rao, R. R., Jineesh, V. K., Arul, M. M., Vengatesan, G., Ramasundaram, S., Sundar, R. and Atmanand, M. A. 2016. Differential bleaching of corals based on El Niño type and intensity in the Andaman Sea, southeast Bay of Bengal. *Environmental monitoring and assessment.* 188(3):175p.
- Longhurst, A. R. and Harrison, W. G. 1989. The biological pump: profiles of plankton production and consumption in the upper ocean. *Prog. Oceanogr.* 22(1):47-123.

- Longhurst, A. R. and Wooster, W. S. 1990. Abundance of oil sardine (*Sardinella longiceps*) and upwelling on the southwest coast of India. *Can. J. Fish. Aquat. Sci.* 47(12):2407-2419.
- Longhurst, A., Sathyendranath, S., Platt, T. and Caverhill, C. 1995. An estimate of global primary production in the ocean from satellite radiometer data. *J. Plankton Res.* 17(6):1245-1271.
- Madhupratap, M., Kumar, S. P., Bhattathiri, P. M. A., Kumar, M. D., Raghukumar, S., Nair, K. K. C. and Ramaiah, N. 1996. Mechanism of the biological response to winter cooling in the northeastern Arabian Sea. *Nature.* 384: 549–552.
- Madhupratap, M., Nair, K. N. V., Gopalakrishnan, T. C., Haridas, P., Nair, K. K. C., Venugopal, P. and Gauns, M. 2001. Arabian Sea oceanography and fisheries of the west coast of India. *Curr. Sci.* 81(4):355-361.
- Madhupratap, M., Shetye, S. R., Nair, K. N. V. and Nair, S. S. 1994. Oil sardine and Indian mackerel: their fishery, problems and coastal oceanography. *Curr. Sci.* 66(5):340–348.
- Mahadevan, A. and Archer, D. 2000. Modelling the impact of fronts and mesoscale circulation on the nutrient supply and biogeochemistry of the upper ocean. *J. Geophys. Res.* 105(C1):1209–1225.
- Mahadevan, A. and Tandon, A. 2006. An analysis of mechanisms for sub mesoscale vertical motion at ocean fronts. *Ocean Model.* 14(3):241-256.
- Martin, S., 2014. An introduction to ocean remote sensing. Cambridge University Press, Cambridge, 511p.
- Miller, P. 2004. Multi-spectral front maps for automatic detection of ocean colour features from SeaWiFS. *Int. J. Rem. Sen.* 25(7-8):1437-1442.

- Miller, P. I. and Christodoulou, S. 2014. Frequent locations of ocean fronts as an indicator of pelagic diversity: application to marine protected areas and renewables. *Marine Policy*. 45:318-329.
- Miller, P. I., Read, J. F. and Dale, A. C. 2013. Thermal front variability along the North Atlantic Current observed using microwave and infrared satellite data. *Deep Sea Res. Part II*. 98(B):244-256.
- Montégut, C. B., Vialard, J., Shenoi, S. S., Shankar, D., Durand, F., Ethé, C. and Madec, G. 2007. Simulated seasonal and interannual variability of the mixed layer heat budget in the northern Indian Ocean. *J. Clim.* 20(13): 3249-3268.
- Muhammad, S., Memon, A. A., Muneeb, M. and Ghauri, B. 2016. Seasonal and spatial patterns of SST in the northern Arabian Sea during 2001–2012. *The Egyptian Journal of Remote Sensing and Space Science*. 19(1):17-22.
- Mumby, P. J., Skirving, W., Strong, A. E., Hardy, J. T., LeDrew, E. F., Hochberg, E. J., Stumpf, R. P. and David, L. T. 2004. Remote sensing of coral reefs and their physical environment. *Mar. Pollut. Bull.* 48(3):219-228.
- Muraleedharan, P. M. and Prasannakumar, S. 1996. Arabian Sea upwelling-A comparison between coastal and open ocean regions. *Curr. Sci.* 71:842-846
- Murtugudde, R., Seager, R. and Thoppil, P. 2007. Arabian Sea response to monsoon variations. *Paleoceanography*. 22(4). 17p
- Nair, R. V. 1953. Studies on the revival of the Indian oil sardine fishery. Proceedings of Indo-Pacific Fisheries Council, 23rd October-7th November 1952, Quezon City, Republic of Philippines. pp. 115–129.
- Nair, R. V. 1959. Notes on the spawning habits and early life history of the oil sardine, *Sardinella longiceps* Cuv and Val. *Indian J. Fish.* 6(2):342–359.



- NASA [National Aeronautics and Space Administration]. 2017. NASA Ocean Color home page [on line]. Available: <https://oceancolor.gsfc.nasa.gov> [17 Jan. 2017].
- Nayak, S. R., Solanki, H. U. and Dwivedi, R. M. 2003. Utilization of IRS P4 ocean colour data for potential fishing zone-A cost benefit analysis. *Ind. J. Mar. Sci.* 32(3):244-248
- Nerem, R. S., Schrama, E. J., Koblinsky, C. J. and Beckley, B. D. 1994. A preliminary evaluation of ocean topography from the TOPEX/POSEIDON mission. *J. Geophys. Res.* 99(C12):24565-24583.
- Ñiquen, M. and Bouchon, M. 2004. Impact of El Niño events on pelagic fisheries in Peruvian waters. *Deep Sea Res. Part II.* 51(6):563-574.
- NOAA [National Oceanic and Atmospheric Administration]. 2017a. El Niño theme page [on line]. Available: [https://www.pmel.noaa.gov/el\\_nino](https://www.pmel.noaa.gov/el_nino) [09 Apr. 2017].
- NOAA [National Oceanic and Atmospheric Administration]. 2017b. Global Climate Report - Annual 2016 [on line] Available: <https://www.ncdc.noaa.gov/sotc/global/201613>. [8 Aug. 2017].
- Nur, N., Jahncke, J., Herzog, M. P., Howar, J., Hyrenbach, K. D., Zamon, J. E., Ainley, D. G., Wiens, J. A., Morgan, K., Ballance, L. T. and Stralberg, D. 2011. Where the wild things are: predicting hotspots of seabird aggregations in the California Current System. *Ecol. Appl.* 21(6):2241-2257.
- OCCCI [Ocean Color Climate Change Initiative]. 2017. Ocean Color CCI home page [on line]. Available: <https://www.oceancolour.org>. [17 Jan. 2017].
- Olson, D. B., Hitchcock, G. L., Mariano, A. J., Ashjian, C. J., Peng, G., Nero, R. W. and Podestá, G. P. 1994. Life on the edge: marine life and fronts. *Oceanography.* 7(2):52-60.



- Owen, R. W. 1981. Fronts and eddies in the sea: mechanisms, interactions and biological effects. Analysis of marine ecosystems. Academic press, London, pp. 197-212.
- Pedlosky, J., 1978. A nonlinear model of the onset of upwelling. *Journal of Physical Oceanography*. 8(2):178-187.
- Perea, L. A., Buitron, B. and Mecklenburg, E. 1998. Reproductive state, partial fecundity and frequency of it spawns from the Peruvian anchoveta to autumn beginnings. *Inf. Inst. Mar Peru*. 138:147-152.
- Pillai, N. G. K., Vivekanandan, E., Ganga, U. and Ramachandran, C. 2009. Marine Fisheries Policy Brief-1. *CMFRI Special Publication*. 100:1-24.
- Pillai, V. N. and Nair, P. G. 2010. Potential fishing zone (PFZ) advisories-Are they beneficial to the coastal fisherfolk? A case study along Kerala coast, South India. *Biol. Forum*. 2(2):46-55.
- Pillai, V. N., Pillai, V. K., Gopinathan, C. P. and Nandakumar, A. 2000. Seasonal variations in the physico-chemical and biological characteristics of the eastern Arabian Sea. *J. Mar. Biol. Ass. India*. 42(1 & 2):1-21.
- Piontkovski, S. A., Al-Gheilani, H. M., Jupp, B. P., Al-Azri, A. R. and Al-Hashmi, K. A. 2012. Interannual changes in the Sea of Oman ecosystem. *Open Mar. Biol. J*. 6:38-52.
- Platt, T., Sathyendranath, S., White, G. N., Fuentes-Yaco, C., Zhai, L., Devred, E. and Tang, C. 2010. Diagnostic properties of phytoplankton time series from remote sensing. *Estuaries. Coast*. 33(2):428-439.
- Podestá, G. P., Browder, J. A. and Hoey, J. J. 1993. Exploring the association between swordfish catch rates and thermal fronts on US longline grounds in the western North Atlantic. *Cont. Shelf Res*. 13(2-3):253-277.

- Polovina, J. J. and Howell, E. A. 2005. Ecosystem indicators derived from satellite remotely sensed oceanographic data for the North Pacific. *ICES J. Mar. Sci.* 62(3):319-327.
- Polovina, J., Uchida, I., Balazs, G., Howell, E. A., Parker, D. and Dutton, P. 2006. The Kuroshio Extension Bifurcation Region: a pelagic hotspot for juvenile loggerhead sea turtles. *Deep Sea Res. Part II.* 53(3):326–333.
- Prasannakumar, S., Madhupratap, M., Dileepkumar, M., Gauns, M., Muraleedharan, P. M., Sarma, V. V. S. S. and DeSouza, S. N. 2000. Physical control of primary productivity on a seasonal scale in central and eastern Arabian Sea. *J. Earth Sci. Syst.* 109(4):431-441.
- Pratt, L. J., Earles, J., Cornillon, P. and Cayula, J. F. 1991. The nonlinear behaviour of varicose disturbances in a simple model of the Gulf Stream. *Deep Sea Res. Part I.* 38(1):591-622.
- Preethika, D. T., Joshi, A. T. and Lokesh, G. B., 2016. Growth performance and trade direction of Indian fish products. *Economic Affairs.* 61(1):65p.
- Puthezath, A. S. 2014. Identification of thermal fronts in the Arabian Sea using MODIS-SST data. M.Sc. (PO&OM) thesis, Kerala University of Fisheries and Ocean Studies, Kochi, pp. 53-64.
- Qasim, S. Z. 1982. Oceanography of the northern Arabian Sea. *Deep Sea Res. Part I.* 29(9):1041-1068.
- Radhakrishna, K., Devassy, V. P., Bhargava, R. M. S. and Bhattathiri, P. M. A. 1978. Primary production in the northern Arabian Sea. *Indian J. Geomarine Sci.* 7 (4):271-275
- Raghavan, B. R., Raman, M., Chauhan, P., Kumar, B. S., Shylini, S. K., Mahendra, R. S. and Nayak, S. R. 2006. Summer chlorophyll-a distribution in eastern Arabian Sea off Karnataka-Goa coast from satellite and in-situ observations.

In: Proceedings of SPIE, 28 November 2006, Goa. Remote sensing of the marine environment. pp. 1-7.

Raja, A. B. T., 1972. Possible explanation for the fluctuation in abundance of the Indian oil sardine *Sardinella longiceps* Valenciennes. Proceedings of the IPFC Symposium on Coastal and High Seas Pelagic Resources. 18-27 November 1971. FAO Regional Office, Bangkok. pp. 241-252.

Rana, A. S., Zaman, Q., Afzal, M. and Haroon, M. A. 2014. Characteristics of sea surface temperature of the Arabian Sea Coast of Pakistan and impact of tropical cyclones on SST. *Pak. J. Meteorol.* 11(21):61-68

Rixen, T., Haake, B. and Ittekkot, V. 2000. Sedimentation in the western Arabian Sea the role of coastal and open-ocean upwelling. *Deep Sea Res. Part II: Topical Studies in Oceanography.* 47(9): 2155-2178.

Rixen, T., Haake, B., Ittekkot, V., Guptha, M. V. S., Nair, R. R. and Schlüssel, P. 1996. Coupling between SW Monsoon-related surface and deep ocean processes as discerned from continuous particle flux measurements and correlated satellite data. *J. Geophys. Res.* 101(C12):28569-28582.

Roberts, J. J., Best, B. D., Dunn, D. C., Treml, E. A. and Halpin, P. N. 2010. Marine Geospatial Ecology Tools: An integrated framework for ecological geoprocessing with ArcGIS, Python, R, MATLAB, and C++. *Environ. Model. Softw.* 25(10):1197-1207.

Royer, F., Fromentin, J. M. and Gaspar, P. 2004. Association between Bluefin tuna schools and oceanic features in the western Mediterranean. *Mar. Ecol. Prog. Ser.* 269:249-263.

Rutllant, J. A., Rosenbluth, B. and Hormazabal, S. 2004. Intraseasonal variability of wind-forced coastal upwelling off central Chile (30 S). *Continental Shelf Res.* 24(7):789-804.

- Ryan, J. P., Yoder, J. A. and Cornillon, P. C. 1999. Enhanced chlorophyll at the shelfbreak of the Mid-Atlantic Bight and Georges Bank during the spring transition. *Limnol. Oceanogr.* 44(1):1–11.
- Sabarros, P. S., Grémillet, D., Demarcq, H., Moseley, C., Pichegru, L., Mullers, R. H., Stenseth, N. C. and Machu, E. 2014. Fine-scale recognition and use of mesoscale fronts by foraging Cape gannets in the Benguela upwelling region. *Deep Sea Res. Part II.* 107:77-84.
- Sarma, V. V. S. S., Delabehra, H. B., Sudharani, P., Remya, R., Patil, J. S. and Desai, D. V. 2015. Variations in the inorganic carbon components in the thermal fronts during winter in the northeastern Arabian Sea. *Mar. Chem.* 169:16-22.
- Scales, K. L., Miller, P. I., Hawkes, L. A., Ingram, S. N., Sims, D. W. and Votier, S. C. 2014. REVIEW: On the Front Line: frontal zones as priority at-sea conservation areas for mobile marine vertebrates. *J. Appl. Ecol.* 51(6): 1575-1583.
- Schott, F. 1983. Monsoon response of the Somali Current and associated upwelling. *Prog. Oceanogr.* 12(3): 357-381.
- Schott, F., Swallow, J. C. and Fieux, M. 1990. The Somali Current at the equator: annual cycle of currents and transport in the upper 1000 m and connection to neighboring latitudes. *Deep Sea Res.* 37(12):1825-1848.
- Scott, B. E., Langton, R., Philpott, E. and Waggitt, J. J. 2014. Seabirds and marine renewables: are we asking the right questions? In: Shields, M.A. and Payne, A.I.L. (eds), *Marine Renewable Energy Technology and Environmental Interactions*. Springer, Netherlands, pp. 81–92.
- Scott, B. E., Sharples, J., Ross, O. N., Wang, J., Pierce, G. J. and Camphuysen, C. J. 2010. Sub-surface hotspots in shallow seas: fine-scale limited locations of

top predator foraging habitat indicated by tidal mixing and sub-surface chlorophyll. *Mar. Ecol. Prog. Ser.* 408:207–226.

Shankar, D. and Shetye, S. R. 1997. On the dynamics of the Lakshadweep high and low in the southeastern Arabian Sea. *J. Geophys. Res.* 102(C6):12551-12562.

Shankar, D., Vinayachandran, P. N. and Unnikrishnan, A. S. 2002. The monsoon currents in the north Indian Ocean. *Prog. Oceanogr.* 52(1):63-120.

Shetye, S. R. 1986. A model study of the seasonal cycle of the Arabian Sea surface temperature. *J. Mar. Res.* 44(3):521-542.

Skov, H. and Durinck, J. 1998. Constancy of frontal aggregations of sea-birds at the shelf break in the Skagerrak. *J. Sea Res.* 39(3):305–311.

Solanki, H. U., Dwivedi, R. M. and Nayak, S. R. 2001. Synergistic analysis of SeaWiFS chlorophyll concentration and NOAA-AVHRR SST features for exploring marine living resources. *Int. J. Rem. Sen.* 22(18):3877-3882

Solanki, H. U., Dwivedi, R. M., Nayak, S. R., Gulati, D. K., John, M. E. and Somavanshi, V. S. 2003. Potential Fishing Zone (PFZs) forecast using satellite data derived biological and physical processes. *J. Ind. Soci. Rem. Sen.* 31(2):67-69.

Solanki, H. U., Dwivedi, R. M., Nayak, S. R., Somvanshi, V. S., Gulati, D. K. and Pattanayak, S. K. 2003. Fishery forecast using OCM chlorophyll concentration and AVHRR SST: validation results off Gujarat coast, India. *Int. J. Remote Sensing.* 24(18):3691-3699.

Solanki, H. U., Mankodi, P. C., Nayak, S. R. and Somvanshi, V. S. 2005. Evaluation of remote-sensing based potential fishing zones (PFZs) forecast methodology, *Cont. Shelf Res.* 25(18):2163-2173.

- Solanki, H. U., Pradhan, Y., Dwivedi, R. M., Nayak, S. R., Gulati, D. K. and Somvanshi, V. S. 2005. Application of QuikSCAT Sea Winds data to improve remotely sensed Potential Fishing Zones (PFZs) forecast methodology: Preliminary validation results. *Ind. J. Mar. Sci.* 34(4):441-448
- Springer, A. M., McRoy, C. P. and Flint, M. V. 1996. The Bering Sea GreenBelt: shelf-edge processes and ecosystem production. *Fish. Oceanogr.* 5(3-4): 205–223.
- Subrahmanyam, B., Rao, K. H., Rao, S. N., Murty, V. S. N. and Sharp, R. J. 2002. Influence of a tropical cyclone on chlorophyll-a concentration in the Arabian Sea. *Geophys. Res. Lett.* 29(22):4p
- Subrahmanyam, R. 1959. Studies on the phytoplankton of the west coast of India. *Proc. of the Indian Academy of Sciences.* 50(3):113-187.
- Sugimoto, T., Kimura, S. and Tadokoro K. 2001. Impact of El Niño events and climate regime shift on living resources in the western North Pacific. *Prog. Oceanogr.* 49(1):113– 127.
- Taylor, J. R. and Ferrari, R. 2011. Ocean fronts trigger high latitude phytoplankton blooms. *Geophys. Res. Lett.* 38(23):24.
- Thorne, L. and Read, A. 2013. Fine-scale biophysical interactions drive prey availability at a migratory stopover site for Phalaropus spp. In the Bay of Fundy, Canada. *Mar. Ecol. Prog. Ser.* 487:261–273.
- Thurman, H. and Trujillo, A. 1999. Essentials of Oceanography, Prentice Hall, Upper Saddle River, New Jersey, 542p.
- Tijani, K., Chiaradia, M. T., Morea, A., Nutricato, R., Guerriero, L. and Pasquariello, G. 2015. Fishing forecasting system in Adriatic Sea-A model approach based on a normalized scalar product of the SST gradient and CHL

- gradient vectors. In: Geoscience and Remote Sensing Symposium (IGARSS), 26-31 July 2015, Milan, Italy, pp. 2257-2260.
- Treml, E. A., Halpin, P. N., Urban, D. L. and Pratson, L. F. 2008. Modelling population connectivity by ocean currents, a graph – theoretic approach for marine conservation. *Landsc. Ecol.* 23(1):19-36.
- Turner, W., Spector, S., Gardiner, N., Fladeland, M., Sterling, E. and Steininger, M. 2003. Remote sensing for biodiversity science and conservation. *Trends Ecol. Evol.* 18(6):306-314.
- Tynan, C. T., Ainley, D. G., Barth, J. A., Cowles, T. J., Pierce, S. D. and Spear, L. B. 2005. Cetacean distributions relative to ocean processes in the northern California Current System. *Deep Sea Res. Part II.* 52(1):145–167.
- Ullman, D. S. and Cornillion, P. C. 2000. Evaluation of front detection methods for satellite derived SST data using in situ observations. *J. Atmos. Ocean. Technol.* 17(12):1667–1675.
- Vialard, J., Jayakumar, A., Gnanaseelan, C., Lengaigne, M., Sengupta, D. and Goswami, B. N. 2012. Processes of 30–90 days sea surface temperature variability in the northern Indian Ocean during boreal summer. *Clim. Dyn.* 38(9-10):1901-1916.
- Vipin, P., Sarkar, K., Aparna, S. G., Shankar, D., Sarma, V. V. S. S., Gracias, D. G., Krishna, M. S., Srikanth, G., Mandal, R., Rao, E. R. and Rao, N. S. 2015. Evolution and sub-surface characteristics of a sea-surface temperature filament and front in the northeastern Arabian Sea during November–December 2012. *J. Mar. Syst.* 150:1-11.
- Vitousek, P. M., Mooney, H. A., Lubchenco, J. and Melillo, J. M. 1997. Human domination of Earth's ecosystems. *Science.* 277(5325):494-499.



- Vivekanandan, E. 2010. Impact of Climate Change on Indian Marine Fisheries and Options for Adaptation. *Souvenir: Lobster Research in India*, pp. 65-71.
- Vivekanandan, E. 2013. Impact and adaptation options for Indian marine fisheries to climate change. In Winter School on ICT-oriented Strategic Extension for Responsible Fisheries Management. pp. 63-72.
- Wang, C., Wang, W., Wang, D. and Wang, Q. 2006. Inter annual variability of the South China Sea associated with El Niño. *J. Geophys Res.* 111(C3).1-19
- Ware, D. M. and Thomson, R. E. 2005. Bottom-up ecosystem trophic dynamics determine fish production in the Northeast Pacific. *Science.* 308(5726): 1280-1284.
- Weller, R. A., Baumgartner, M. F., Josey, S. A., Fischer, A. S. and Kindle, J. C. 1998. Atmospheric forcing in the Arabian Sea during 1994–1995: observations and comparisons with climatology and models. *Deep Sea Res. Part II: Topical Studies in Oceanography.* 45(10-11): 1961-1999.
- Weller, R. A., Fischer, A. S., Rudnick, D. L., Eriksen, C. C., Dickey, T. D., Marra, J., Fox, C. and Leben, R. 2002. Moored observations of upper-ocean response to the monsoons in the Arabian Sea during 1994–1995. *Deep Sea Res. Part II: Topical Studies in Oceanography.* 49(12): 2195-2230.
- Wiebinga, C. J., Veldhuis, M. J. and De Baar, H. J. 1997. Abundance and productivity of bacterioplankton in relation to seasonal upwelling in the northwest Indian Ocean. *Deep Sea Res. Part I.* 44(3):451-476.
- Wiggert, J. D., Murtugudde, R. G. and McClain, C. R. 2002. Processes controlling interannual variations in wintertime (Northeast Monsoon) primary productivity in the central Arabian Sea. *Deep Sea Res. Part II: Topical Studies in Oceanography.* 49(12): 2319-2343.

- Witherington, B. 2002. Ecology of neonate loggerhead turtles inhabiting lines of downwelling near a Gulf Stream front. *Mar. Biol.* 140(4):843–853.
- WMO [World Meteorological Organization]. 2016. WMO provisional Statement on the Status of the Global Climate in 2016 [on line] Available:[https://www.uncclearn.org/sites/default/files/inventory/wmo2016\\_0.pdf](https://www.uncclearn.org/sites/default/files/inventory/wmo2016_0.pdf) [8 Aug. 2017].
- Yazdi, K. S. and Shakouri, B. 2010. The effects of climate change on aquaculture. *International Journal of Environmental Science and Development*, 1(5): 378.
- Yi, X. 2016. Impact of large-scale climate variability on the Arabian Sea coastal upwelling system. M.Sc. thesis, University of Hamburg, Hamburg, pp. 1-68
- Zainuddin, M. 2011. Skipjack Tuna in relation to sea surface temperature and chlorophyll-a concentration of Bone Bay using remotely sensed satellite data. *Jurnal Ilmu dan Teknologi Kelautan Tropis*. 3(1):82-90
- Zainuddin, M. and Jamal, M. 2009. Satellite remote sensing and geographic information system of potential fishing zones and migration pattern of Skipjack Tuna in Bone Bay, South Sulawesi. In: International Proceeding of World Ocean Conference. Manado.
- Zainuddin, M., Kiyofuji, H., Saitoh, K. and Saitoh, S. I. 2006. Using multi-sensor satellite remote sensing and catch data to detect ocean hot spots for albacore (*Thunnusalalunga*) in the northwestern North Pacific. *Deep Sea Res. Part II*. 53(3):419- 431.
- Zainuddin, M., Saitoh, S. I. and Saitoh, K. 2004. Detection of potential fishing ground for albacore tuna using synoptic measurements of ocean color and thermal remote sensing in the northwestern North Pacific. *Geophys. Res. Lett.* 31(20):4p

**INTER-ANNUAL VARIABILITY OF THERMAL AND  
CHLOROPHYLL FRONTS IN SELECTED PARTS OF  
EASTERN ARABIAN SEA AND THEIR RELATION TO  
MARINE FISHERY**

*by*

**ANANTH C BABU**

**(2012 - 20 - 103)**

**THESIS ABSTRACT**

**Submitted in partial fulfilment of the  
requirements for the degree of**

**B.Sc. – M.Sc. (Integrated) Climate Change Adaptation**

**Faculty of Agriculture**

**Kerala Agricultural University**



**ACADEMY OF CLIMATE CHANGE EDUCATION AND RESEARCH**

**VELLANIKKARA, THRISSUR – 680 656**

**KERALA, INDIA**

**2017**

## CHAPTER 7

### ABSTRACT

In the marine ecosystem, distribution of fish, as well as abundance, is determined by the presence of conditions favourable for their existence. Among various oceanic features, frontal zones are important sites promoting fish aggregation and these zones are found to be ideal habitats for fish. Therefore, areas with higher incidence of fronts are likely to be associated with higher fish production, than those with lower frontal incidence. An evaluation of this concept based on total thermal/chlorophyll frontal area of the eastern Arabian Sea (50-80°E; 0 to 30°N), was performed for the period July 2002 to December 2016. This work utilized 8-day averaged satellite Sea Surface Temperature observations (SST) from MODIS/AQUA sensor as well as 8-day averaged satellite chlorophyll a concentration (Chl-a) from the Ocean Colour Climate Change Initiative (OC-CCI) project. Frontal identification was based on Cayula-Cornillon (1992) single-image edge detection algorithm on the satellite SST/Chl-a image in ArcGIS platform.

Seasonal variation of thermal fronts showed maximum frontal coverage (0.5 – 0.6 million km<sup>2</sup>) during the winter period. Thermal fronts have their lowest incidence (0.2 – 0.3 million km<sup>2</sup>) during post and pre-monsoon period, and moderate existence during the summer monsoon (0.3 – 0.4 million km<sup>2</sup>). Chlorophyll fronts showed a slightly different pattern with highest frontal coverage (0.5- 0.6 million km<sup>2</sup>) during winter period followed by pre and post monsoon period (0.4 – 0.5 million km<sup>2</sup>). Chlorophyll fronts had their lowest incidence (0.2 – 0.3 million km<sup>2</sup>) during summer monsoon period. Possible physical reasons for the seasonal variation in thermal and chlorophyll front incidence are discussed. Analysis of inter-annual variability of thermal fronts indicated an increasing trend during 2015 and 2016 whereas chlorophyll frontal area showed a sudden drop in values from mid-2012 onwards. During this period, the usual seasonal variation in frontal zones is not observed. The mechanism

responsible for this unusual behaviour was also analysed. Spatial variability of frontal zones in the Arabian Sea indicated that the pattern of variability in the west is different from that of the eastern Arabian Sea. The impact of thermal as well as chlorophyll frontal area on fisheries during the inter-annual cycle is also discussed.

174270

